

SOME COORDINATION COMPOUNDS OF
SILICON TETRAFLUORIDE

by

J.P. Guertin, B.Sc.

A Thesis submitted to the Faculty of Graduate
Studies and Research of McGill University
in partial fulfilment of the requirements
for the degree of Doctor of Philosophy

From the Inorganic Chemistry Laboratory
of Dr. M. Onyszchuk

McGill University,
Montreal, P.Q.
Canada

July, 1964

To my parents

To Huguette

ACKNOWLEDGEMENTS

The author wishes to thank Dr. M. Onyszchuk for his guidance and continual encouragement in making this investigation possible.

The author is indebted to Dr. A. Taurins and Dr. C. Stammer for the proton magnetic resonance measurements.

The author is grateful to Dr. J.T. Edward and to Dr. M.A. Whitehead for their helpful discussions.

TABLE OF CONTENTS

	<u>page</u>
INTRODUCTION	1
OUTLINE OF THE RESEARCH PROBLEM	10
EXPERIMENTAL	12
Apparatus	12
Materials	14
Methods	18
Analyses	28
RESULTS	32
The Interaction of SiF ₄ with Methanol	33
Coordination of SiF ₄ with Aliphatic Cyclic Ethers and Dimethyl Ether	51
Coordination of SiF ₄ with Pyridine and other Nitrogen Electron-Pair Donor Molecules	96
Attempted Preparation of SiF ₄ Complexes with Hydrogen Sulfide, Dimethyl Sulfide, Phosphine, and Nitromethane	136
DISCUSSION	140
The Interaction of SiF ₄ with Methanol	140
Coordination of SiF ₄ with Aliphatic Cyclic Ethers and Dimethyl Ether	149

<u>TABLE OF CONTENTS</u> (cont'd.)	<u>page</u>
Coordination of SiF ₄ with Pyridine and other Nitrogen Electron-Pair Donor Molecules	170
Attempted Preparation of SiF ₄ Complexes with Hydrogen Sulfide, Dimethyl Sulfide, Phosphine, and Nitromethane	185
SUMMARY AND CONTRIBUTIONS TO KNOWLEDGE	188
REFERENCES	191
PUBLICATION	197

INTRODUCTION

The preparation of the first complex compound of BF_3 , $\text{BF}_3 \cdot \text{NH}_3$, was reported by Gay-Lussac and Thenard (1) more than 150 years ago. Some time afterwards the first SiF_4 complex, $\text{SiF}_4 \cdot 2\text{NH}_3$, was prepared (2). In 1890, Besson (3) isolated crystalline $\text{SiF}_4 \cdot \text{PH}_3$, but a temperature of -22° and a pressure of 50 atmospheres were necessary. This is the only SiF_4 complex reported containing a phosphorus electron-pair donor molecule and none have been reported with sulfur electron-pair donor molecules.

Compounds which are formed by the combination of two or more species, the atoms of which seem to be in their maximum valency, are called molecular addition compounds (or adducts); they are also broadly referred to as complex or coordination compounds. The term, coordination compound, should only be used if the bonding between the species is of the coordinate covalent type. A coordinate bond, first described by N.V. Sidgwick, is one in which two electrons shared between the two atoms forming the bond were originally associated with one atom. The molecule containing the atom which provides the shared electron-pair is called a Lewis base (4) and the molecule containing the atom which accepts a share in the electron-pair is called a Lewis acid. Any substance with one or more nonbonded electron-pairs in its valency shell orbitals is a potential Lewis base capable of forming a coordinate bond with a substance which has one or more vacant nonbonded orbitals, i.e., a Lewis acid. For example, in the reaction of SiF_4 with NH_3 to produce the

adduct, $\text{SiF}_4 \cdot 2\text{NH}_3$, SiF_4 is the electron-pair acceptor (Lewis acid) by virtue of its vacant 3d-orbitals and NH_3 is the electron-pair donor (Lewis base) because of the lone electron-pair on the nitrogen atom.

Ground state silicon (atomic number, 14) has an electronic configuration: $1s^2, 2s^2, 2p^6, 3s^2, 3p^2, 3d^0$, the excited states of which should theoretically allow the silicon atom to acquire a maximum covalency of nine by using its five vacant 3d-orbitals in bonding. However, in practice, the maximum covalency attained is six. Thus, in terms of the valence bond theory SiF_4 has a tetrahedral structure arising from sp^3 hybridization of the silicon atom. There is a change to sp^3d^2 hybridization during the formation of the $\text{SiF}_4 \cdot 2\text{NH}_3$ complex. The bonding characteristics of the silicon atom, in terms of the valence bond theory, are summarized in Fig. 1.

In the $\text{SiF}_4 \cdot 2\text{NH}_3$ each NH_3 molecule forms a coordinate bond with SiF_4 by the overlap of its filled nonbonded sp^3 -hybrid orbital with a vacant sp^3d^2 -hybrid orbital. There are two possible geometrical arrangements of the valence shell electrons in $\text{SiF}_4 \cdot 2\text{NH}_3$; these are illustrated in Fig. 2.

Complex compounds of the molecular addition type are named (5) simply by stating the name of the Lewis acid followed by a hyphen and the name of the Lewis base. The respective number of molecules are shown with Arabic numerals. For example, $\text{SiF}_4 \cdot 2\text{NH}_3$ is named silicon tetrafluoride-2-ammonia.

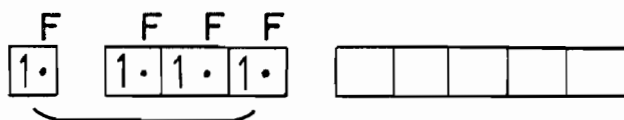
It is only in the last 11 years that most of the known SiF_4

FIG. 1

The changes in the bonding characteristics of the silicon
atom in SiF_4 during the formation of $\text{SiF}_4 \cdot 2\text{NH}_3$

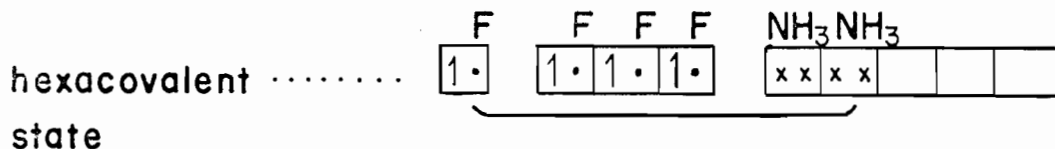
Si (Z=14): $1s^2, 2s^2, 2p^6, 3s^2, 3p^2, 3d^0$ ground state

$1s^2, 2s^2, 2p^6, 3s^1, 3p^3, 3d^0$ tetravalent state



sp^3 hybridization, tetrahedral,
as in SiF_4

$1s^2, 2s^2, 2p^6, 3s^1, 3p^3, 3d^0$



sp^3d^2 hybridization, octahedral,
as in $\text{SiF}_4 \cdot 2\text{NH}_3$

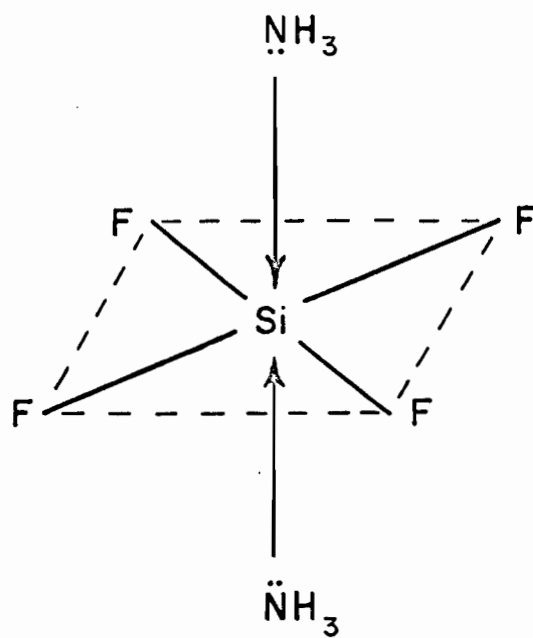
N (Z=7): $1s^2, 2s^2, 2p^3$ ground state



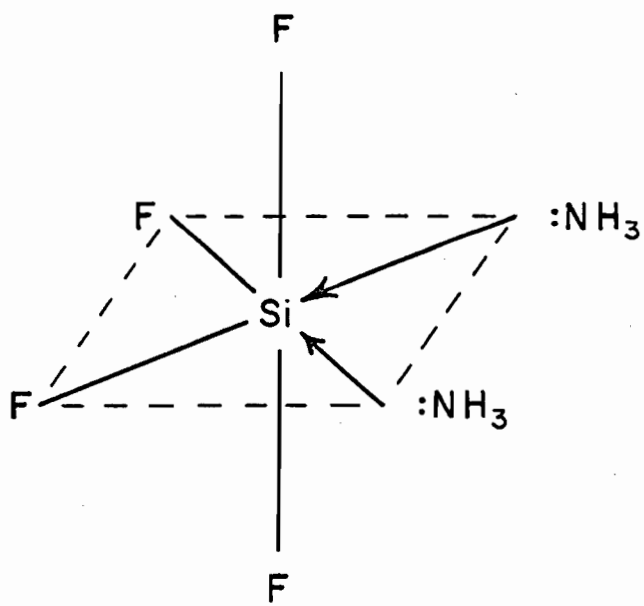
sp^3 hybridization, tetrahedral,
as in NH_3 (one lone electron-pair)

FIG. 2

The two possible structures of $\text{SiF}_4 \cdot 2\text{NH}_3$



TRANS



CIS

complexes with nitrogen electron-pair donor molecules have been prepared. Most of these complexes have 1:2 mole ratios (or 1:1 for SiF_4 with a bidentate donor). Only $\text{SiF}_4 \cdot (\text{CH}_3)_3\text{N}$ (6-9) and $\text{SiF}_4 \cdot \text{C}_5\text{H}_5\text{N}$ (10,11) have been reported as monodentate 1:1 complexes of SiF_4 with nitrogen electron-pair donor molecules. The interaction of SiF_4 with $\text{C}_5\text{H}_5\text{N}$ has also been claimed to produce $\text{SiF}_4 \cdot 3/2\text{C}_5\text{H}_5\text{N}$ (12) and $\text{SiF}_4 \cdot 2\text{C}_5\text{H}_5\text{N}$ (8,12).

Three main techniques were used to prepare the SiF_4 complexes with nitrogen electron-pair donor molecules. (i) The direct quantitative vacuum synthesis was used for the preparation of $\text{SiF}_4 \cdot (\text{CH}_3)_3\text{N}$ (6-9), $\text{SiF}_4 \cdot 2(\text{CH}_3)_3\text{N}$ (6-8), $\text{SiF}_4 \cdot 2\text{NH}_3$ (2,13-15), $\text{SiF}_4 \cdot \text{NH}_2(\text{CH}_2)_2\text{NH}_2$ (16), $\text{SiF}_4 \cdot \text{HCON}(\text{CH}_3)_2$ (17), and $\text{SiF}_4 \cdot 2\text{N}_2\text{H}_4$ (18). (ii) Tensimetric titrations (pressure-composition isotherms) were also done for $\text{SiF}_4 \cdot (\text{CH}_3)_3\text{N}$ (6,7), $\text{SiF}_4 \cdot 2(\text{CH}_3)_3\text{N}$ (6,7) and $\text{SiF}_4 \cdot 2\text{N}_2\text{H}_4$ (18). (iii) Bubbling SiF_4 gas through a dilute solution of the Lewis base in an "inert" solvent such as acetonitrile, benzene, or diethyl ether, yielded the following complexes: $\text{SiF}_4 \cdot \text{C}_5\text{H}_5\text{N}$ (10,11), $\text{SiF}_4 \cdot 3/2\text{C}_5\text{H}_5\text{N}$ (12), $\text{SiF}_4 \cdot 2\text{C}_5\text{H}_5\text{N}$ (8,12), and complexes of SiF_4 with 14 other nitrogen electron-pair donor molecules (10,19). In every case the complexes were stable white solids at 25° and could be purified by vacuum sublimation.

Attempts have been made to apply these techniques to the preparation of complexes of SiF_4 with oxygen electron-pair donor molecules, but were less successful. Using the bubbling technique, Muetterties (10) prepared $\text{SiF}_4 \cdot 2(\text{CH}_3)_2\text{SO}$, $\text{SiF}_4 \cdot 2(\text{CH}_3)_2\text{NCHO}$, and $\text{SiF}_4 \cdot x\text{CH}_3\text{COCH}_2\text{COCH}_3$; the last is a very weak complex of uncertain composition. The complexes, $\text{SiF}_4 \cdot 2(\text{CH}_3)_3\text{NO}$, $\text{SiF}_4 \cdot 2\text{C}_5\text{H}_5\text{NO}$, $\text{SiF}_4 \cdot 2(\text{C}_6\text{H}_5)_3\text{PO}$, and $\text{SiF}_4 \cdot 2(\text{C}_6\text{H}_{11})_3\text{PO}$,

have been prepared by precipitation from chloroform solution (20); it is claimed that coordination occurs through the oxygen atom. Gierut et al. (13) reported briefly that SiF_4 reacts with alcohols in a 1:4 mole ratio, yielding unstable addition compounds $\text{SiF}_4 \cdot 4\text{ROH}$, where R is CH_3 , C_2H_5 , $\text{iso-C}_3\text{H}_7$, and $\text{iso-C}_5\text{H}_{11}$. These results were confirmed by Topchiev and Bogomolova (21), who also suggested that the complex is ionic and contains hexavalent silicon. However, Holzapfel et al. (22) reported that SiF_4 and CH_3OH produce 1:6 and 1:8 complexes only. Schmeisser and Elischer (23) were the only workers to use some temperature control in the preparation of complexes of SiF_4 with either nitrogen or oxygen electron-pair donor molecules. At low temperature they were able to prepare $\text{SiF}_4 \cdot 2(\text{CH}_2)_2\text{O}$ which decomposes at $10-15^\circ$ to give 1,4-dioxane.

The reasons for discussing these methods of preparation have been to point out the emphasis by previous workers on the isolation of complexes which are stable solids at 25° . Except for the preparation of $\text{SiF}_4 \cdot 2(\text{CH}_2)_2\text{O}$, few other attempts to prepare complexes of SiF_4 with aliphatic and cyclic ethers have been reported. Little information is available about the structure of these complexes. The octahedral structure, with either cis or trans arrangement of ligands, has previously been postulated (10,16-19). Muetterties (10) has been able to tentatively assign a trans configuration to the 1:2 complexes of SiF_4 that he prepared. He observed only a single F^{19} magnetic resonance for these complexes in solution, proving that all four fluorine atoms are equivalent. This would not be the case in a cis octahedral structure. Aggarwal and Onyszchuk (18) reported infrared data indicating a cis

configuration for $\text{SiF}_4 \cdot 2\text{N}_2\text{H}_4$, but their results are not conclusive since their infrared data do not extend below 650 cm^{-1} .

Table 1 contains a complete list of the previously prepared complexes of SiF_4 with nitrogen and oxygen electron-pair donor molecules. The research in this laboratory was prompted, in part, by the general lack of information in the literature regarding the properties and structures of the coordination compounds of SiF_4 .

TABLE 1

Previously prepared complexes of SiF_4 with nitrogen
and oxygen electron-pair donor molecules

Complexes with nitrogen donors		Complexes with oxygen donors	
Complex	Reference	Complex	Reference
$\text{SiF}_4 \cdot (\text{CH}_3)_3\text{N}$	6-9	$\text{SiF}_4 \cdot 2(\text{CH}_3)_2\text{SO}$	10
$\text{SiF}_4 \cdot 2(\text{CH}_3)_3\text{N}$	6-8	$\text{SiF}_4 \cdot 2(\text{CH}_3)_2\text{NCHO}$	10
$\text{SiF}_4 \cdot \text{C}_5\text{H}_5\text{N}$	10,11	$\text{SiF}_4 \cdot x \text{CH}_3\text{COCH}_2\text{COCH}_3$	10
$\text{SiF}_4 \cdot 3/2\text{C}_5\text{H}_5\text{N}$	12	(x is uncertain)	
$\text{SiF}_4 \cdot 2\text{C}_5\text{H}_5\text{N}$	8,12	$\text{SiF}_4 \cdot 4\text{CH}_3\text{OH}$	13,21
$\text{SiF}_4 \cdot 2\text{NH}_3$	2, 13-15	$\text{SiF}_4 \cdot 6\text{CH}_3\text{OH}$	22
$\text{SiF}_4 \cdot \text{NH}_2(\text{CH}_2)_2\text{NH}_2$	16	$\text{SiF}_4 \cdot 8\text{CH}_3\text{OH}$	22
$\text{SiF}_4 \cdot 2\text{HCON}(\text{CH}_3)_2$	17	$\text{SiF}_4 \cdot 2(\text{CH}_2)_2\text{O}$	23
$\text{SiF}_4 \cdot 2\text{N}_2\text{H}_4$	18	$\text{SiF}_4 \cdot 2(\text{C}_6\text{H}_5)_3\text{PO}$	20
$\text{SiF}_4 \cdot 2\text{C}_6\text{H}_5(\text{CH}_3)_2\text{N}$	10	$\text{SiF}_4 \cdot 2(\text{C}_6\text{H}_{11})_3\text{PO}$	20
$\text{SiF}_4 \cdot 2,4-(\text{CH}_3)_2\text{C}_5\text{H}_3\text{N}$	10	$\text{SiF}_4 \cdot 2(\text{CH}_3)_2\text{NO}$	20
$\text{SiF}_4 \cdot 2(\text{CH}_3)_2\text{C}=\text{NOH}$	10	$\text{SiF}_4 \cdot 2\text{C}_5\text{H}_5\text{NO}$	20

(cont'd.)

TABLE 1 (cont'd.)

Complexes with nitrogen donors		Complexes with oxygen donors	
Complex	Reference	Complex	Reference
$\text{SiF}_4 \cdot \text{C}_6\text{H}_3(\text{OH})\text{C}_3\text{H}_3\text{N}$	10		
$\text{SiF}_4 \cdot 2$ ethylenimine	19		
$\text{SiF}_4 \cdot 2$ p-chloroaniline	19		
$\text{SiF}_4 \cdot 2$ quinoline	19		
$\text{SiF}_4 \cdot 2$ p-aminophenol	19		
$\text{SiF}_4 \cdot 2$ β -naphthylamine	19		
$\text{SiF}_4 \cdot 2$ p-aminobenzoic acid	19		
$\text{SiF}_4 \cdot$ piperazine	19		
$\text{SiF}_4 \cdot$ phenylhydrazine	19		
$\text{SiF}_4 \cdot$ o-nitroaniline	19		
$\text{SiF}_4 \cdot$ o-phenylenediamine	19		
$\text{SiF}_4 \cdot \alpha, \alpha'$ -dipyridyl	19		

Outline of the Research Problem

1. The interaction of SiF_4 with CH_3OH was undertaken partly because CH_3OH is a potential electron-pair donor molecule but mainly with the object of clarifying the conflicting results reported in the literature pertaining to the combining ratio and structure of the complex formed (p. 6).
2. Similarly, confusion exists in the literature concerning the interaction of SiF_4 with $\text{C}_5\text{H}_5\text{N}$ (p. 5). Various authors obtained different combining ratios and no attempts were made to elucidate the structure of the complex formed, i.e., as to whether it has a cis or trans configuration.
3. No complexes have been reported between SiF_4 and either sulfur or phosphorus electron-pair donor molecules (except $\text{SiF}_4 \cdot \text{PH}_3$ produced under high pressure). Sulfur and phosphorus show strong donor activity towards GeF_4 (24). Also complexes such as $\text{SiCl}_4 \cdot 2\text{PR}_3$ (where R is C_6H_5 and C_6H_{11}) and $\text{SiBr}_4 \cdot 2\text{PR}'_3$ (where R' is C_3H_7 and C_6H_{11}) have been reported (20). It was therefore desirable to determine whether or not SiF_4 would coordinate at low temperatures and at moderate pressure with H_2S , $(\text{CH}_3)_2\text{S}$, and PH_3 .
4. Few coordination compounds of SiF_4 with oxygen electron-pair donor molecules have been reported. Because of the lack of steric hindrance it was thought that the simple aliphatic cyclic ethers might form complexes with SiF_4 . Phenyl ethyl ether and isopropyl ether have been reported not to coordinate with SiF_4 (13) at 25° . At the same time

it was of interest to obtain the relative basicity of these ethers with change in ring size. It was hoped that with improved vacuum techniques it would be possible to detect and isolate complexes which are stable only at low temperatures.

5. This research was part of a general investigation of the relative electron acceptor power of SiF_4 and GeF_4 towards oxygen, sulfur, nitrogen, and phosphorus electron-pair donor molecules.

EXPERIMENTAL

1. Apparatus

(i) Vacuum System

Volatile materials were manipulated in a standard pyrex glass high-vacuum system similar to those previously described (25-27). Pressure measurements were made in the absence of mercury to an accuracy of ± 0.1 mm with a delicate soft glass spoon gauge used as a "null" indicator. The use of ground glass joints fitted with Viton rubber O-rings (Ace Glass Incorporated) was the only major improvement over previous vacuum systems used in this laboratory. A minor improvement consisted in making the inside of the LeRoy low-temperature fractionation columns (28) visible by spiraling the fiberglass encased Nichrome heating wire directly onto the glass.

Liquid air (-195°) was used for the transfer of volatile compounds. Constant temperature baths in the range -163 to 0° were prepared by cooling a suitable organic solvent with liquid air until a "slush" was obtained (26). Temperatures were measured to $\pm 0.1^\circ$ by means of a sensitive potentiometer and copper-constantan thermocouples with an ice-water mixture as a reference junction.

Liquids with boiling points above room temperature were quantitatively measured with a small weighing tube consisting of a graduated tube (capacity ~ 10 ml) equipped with a stopcock and standard joint for attachment to the vacuum system. The liquid and its vapor were condensed to an involatile solid by liquid air, the vessel was evacuated,

and the substance was transferred to the desired part of the apparatus by condensation with liquid air. The weight of substance was found by difference. Corrosive liquids were quantitatively measured and transferred using a serum-capped (Suba Seal) reaction vessel and a syringe equipped with a stopcock (29). Gases at room temperature were quantitatively determined by vapor density measurements using the Ideal Gas equation in the form $n = \frac{PV}{RT}$.

Molecular weights of gases and volatile liquids were determined to an accuracy usually better than $\pm 1\%$ by weighing a sample at measured temperature and pressure in a bulb of known volume, and subsequent application of the Ideal Gas equation in the form $M = \frac{WRT}{PV}$.

(ii) Dry Box

Hygroscopic solids and nonvolatile liquids were manipulated in an evacuable "dry box" filled with dry nitrogen. A small open dish of P_2O_5 placed inside the box assured the maintenance of dry conditions during operation.

(iii) Infrared Spectrometry

Infrared spectra in the range $4000-650 \text{ cm}^{-1}$ were recorded on Perkin-Elmer Model 21 and Infracord spectrophotometers equipped with NaCl optics. When greater resolution was required spectra were measured on a grating Perkin-Elmer Model 421 spectrophotometer. This instrument was also used for measurements in the $650-265 \text{ cm}^{-1}$ range by replacing the grating with a CsBr prism interchange unit.

Spectra of solids were taken in KBr pellets or in Nujol or Fluorolube mulls. Volatile solids were prepared for infrared measurements by subliming a thin film of the substance on a NaCl plate maintained at a sufficiently low temperature. The spectra of liquids were taken using fixed or variable space NaCl liquid cells or more simply using a thin film between two NaCl plates. The spectra of gases were taken at known pressures using a cylindrical gas cell of 10 cm length and 2.5 cm radius equipped with Viton O-rings and screw caps for the 7.5 mm thick NaCl windows.

Measurements in the 650-265 cm^{-1} range were made on samples in pure liquid or in Nujol mull form placed between CsBr plates, whose delicate surfaces were protected by 7.0 micron thin polyethylene film (Dow Chemical Company "Handi-Wrap"). This film does not absorb in the 650-265 cm^{-1} region. It was found that thin KBr pellets could also be used for measurements down to 300 cm^{-1} .

2. Materials

In general, solids were purified by several recrystallizations from a suitable solvent and by several vacuum sublimations. Their purity was checked by melting point and infrared measurements. Liquids were purified by refluxing over a suitable drying agent followed by fractional distillation. Their purity was checked by boiling point and infrared measurements. If a liquid was sufficiently volatile further purification was achieved by low-temperature vacuum distillation and its purity was further checked by vapor pressure (v.p.) and gas phase molecular weight

(M) measurements. Gases were purified by several low-temperature vacuum distillations usually using a LeRoy still. Their purity was checked by vapor pressure, molecular weight, and infrared measurements. Table 2 shows the materials used in this work with the exception of common laboratory chemicals used only occasionally.

TABLE 2

Materials used in this work

Substance Name	Formula	Commercial source	Method of purification	Purity Check			
				m.p., Required	b.p., Found	v.p., Calc'd.	Mol. Wt. (M) Found
silicon tetra- fluoride	SiF ₄	Matheson	LeRoy still	v.p. 80 mm at -115° (30)	78.5 mm	104.1	104.1
methanol	CH ₃ OH	Fisher	Refluxed with Mg/I ₂ , Distilled (32)	b.p. 64.6° (31)	63-64°	32.0	32.3
ethylene oxide	(CH ₂) ₂ O	Matheson	LeRoy still	v.p. 170 mm at -23° (30)	167 mm	44.05	44.0
trimethylene oxide	(CH ₂) ₃ O	K and K Labs.	Refluxed with KOH, Distilled, LeRoy still	b.p. 46° (33)	46-47°	58.1	58.3
tetrahydro- furan	(CH ₂) ₄ O	Fisher	Refluxed with Na, Distilled	b.p. 64-66° (31)	65°	72.1	73.0
tetrahydro- pyran	(CH ₂) ₅ O	Anachemia	"	b.p. 81-82° (31)	82.5°	86.1	87.0
dimethyl ether	(CH ₃) ₂ O	Matheson	LeRoy still	v.p. 285 mm at -45° (30)	282 mm	46.1	45.7
1,4-dioxane	(CH ₂ CH ₂ O) ₂	Fisher	Refluxed with Na, Distilled	b.p. 101.5° (31)	101-102°	88.1	89.0
nitromethane	CH ₃ NO ₂	"	Refluxed with CaH ₂ , Distilled	b.p. 101° (31)	101.5°	61.0	62.0
diethyl ether	(C ₂ H ₅) ₂ O	Mallinckrodt	None	b.p. 34.6° (31)	-	74.1	-

. . . .

TABLE 2 (cont'd.)

Substance		Commercial source	Method of purification	Purity Check			
Name	Formula			m.p., b.p., v.p.		Mol. wt. (M)	
				Required	Found	Calc'd.	Found
pyridine	C ₅ H ₅ N	Fisher	Refluxed with CaH ₂ , Distilled	b.p. 115.3° (31)	116°	79.1	80.0
Ethylene-diamine	NH ₂ (CH ₂) ₂ NH ₂	"	"	b.p. 116.1° (31)	117°	60.1	60.5
pyrrolidine	(CH ₂) ₄ NH	"	"	b.p. 88.5° (31)	86°	71.1	72.0
piperidine	(CH ₂) ₅ NH	"	"	b.p. 106.3° (31)	106°	85.15	85.8
acetonitrile	CH ₃ CN	"	"	b.p. 82° (31)	82°	41.05	41.3
ammonia	NH ₃	Matheson	LeRoy still	v.p. 405 mm at -45° (30)	401 mm	17.0	17.0
hydrogen sulfide	H ₂ S	"	"	v.p. 270 mm at -78° (30)	268 mm	34.1	34.1
dimethyl sulfide	(CH ₃) ₂ S	"	"	v.p. 180 mm at 0° (30)	181 mm	62.1	62.0
phosphine	PH ₃	P (yellow) + KOH (50%), boil (37)	"	v.p. 130 mm at -115° (30)	128 mm	34.0	34.0
naphthalene	C ₁₀ H ₈	Fisher	None	m.p. 80.2° (31)	79-80°	128.2	-
anthracene	C ₁₄ H ₁₀	"	Recrystallized (in the dark) from ethanol	m.p. 217° (31)	215-217°	178.2	-
48% hydrofluoric acid	48% HF (aq.)	"	None	-	-	-	-

3. Methods

(i) Quantitative Synthesis

In a typical experiment, SiF_4 (x mmole) was condensed over B^* (y mmole) at -195° , and the mixture was slowly warmed to 25° using proper constant temperature slush baths. This technique provided a "heat sink" for the heat produced by the interaction, thus minimizing the possible degradation of B. In cases where B could polymerize, the temperature had to be kept as low as possible at all times. Vacuum distillation of the excess component at as low a temperature as possible at which no other components or complex were volatile, allowed the determination of how much of it had reacted. For example, if SiF_4 had been in excess and vacuum distillation had yielded SiF_4 (z mmole), then SiF_4 (x - z mmole) would have reacted with B (y mmole) in a mole ratio $1 : \frac{y}{x - z}$, corresponding to the complex, $\text{SiF}_4 \cdot \frac{y}{x - z} \text{B}$.

The apparatus limited the pressure conditions to less than one atmosphere. It is possible that high pressures could produce a very different type of compound.

(ii) Tensimetric Titration

Preliminary experiments were generally needed to determine the most suitable temperature at which to measure total pressures (T_p) and to allow the reaction (T_r) to occur. These consisted of a few trial quantitative syntheses at different temperatures. T_p was chosen as low as possible to minimize dissociation of the complex but not low enough to

* Any substance with possible electron donor capacity, i.e., a Lewis base.

condense SiF_4 (b.p. -94.8°); whenever possible -78° was used because of the convenient dry ice-ethanol constant temperature slush bath available. T_r was chosen as high as possible for best interaction but not high enough to cause polymerization; whenever possible 25° was used.

Measured amounts of B (p. 18) were added in successive small amounts (~ 3 m mole at a time) to a fixed quantity of SiF_4 . After each addition, the mixture was warmed to T_r for about 15 minutes before it was slowly cooled to T_p , at which temperature pressure measurements were made. The process was stopped only after the "end" point had been passed and no other inflections could be observed. A plot of total pressure against the quantity of B added showed a linear decrease in the pressure (due to the formation of less volatile complex) until all the SiF_4 had been used up. Then a "break" in the curve occurred and the pressure became constant at the vapor pressure of B at T_p . The point of inflection indicated the mole ratio in which SiF_4 and B had combined. Similarly, reverse tensimetric titrations were done by adding measured amounts of SiF_4 (~ 3 m mole at a time) to a fixed quantity of B. In this case, the pressure remained constant until the "end" point, after which it increased linearly.

This method of indicating the formation of complexes has certain advantages over other methods. It can detect the simultaneous formation of more than one complex and the formation of a complex with an appreciable dissociation pressure under the chosen experimental conditions.

(iii) Other Methods of Preparation

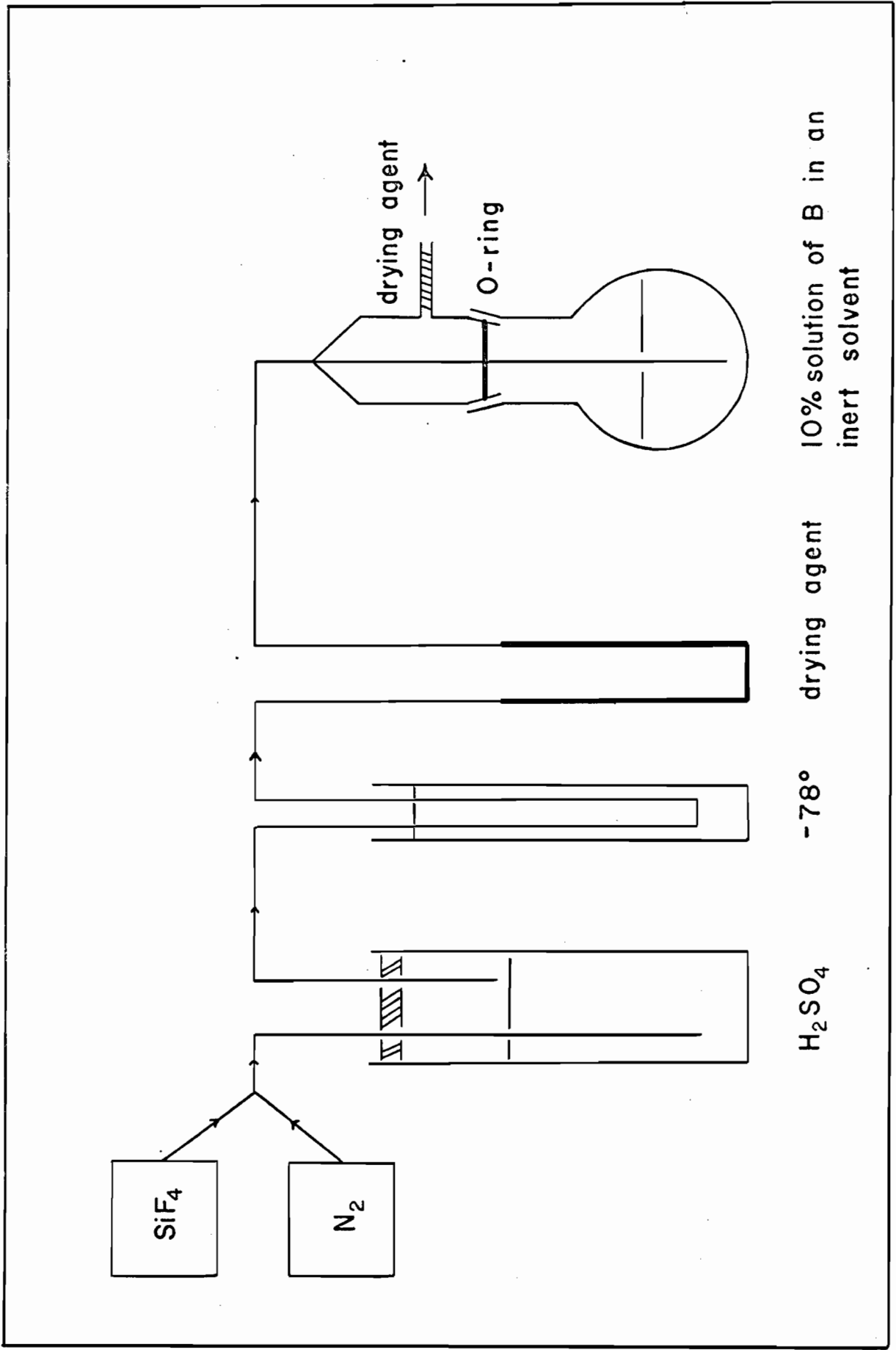
The methods described in (i) and (ii) were applicable in all cases; but if we knew from previous data that a certain complex would be a stable involatile solid at 25°, then easier methods of preparation could be used. Using a "bubbling train" (Fig. 3) dry nitrogen was passed through a 10% solution of B (p. 18) in a volatile inert solvent (b.p. < 100°). After thorough flushing of the apparatus, SiF₄ was bubbled through the solution until complex formation had ceased. The solvent was then evaporated from the solid complex and the complex was washed several times with pure dry solvent to remove any unreacted B and finally, dried by suction or in a vacuum. This method had the following advantages over methods (i) and (ii): (a) no vacuum system was needed, (b) faster preparation, (c) larger quantities of complex per experiment could be prepared, (d) smaller complex particle size, and (e) the dispersion effect of the solvent resulted in purer product, especially when the Lewis base was sensitive to thermal decomposition. A second method involved the use of the vacuum system but quantities of SiF₄ and B need not have been measured exactly. SiF₄ was condensed over a solution of B in an inert solvent at -195°. The mixture was slowly warmed and stirred magnetically as soon as it liquified. The dry solid complex was isolated using the same method described in the bubbling technique.

(iv) Proton Nuclear Magnetic Resonance

Proton magnetic resonance measurements were made only on the SiF₄-CH₃OH system. Spectra were recorded on a high-resolution Varian spectrometer (HR 60) with a fixed frequency of 60 Mc. Pure benzene

FIG. 3

The bubbling "train" for the preparation of stable
involatile solid complexes at 25°



SiF_4

N_2

H_2SO_4

-78°

drying agent

O-ring

10% solution of B in an inert solvent

contained in a sealed capillary was used as the external standard ($\tau = 2.734$ p.p.m.). It was placed in a pyrex tube, 17 cm long and 5 mm outside diameter, into which solutions of known mole ratio of SiF_4 to CH_3OH were condensed. Solutions with mole ratios, $\text{SiF}_4/\text{CH}_3\text{OH}$, greater than 0.4 were not prepared because the sealed glass tubes might have exploded due to internal pressures in the tens of atmospheres. The sample tube was sealed off in a vacuum at a constriction. The side band technique was used to obtain the τ -values for the OH and CH_3 peaks. The distance from the reference peak to the side band was 1τ (60 c.p.s.), from which the mm- τ equivalence was calculated.

(v) Dissociation Pressures

Heats of dissociation were only measured for the SiF_4 -aliphatic cyclic ethers and SiF_4 -dimethyl ether systems. Dissociation pressures of the nitrogen electron donor complexes with SiF_4 were too small to be measured accurately with the available apparatus.

Solid $\text{SiF}_4 \cdot 2(\text{ether})$ complexes were prepared at low temperatures as described in section 3(i) using the necessary precautions described in the Results section, and their temperature was increased slowly until a pressure of about 0.5 mm was observed. Thereafter, pressure measurements were made at intervals of about 5 or 10°. To be certain that an equilibrium existed at each temperature, a sample of the gas above the solid complex was pumped off and a constant pressure was re-established. True equilibrium existed at a given temperature if the pressure before and after the pumping off procedure were identical. Pressure-temperature measurements were made until the complex decomposed irreversibly, as

evident by an abnormally large pressure increase and failure to observe identical pressures before and after the pumping off operation. Equilibrium pressures were approached from above as well as from below a given temperature to be sure that these were identical indicating a reversible dissociation. Values of heat of dissociation were calculated from the slopes of the linear $\log p_{\text{mm}}$ against T^{-1} plots using the integrated form of the Clausius-Clapeyron equation, $\Delta H^\circ = - \frac{2.303 R \log \Delta p}{\Delta (T^{-1})}$, where $R = 1.987 \text{ cal deg}^{-1} \text{ mole}^{-1}$ and ΔH° is given in cal mole^{-1} .

The method gave $\Delta H_{\text{dissc.}}^\circ$ to an estimated accuracy of $\pm 0.3 \text{ kcal mole}^{-1}$. This was based on the following possible experimental errors,

temperature T ($^\circ\text{C}$) , ± 0.2

pressure P (mm) , ± 0.1

and recalculating $\Delta H_{\text{dissc.}}^\circ$ using pressure-temperature errors at the two points, $p = 20 \text{ mm}$ and $p = 2 \text{ mm}$, to produce a maximum and a minimum $\Delta H_{\text{dissc.}}^\circ$. The actual error was probably no worse than half the maximum possible error due to the averaging process. The human error in reading the slope from the straight line was less than $\pm 0.05 \text{ kcal mole}^{-1}$, as five different co-workers read the slope within this accuracy.

(vi) Conductivity

Conductivity measurements were made using a conductivity bridge (Industrial Instruments Model RC 16 B2) and a cell having a cell constant of 0.01. The instrument had a conductivity range of 4×10^{-9} to $5 \times 10^{-2} \text{ mho cm}^{-1}$. Transfers of solutions and measurements were made in a nitrogen-

filled dry box to avoid hydrolysis by atmospheric moisture. A sample with the highest concentration of complex in solution was transferred to the conductivity cell and its conductivity was measured. Solutions of lower concentration were prepared by successive dilutions with the solvent and their conductivity was measured. Plots of molar conductance against (concentration)^{1/2} were obtained. The molar conductances were calculated using the equation, $\mu = \frac{10^3 k}{c}$

where $k =$ specific conductance, mho cm^{-1}

$c =$ concentration, mole l^{-1}

$\mu =$ molar conductance, mho $\text{cm}^2 (\text{g-mole})^{-1} \text{l}^{-1}$

and $k = (\text{cell constant}) \times (\text{conductivity reading})$. In the case of a weak electrolyte (as $\text{SiF}_4 \cdot 4\text{CH}_3\text{OH}$ in methanol), an empirical method (34) was used to obtain an estimate of the molar conductance at infinite dilution (μ_0), the equilibrium constant for dissociation (K), and the degree of dissociation (α_c) at a given concentration. A plot of μ^{-1} against $c^{1/2}$ (for $0 < c^{1/2} < 0.1$), a straight line having the equation $\mu^{-1} = A + bc^{1/2}$ where A is the μ^{-1} intercept and b is the slope, was extrapolated to $c^{1/2} = 0$. This apparently gave $A = \mu_0^{-1}$ but in fact these μ_0 values are higher than accepted values by a factor of $3/2$, thus $\mu_0 (\text{true}) = 2/3 A$. The equilibrium constant was given by $K = (\mu_0 b)^{-2}$ and the degree of dissociation by $\alpha_c = \mu_c \mu_0^{-1}$. In the case of a strong electrolyte, as $(\text{C}_5\text{H}_5\text{NH})_2\text{SiF}_6$ in nitromethane, extrapolation of the linear μ against $c^{1/2}$ plot (for $0 < c^{1/2} < 0.05$) to $c^{1/2} = 0$ gave μ_0 directly. In this case, $K \rightarrow \infty$ and $\alpha \rightarrow 1$ for a dilute solution.

(vii) Cryoscopic Molecular Weight Determination

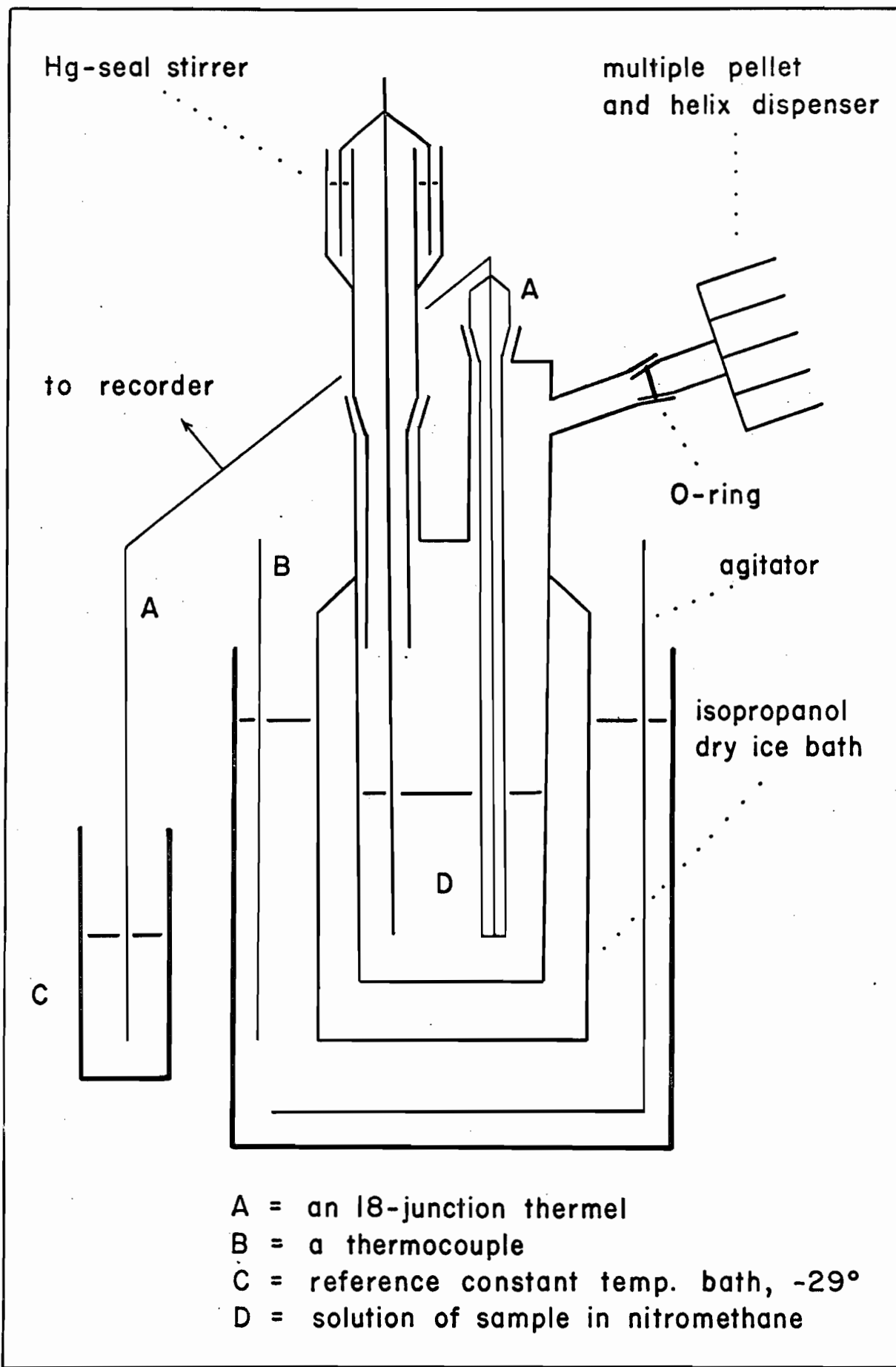
A simple freezing point depression apparatus was designed for the molecular weight determination of $\text{SiF}_4 \cdot 2\text{C}_5\text{H}_5\text{N}$ in nitromethane. The method could be applied for any hygroscopic compound in a solution with a freezing point below 25° . A novel method of seeding the solution was perfected.

Instead of using a Beckmann thermometer, it was found more convenient to use a multi-junction thermocouple assembly consisting of an 18-junction thermel (35) connected to a Honeywell recorder Model Y143X18 (maximum sensitivity, $1 \mu\text{V}$) for the measurement of temperature changes greater than 0.01° . The fused thermocouple ends (No. 30 gauge, Cu-Constantan) were cleaned with concentrated aqueous KCN (to remove oxides), washed, dried, and insulated with red glyptol varnish (No. 90, G C Electronics Co., L.A., Calif.). Their total resistance was checked before and after insertion of each 18-junction end into 30 cm long ground glass cones with stems. One end of the thermel was kept at -29° using a constant temperature slush bath of nitromethane and the other in the sample solution. The temperature of the sample solution was controlled adequately with an external isopropyl alcohol bath, the temperature of which was controlled by the periodic addition of dry ice chips. The apparatus was kept moisture-free by using a mercury-seal spiral-blade glass stirrer and a multiple sample (pellet) dispenser fitted with a "dry tube" and a container of glass helices (column packing type), as shown in Fig. 4.

In a typical experiment, the freezing point of the pure solvent (~ 50 ml) was determined initially. The proper cooling rate was achieved

FIG. 4

Cryoscopic molecular weight apparatus



by maintaining the outer bath at 5° below the freezing point of the pure solvent. Vigorous stirring was essential. When it was judged that the temperature of the solvent was below its freezing point a precooled helix (by liquid air) was dropped into it to minimize the supercooling. If the solvent did not freeze, then the seeding was repeated. Fig. 5 shows a typical cooling curve recorded on chart paper. The temperature "plateau" was taken as the freezing point of the pure solvent. The solvent was allowed to warm up to 25° and a weighed pellet of sample (~50 mg) was dissolved into it. The freezing point of the resultant solution was determined as described for the pure solvent making sure that the seeding gave about the same degree of supercooling as with the pure solvent (not greater than 0.2° below the freezing point). Further additions of sample to the solution with subsequent freezing point determinations were done until the solution became saturated. A plot of the voltage reading (v) (freezing point) against the weight of sample (w) was obtained. The molecular weight was found from the slope of this plot using the equation, $M = K_f \left| \frac{\Delta w}{\Delta v} \right|$, where $\left| \frac{\Delta v}{\Delta w} \right|$ = absolute value of the slope

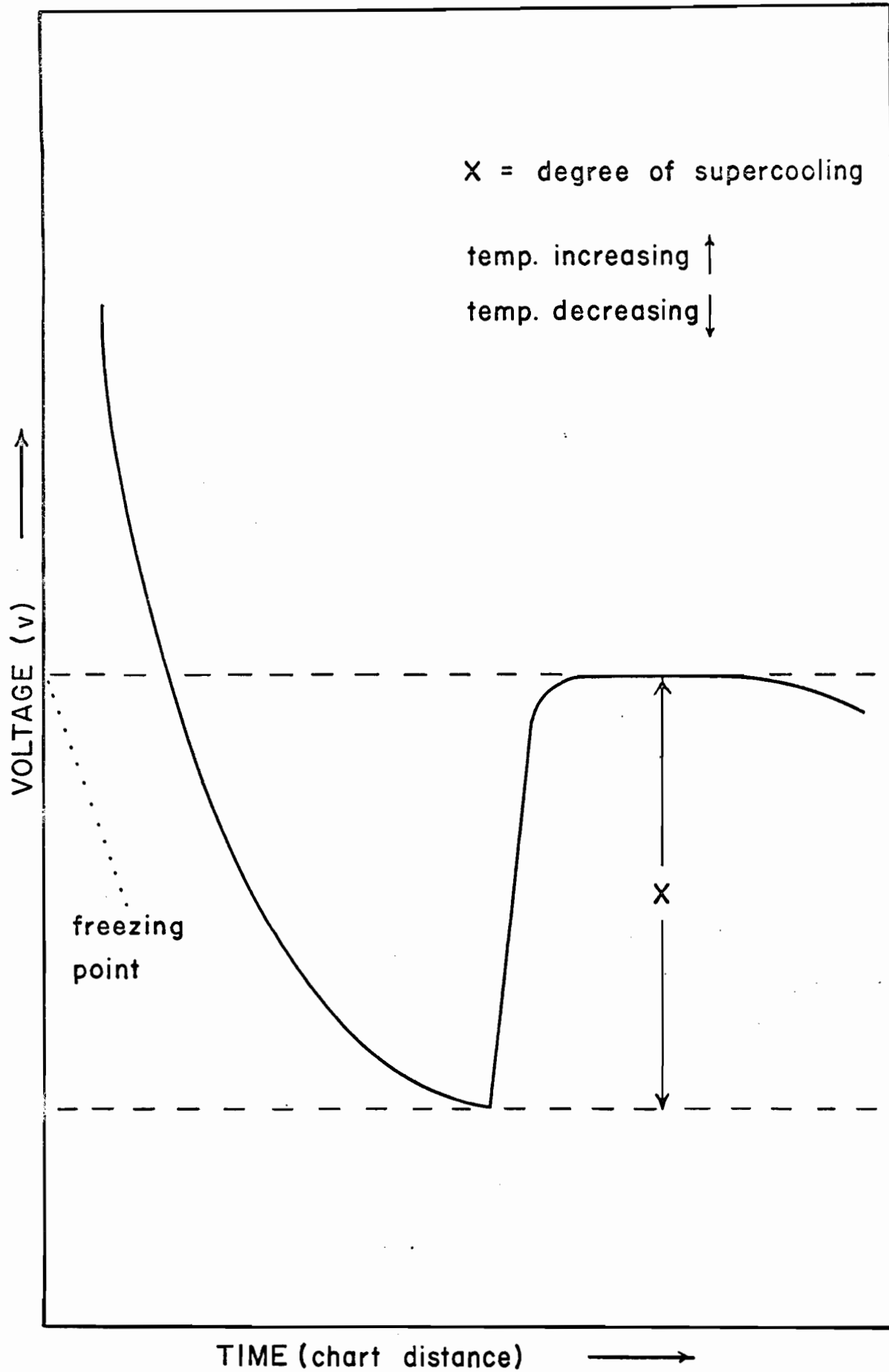
M = apparent molecular weight

K_f = relative freezing point constant
for the solvent.

K_f was determined from a v. against w. plot for a sample of known M (a calibration). In this work naphthalene (M = 128.2) and anthracene (M = 178.2) were used in the calibration. The method gave molecular weights to an accuracy of about 10%. The main source of error was probably due to the difficulty in keeping the reference slush bath at an absolutely constant temperature. This difficulty was minimized or overcome by making

FIG. 5

A typical cryoscopic cooling curve



the slush bath perfectly homogeneous. More recently, all-glass low-temperature range thermistors connected through a thermometric bridge (E.H. Sargent and Co.) have been obtained. These will eliminate the need for a constant temperature reference bath.

The main advantages of the "helix seeding" method are (a) the system need never be exposed to moist air, (b) freezing occurs almost instantly on seeding, thus obtaining better control on the degree of supercooling, (c) the negligible thermal and chemical effect of the helices on the system, and (d) its ease of operation.

4. Analyses

(i) Fluorine

All stable solid complexes prepared were analyzed for fluorine using the gravimetric method of Belcher and Tatlow (36).

Sufficient sample was dissolved in a minimum amount of water containing 5-10 pellets of KOH to yield 30 to 60 mg of fluorine. With 20 mg of fluorine the results are about 0.5% lower than theoretical, and with 10 mg about 1% lower. There was no need to remove the liberated Lewis base since it did not interfere with the analysis. Gentle heating was used to facilitate solution of the sample. After cooling the solution, 8 drops of a 0.1% solution of methyl red were added, and 5N HNO₃ was slowly added until the indicator just turned pink. After adding 0.5 ml of 30% acetic acid solution, the solution was heated to 60-70°. Meanwhile, 200 ml of a filtered saturated PbCl₂ solution containing 0.5 ml of 30% acetic acid solution were heated nearly to a boil. The hot PbCl₂ solut-

ion was added to the warm sample solution and the mixture was left to digest overnight. If the addition had been reversed (as it was according to Belcher and Tatlow) it would have been necessary to wash the sample beaker. The next day the precipitate obtained was filtered through a weighed No. 4 sintered glass crucible. The beaker was washed twice with 15 ml portions of filtered saturated PbCl_2 solution in order to remove all the precipitate, then washed with a jet from a wash bottle containing filtered saturated PbCl_2 solution, and finally the precipitate was washed twice with 15 ml portions of filtered saturated PbClF solution and twice with 15 ml portions of dry acetone. The crucible was dried by suction, wiped off, and dried in an oven at 120° for one hour. After cooling in a desiccator for 30 minutes, the crucible with its precipitate was weighed, the reading always being taken after 30 seconds on the balance pan. This gave the weight of PbClF precipitated. The %F was calculated by the following method:

$$\%F = \frac{\text{weight of F in the sample}}{\text{weight of sample}},$$

where the weight of F in the sample = (weight of precipitate) X (% of F in PbClF)

$$\text{and the \%F in PbClF} = \frac{(\text{at. w. F}) (100)}{(\text{at. w. PbClF})} = \frac{(19.0) (100)}{261.6} = 7.263\%.$$

Finally,

$$\%F = \frac{(\text{weight of precipitate}) X (0.07263)}{\text{weight of sample}}.$$

The method usually gave the %F with an accuracy of better than 0.2% for absolute values in the range $25\% < \%F < 50\%$.

(ii) Ultraviolet (displacement reaction)

The quantitative amount of pyridine displaced by ethylenediamine from the complex, $\text{SiF}_4 \cdot 2\text{C}_5\text{H}_5\text{N}$, was measured using a Perkin-Elmer Model 350 ultraviolet spectrophotometer. After the interaction of $\text{SiF}_4 \cdot 2\text{C}_5\text{H}_5\text{N}$ with $\text{NH}_2(\text{CH}_2)_2\text{NH}_2$, the volatile material was condensed into a small tube of known weight and the weight of liquid was obtained. A portion of this liquid was dissolved in absolute ethanol to produce a very dilute solution ($\sim 1 \times 10^{-4} \text{ g.l}^{-1}$) and its ultraviolet spectrum was obtained. Similarly, the ultraviolet spectrum of a standard $\text{C}_5\text{H}_5\text{N}$ solution in absolute alcohol was obtained as well as that of a standard $\text{NH}_2(\text{CH}_2)_2\text{NH}_2$ solution. There was no interference in the absorbances of $\text{C}_5\text{H}_5\text{N}$ and $\text{NH}_2(\text{CH}_2)_2\text{NH}_2$ occurring at 256 and 220 μ , respectively. The 256 μ absorbance was used for the calculations. The magnitudes (peak heights) of the sample and standard solution absorbance were measured. From these measurements, the concentration of $\text{C}_5\text{H}_5\text{N}$ in the sample solution was calculated using Beer's equation (assumed to be valid in the dilute concentration range),

$$A = \epsilon c l$$

where A = absorbance

ϵ = molecular extinction coefficient

c = concentration (g.l^{-1})

l = cell path length

For the standard $\text{C}_5\text{H}_5\text{N}$ solution

$$A_1 = \epsilon_{\text{py}} c_1 l$$

py = pyridine

For the sample solution

$$A_2 = \epsilon_{\text{py}} c_2 l$$

Dividing one equation by the other

$$\frac{A_1}{A_2} = \frac{c_1}{c_2} \quad \text{where only } c_2 \text{ is unknown.}$$

The percent C_5H_5N in the sample (and therefore in the liquid product) was given by $\frac{c_2}{\text{sample concentration}} \times 100$, from which the total amount of C_5H_5N displaced was calculated.

RESULTS

The experimental results are conveniently grouped under the following main headings:

- I. The interaction of SiF_4 with methanol.
- II. Coordination of SiF_4 with aliphatic cyclic ethers and dimethyl ether.
- III. Coordination of SiF_4 with pyridine and other nitrogen electron-pair donor molecules.
- IV. Attempted preparation of SiF_4 complexes with hydrogen sulfide, dimethyl sulfide, phosphine and nitromethane.

I. The Interaction of SiF_4 with Methanol

(i) Preparation of $\text{SiF}_4 \cdot 4\text{CH}_3\text{OH}$

In a typical experiment, SiF_4 (10.48 mmole) was combined with CH_3OH (8.44 mmole) and the mixture was kept at 25° for 30 minutes. Unreacted SiF_4 (8.32 mmole) was recovered by distillation at -65° , and a colorless solid remained. These results show that SiF_4 and CH_3OH had combined in a mole ratio of 1:3.91, producing the complex, $\text{SiF}_4 \cdot 4\text{CH}_3\text{OH}$. The 1:4 mole ratio was not always reproducible, and values in the range 1:3.75 to 1:4.20 were also obtained. The complex was a liquid at 25° and froze to a colorless solid at about -20° .

(ii) Tensimetric Titration

A tensimetric titration of SiF_4 (5.43 mmole) with CH_3OH (Fig. 6, Table 3) confirmed the formation of only a 1:4 complex. After each addition of CH_3OH to SiF_4 in this titration, the mixture was warmed to 25° and then cooled to -78° , at which temperature pressure measurements were made. As shown in Fig. 6, the pressure decreased linearly and approached zero after the mole ratio, $\text{CH}_3\text{OH}/\text{SiF}_4$, became greater than 4. Extrapolation of the linear portion to zero pressure indicated a mole ratio of 4.23 (corresponding to the addition of 23.0 mmole of CH_3OH), confirming the formation of only $\text{SiF}_4 \cdot 4\text{CH}_3\text{OH}$.

In the reverse titration of CH_3OH (44.00 mmole) with SiF_4 (Fig. 7, Table 3) the pressure remained zero until the mole ratio, $\text{CH}_3\text{OH}/\text{SiF}_4$, decreased to 4.68 (i.e., until the addition of 9.40 mmole SiF_4), when the pressure increased rapidly as the mole ratio decreased further.

TABLE 3

Tensimetric titration of SiF_4 with CH_3OH
and CH_3OH with SiF_4

SiF_4 with CH_3OH (Fig. 6)		CH_3OH with SiF_4 (Fig. 7)	
SiF_4 present initially, 5.43 mmole		CH_3OH present initially, 44.00 mmole	
$T_r, 25^\circ; T_p, -78^\circ$		$T_r, 25^\circ; T_p, -78^\circ$	
Total CH_3OH added mmole	Pressure mm	Total SiF_4 added mmole	Pressure mm
0	290.7	0	0
2.88	266.8	4.56	0
5.20	227.0	7.59	0
8.05	195.5	9.07	0
9.65	176.0	10.11	26.0
12.36	132.3	11.37	48.2
14.84	101.6	15.06	135.0
16.83	81.5	18.00	200.0
18.99	55.4	19.84	242.5
21.15	27.6	23.24	322.0
23.37	6.1	25.36	374.5
26.17	0.5		
30.00	0		
31.80	0		

FIG. 6

The tensimetric titration of SiF_4 with CH_3OH

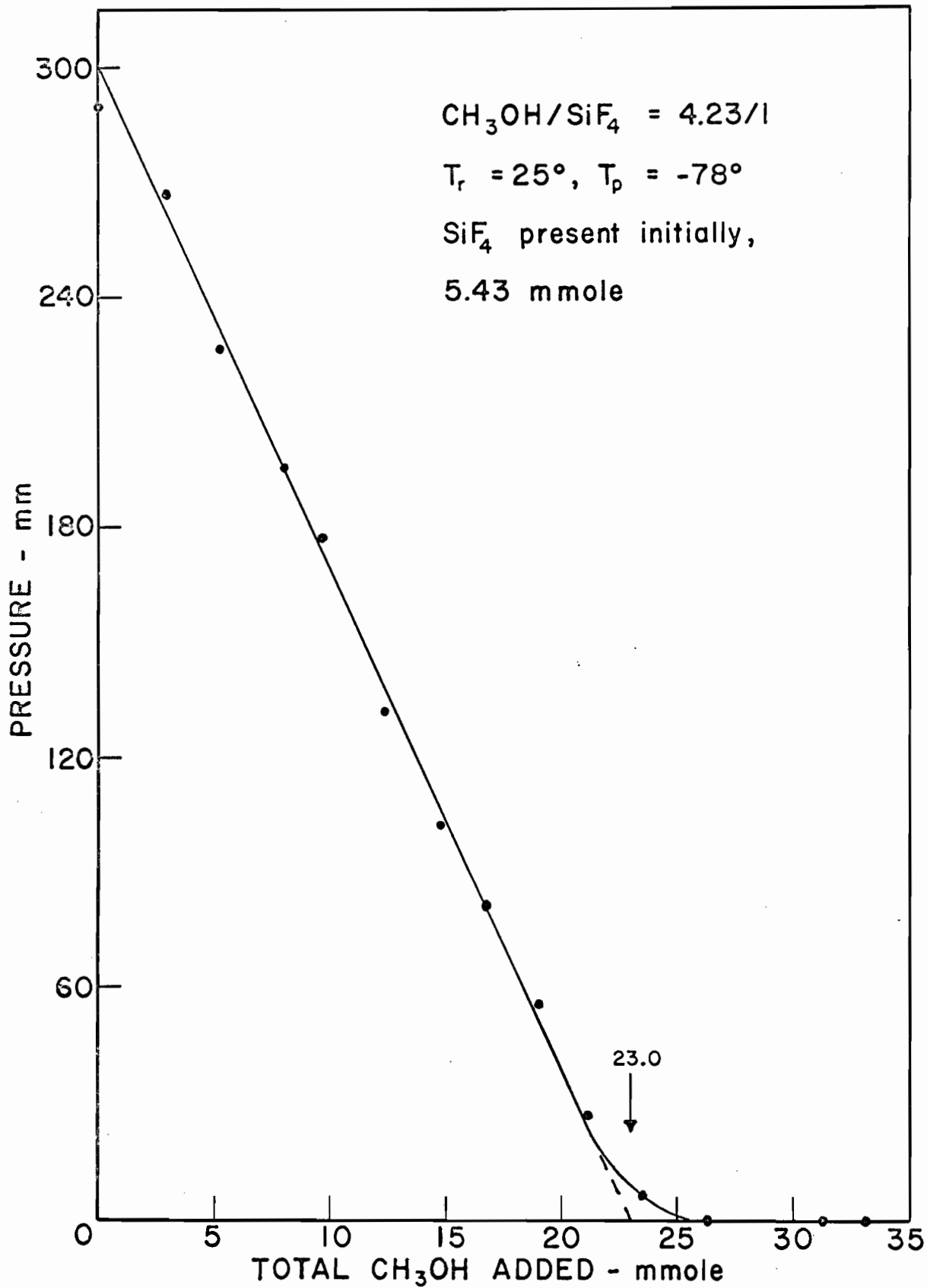
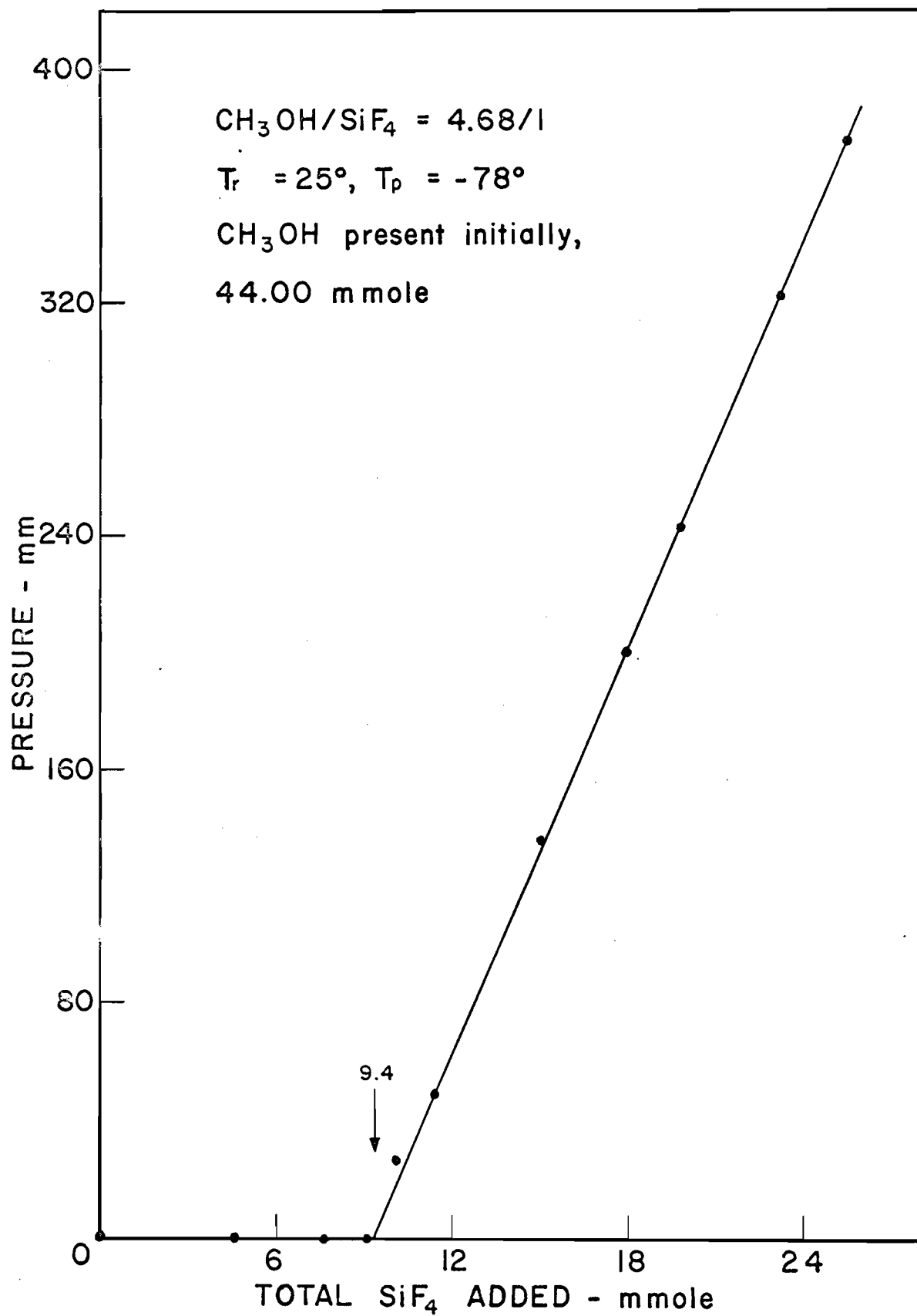


FIG. 7

The tensimetric titration of CH_3OH with SiF_4



(iii) Conductivity of $\text{SiF}_4 \cdot 4\text{CH}_3\text{OH}$

The results and comparisons of the molar conductance of $\text{SiF}_4 \cdot 4\text{CH}_3\text{OH}$, acetic acid (38) and sodium chloride (39) in methanol (Fig. 8, Tables 4, 5) at 25° revealed that $\text{SiF}_4 \cdot 4\text{CH}_3\text{OH}$ was a very weak electrolyte in methanol, with a molar conductance at infinite dilution of $833 \text{ mho cm}^2 (\text{g-mole})^{-1} \text{ l}^{-1}$, an equilibrium constant for dissociation of $2.73 \times 10^{-5} \text{ mole l}^{-1}$, and a degree of dissociation of 4.6% for a solution of 0.01 mole l^{-1} concentration. Table 4 and Fig. 9 were used to obtain the above quantitative data according to the method of Levitt (34). Fig. 10 shows the deviation from a straight line at high concentration ($c^{1/2} > 0.1 \text{ mole}^{1/2} \text{ l}^{-1/2}$) of the plot of the reciprocal molar conductance against the square root of the concentration (μ^{-1} vs $c^{1/2}$).

TABLE 4

Conductivities of $\text{SiF}_4 \cdot 4\text{CH}_3\text{OH}$ in methanol

$\text{SiF}_4 \cdot 4\text{CH}_3\text{OH}$ concentration c , mole l^{-1}	Specific conductance k , mho cm^{-1}	Molar conductance μ , $\text{mho cm}^2 (\text{g-mole})^{-1} \text{l}^{-1}$	$c^{1/2} \times 10^2$ $\text{mole}^{1/2} \text{l}^{-1/2}$	μ^{-1} $\text{ohm cm}^{-2} (\text{g-mole})\text{l}$
3.75	3.0×10^{-3}	0.80	194	1.250
1.87	3.0×10^{-3}	1.60	137	0.625
0.47	1.0×10^{-3}	2.13	68.5	0.470
0.0094	4.0×10^{-4}	42.7	9.7	0.023
0.00090	1.2×10^{-4}	133	3.0	0.0075
0.00019	4.7×10^{-5}	250	1.4	0.0040
0*	5.0×10^{-6}	-	-	

* pure CH_3OH (lit. (54) value: $5 \times 10^{-8} \text{ mho cm}^{-1}$).

TABLE 5

Conductivities of CH₃COOH and NaCl in methanol

CH ₃ COOH in methanol (38) at 25°			NaCl in methanol (34) at 25°		
Concentration c X 10 ⁴ mole l ⁻¹	Molar conductance μ, mho cm ² (g- mole) ⁻¹ l ⁻¹	c ^{1/2} X 10 ² mole ^{1/2} l ^{-1/2}	Concentration c X 10 ⁴ equiv l ⁻¹	Equivalent conductance Λ, mho cm ² (g- equiv) ⁻¹ l ⁻¹	c ^{1/2} X 10 ² equiv ^{1/2} l ^{-1/2}
16.61	89.1	4.07	2N	94.11	1.41
41.62	52.2	6.45	5N	92.09	2.24
74.42	37.6	8.62	10N	89.87	3.16
104.45	31.4	10.75	20N	86.91	4.47
196.56	22.2	14.0	30N	84.84	5.48
345.98	16.9	18.6	50N	81.80	7.08
464.53	14.0	21.6	70N	79.43	8.38
561.81	12.7	23.7	100N	76.71	10.00
μ ₀ = 185.5, K = 2.37 X 10 ⁻¹⁰ mole l ⁻¹			Λ ₀ = 97.61		

FIG. 8

Comparison of the molar conductances of $\text{SiF}_4 \cdot 4\text{CH}_3\text{OH}$,
NaCl, and CH_3COOH in methanol

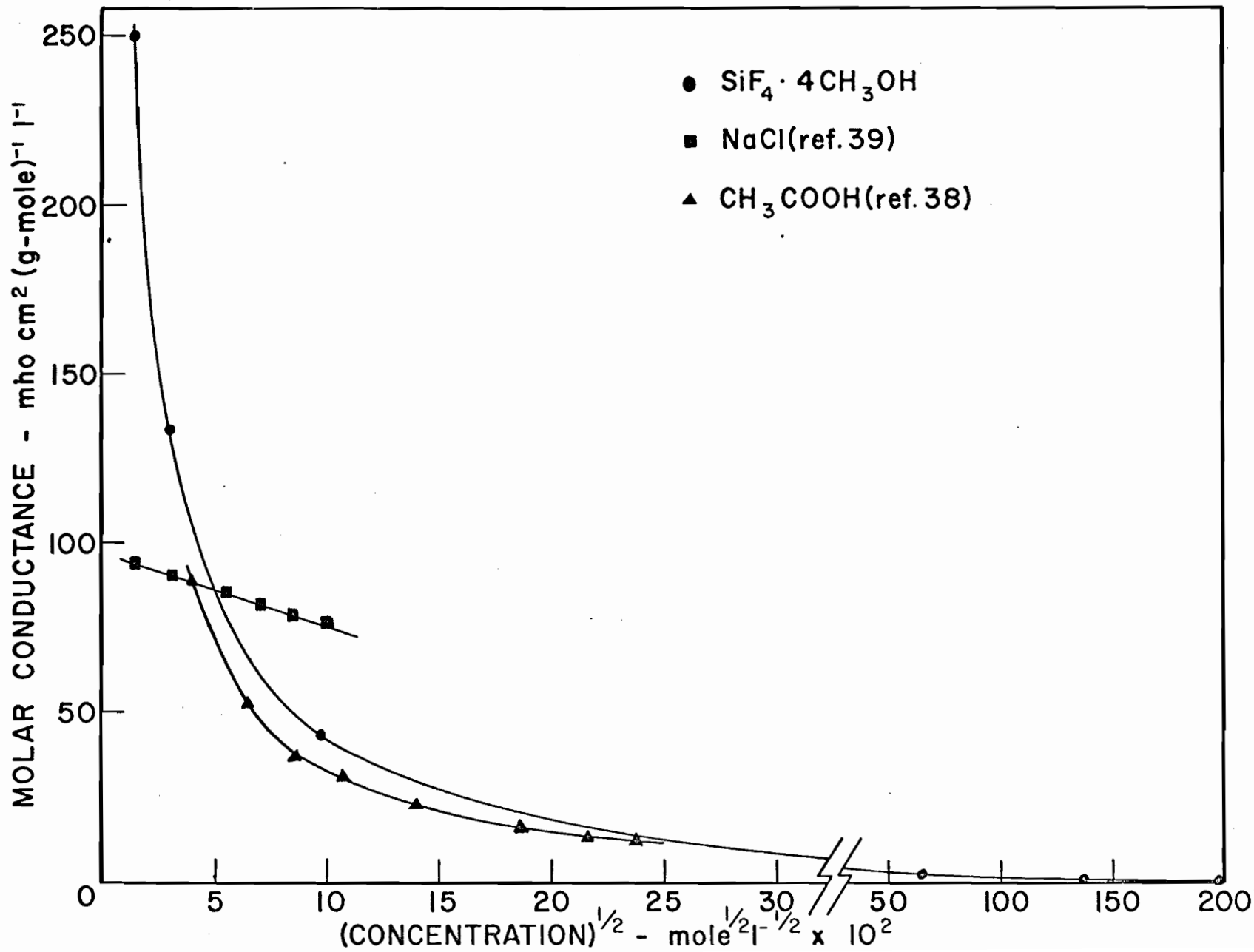


FIG. 9

Plot used in the empirical determination of μ_0 , K , and $\alpha_{0.01}$
for $\text{SiF}_4 \cdot 4\text{CH}_3\text{OH}$ in methanol

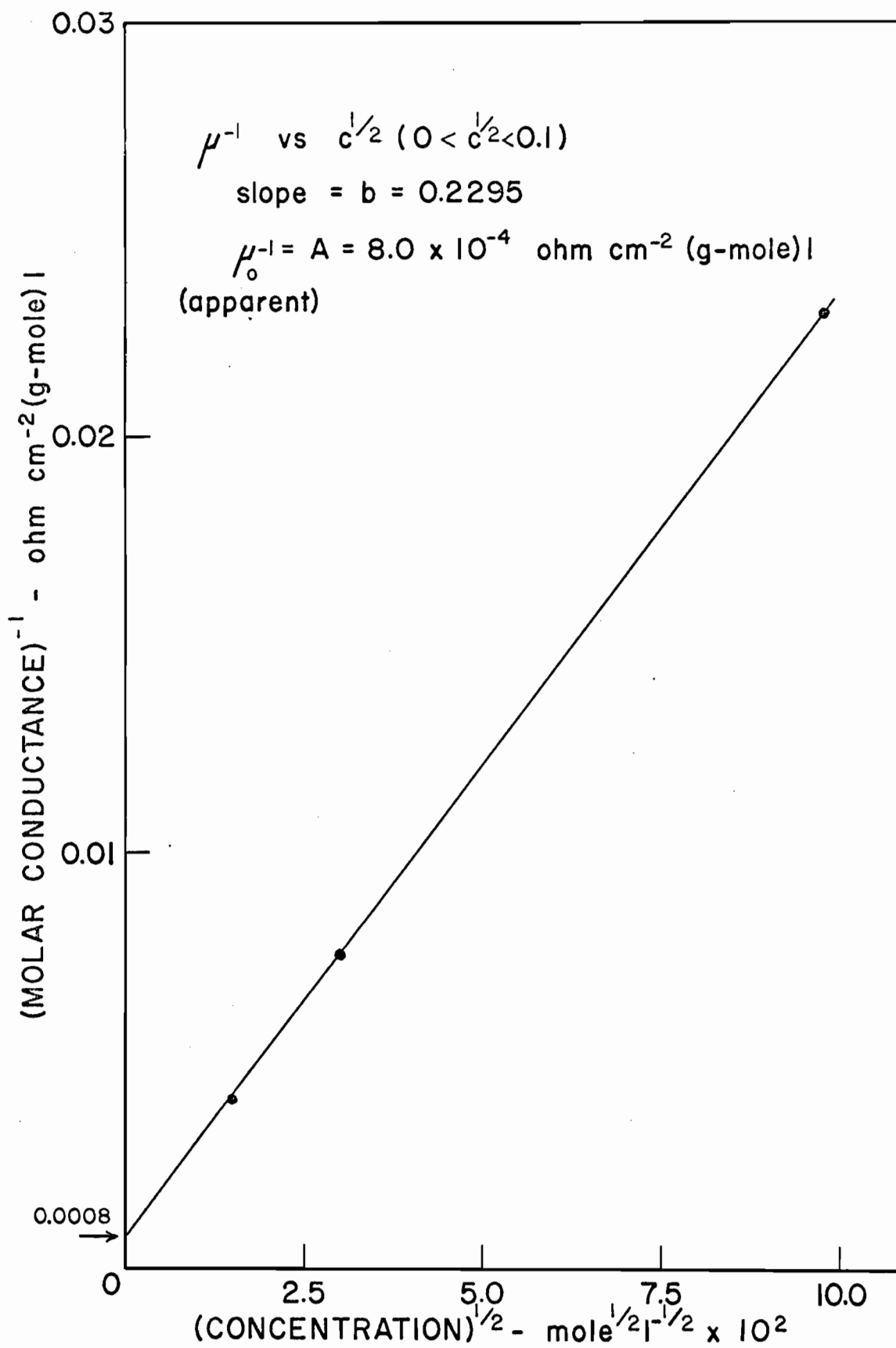
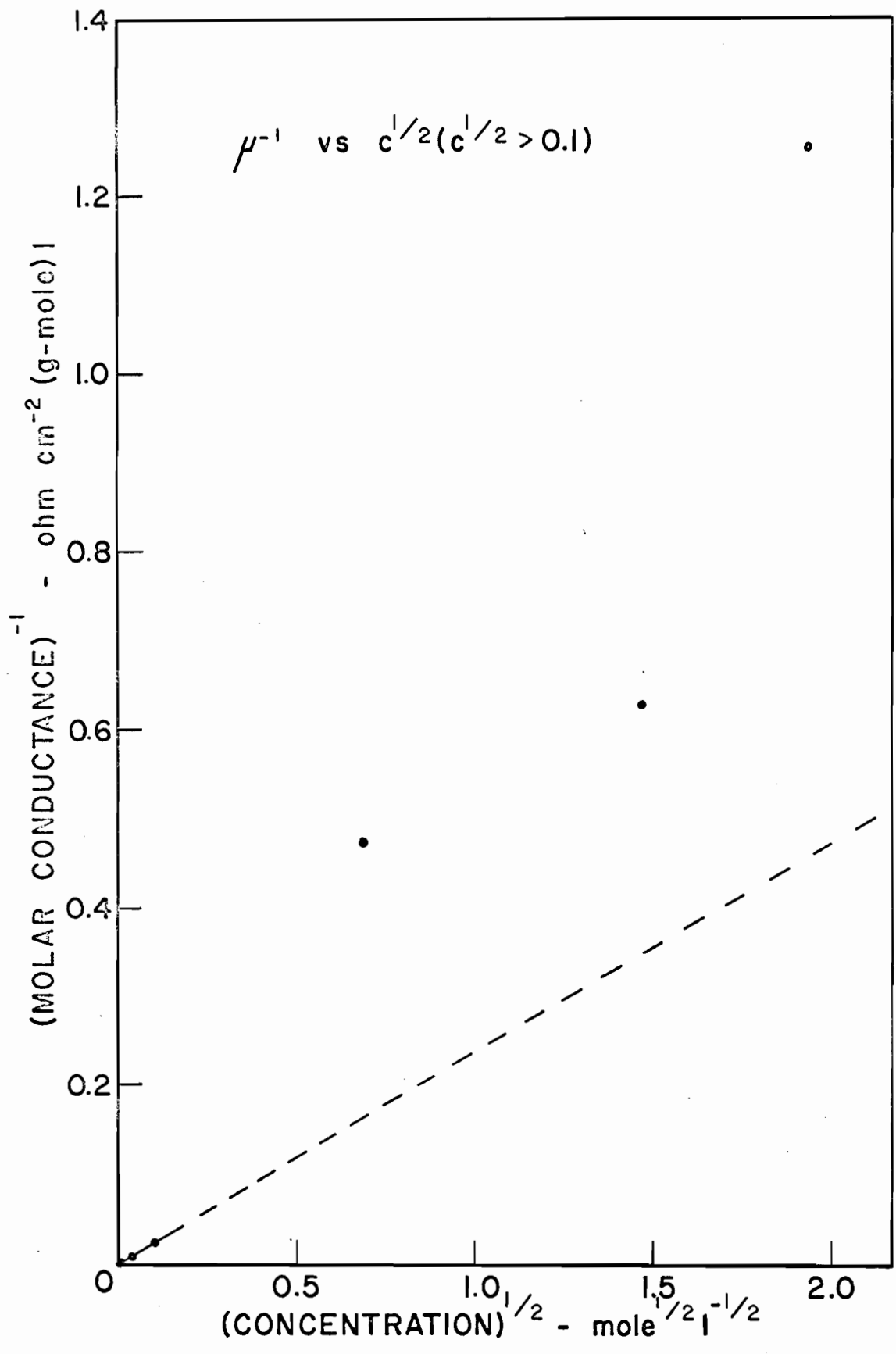


FIG. 10

Deviation of $\mu^{-1} = A + bc^{1/2}$ at higher concentrations
for $\text{SiF}_4 \cdot 4\text{CH}_3\text{OH}$ in methanol



(iv) Infrared Spectrum of $\text{SiF}_4 \cdot 4\text{CH}_3\text{OH}$

Fig. 11 shows the infrared spectrum of liquid $\text{SiF}_4 \cdot 4\text{CH}_3\text{OH}$ and its gaseous products with assignments of absorption frequencies given in Table 6. The indications are that $\text{SiF}_4 \cdot 4\text{CH}_3\text{OH}$ is completely dissociated in the gas phase but not in the liquid phase at 25°.

TABLE 6

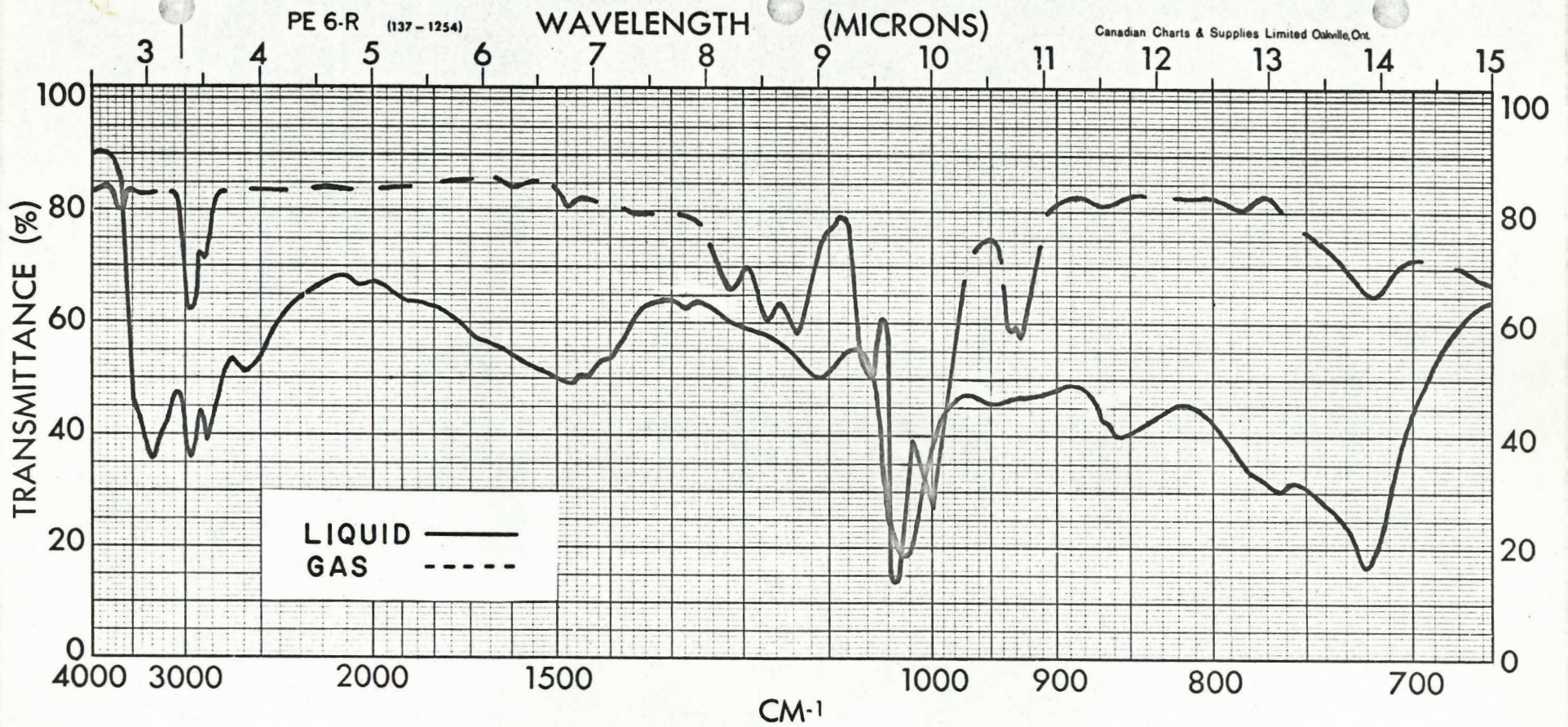
Comparison and assignment of infrared absorption frequencies (cm^{-1})

$\text{SiF}_4 \cdot 4\text{CH}_3\text{OH}$		CH_3OH		SiF_4	Assignment
Gas	Liquid	Gas	Liquid	Gas	
3680w		3680w			$\nu(\text{O-H})$, free
	3300s		3340s		$\nu(\text{O-H})$, H-bonded
2970m	2950s	2950s	2950s		$\nu(\text{C-H})$, antisym.
2870m	2830s	2860m	2840m		$\nu(\text{C-H})$, sym.
	2600m		2500w		combination
1480w	1450m	1450m	1460m		$\delta(\text{CH}_3)$, antisym.
1220m					due to $(\text{CH}_3)_2\text{O}$ impurity
1170m					"
1140m	1110m	1120w	1120m		$\delta(\text{CH}_3)$, sym.
1060m		1050m			[$\nu(\text{Si-F})$ tetrahedral and $\nu(\text{C-O})$, "RQP" for gas phase
1030s	1025s	1030s	1030s	1035vs	
1000s		1010s		1032vs	
930m	950vw				$(\text{CH}_3)_2\text{O}$ impurity
865vw	855m	860w			due to CH_3OH
		835w			"
782w	762m				unidentified
718w	720s				$\nu(\text{Si-F})$ octahedral for SiF_6^{-2}

Note: w = weak, m = medium, s = strong, v = very

FIG. 11

The infrared spectrum of liquid $\text{SiF}_4 \cdot 4\text{CH}_3\text{OH}$ and
its gaseous products



(v) Proton Magnetic Resonance Measurements

Fig. 12 shows the n.m.r. spectrum of a sample of SiF_4 in CH_3OH and also that of pure CH_3OH . Figs. 13 and 14 (Table 7) show the plots of chemical shift (τ) against mole ratio, $\text{SiF}_4/\text{CH}_3\text{OH}$, for the OH and CH_3 peaks, respectively. In Fig. 13 there was an initial linear and rapid decrease in τ -value of the OH peak as the amount of SiF_4 was increased. The slope of this line changed markedly near a mole ratio of 0.2 and finally became constant and less than initially. In Fig. 14 the τ -values of the CH_3 peak decreased gradually and finally levelled off as the concentration of SiF_4 increased. In this case the absolute change was much less.

TABLE 7

The variation of the chemical shift with concentration
for $\text{SiF}_4 \cdot 4\text{CH}_3\text{OH}$ in methanol

Sample concentration, mole ratio $\text{SiF}_4/\text{CH}_3\text{OH}$	Chemical shift (τ) p.p.m.	
	OH peak	CH_3 peak
0	4.712	6.229
0.0202	4.334	6.024
0.0405	4.046	6.128
0.0497	3.863	5.958
0.0670	3.772	6.040
0.0960	3.289	5.793
0.1252	2.766	5.959
0.1435	2.749	5.979
0.2000	2.220	5.849
0.2480	1.703	5.874
0.2620	1.696	5.774
0.2800	1.608	5.782
0.3300	1.424	5.764
0.4010	1.163	5.839

Note: The external standard was benzene ($\tau = 2.734$ p.p.m.).

FIG. 12

The chemical shift of pure CH_3OH and CH_3OH
hydrogen bonded to SiF_4

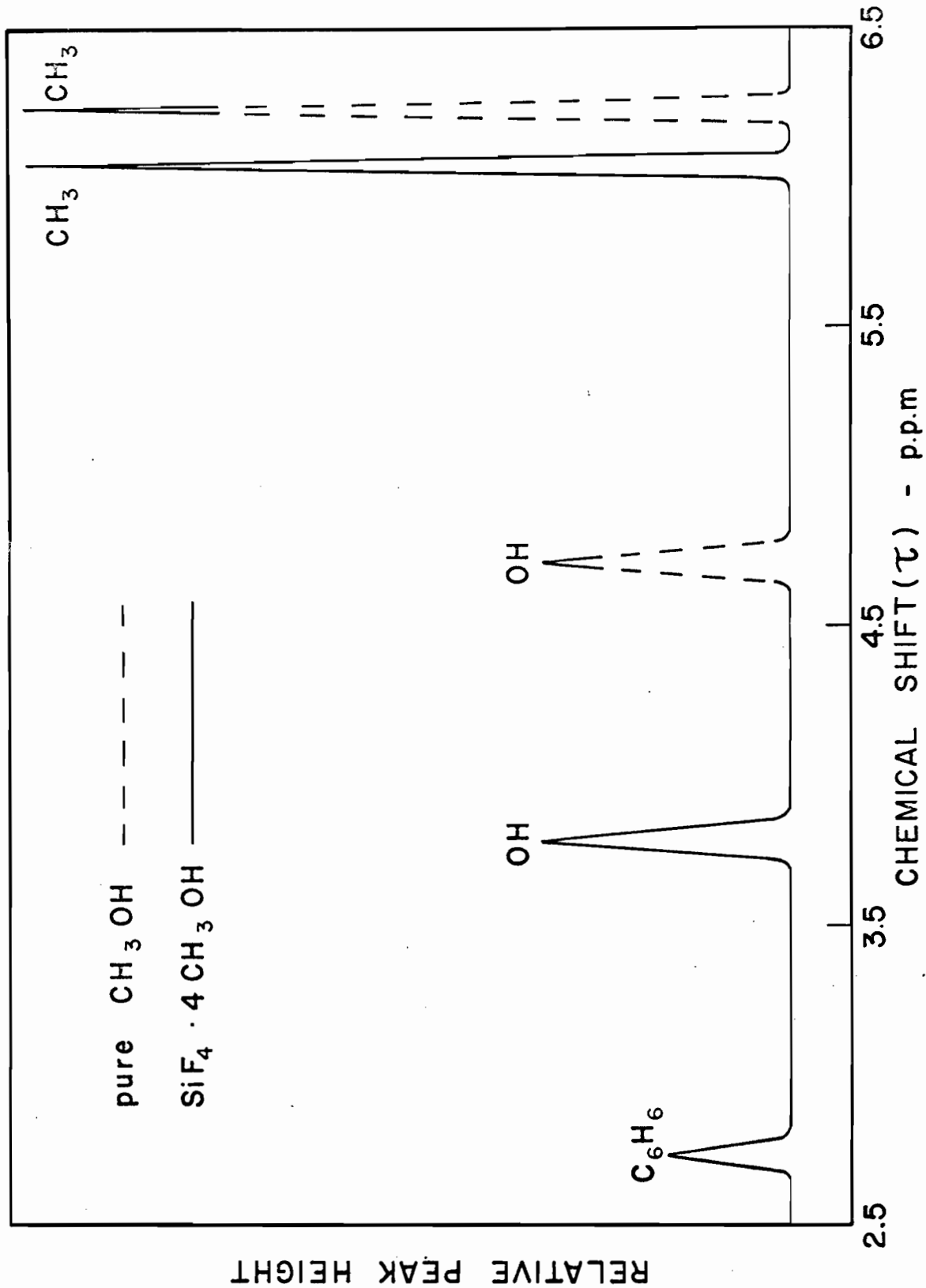


FIG. 13

The variation of the chemical shift of the OH peak
with the mole ratio, $\text{SiF}_4/\text{CH}_3\text{OH}$

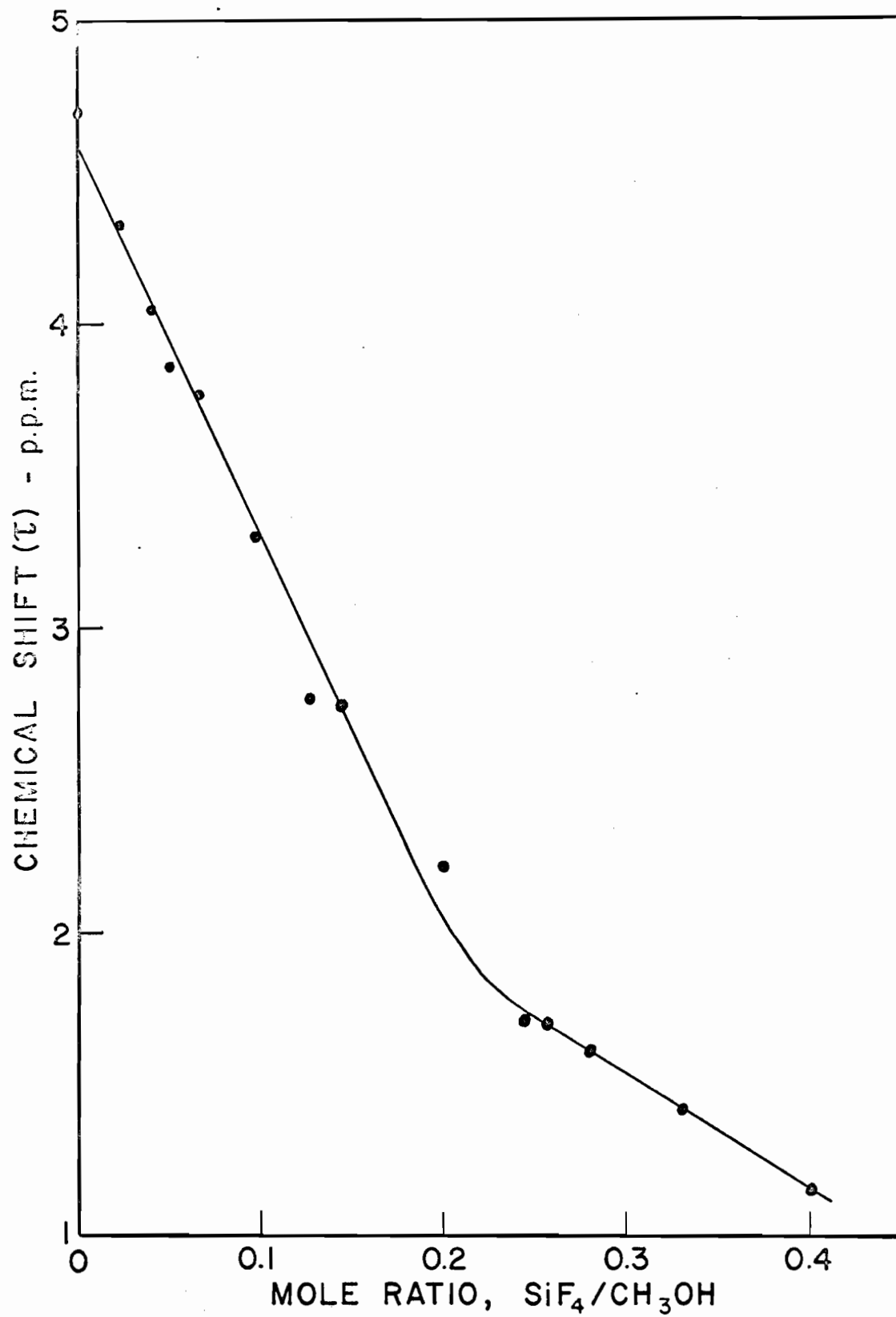
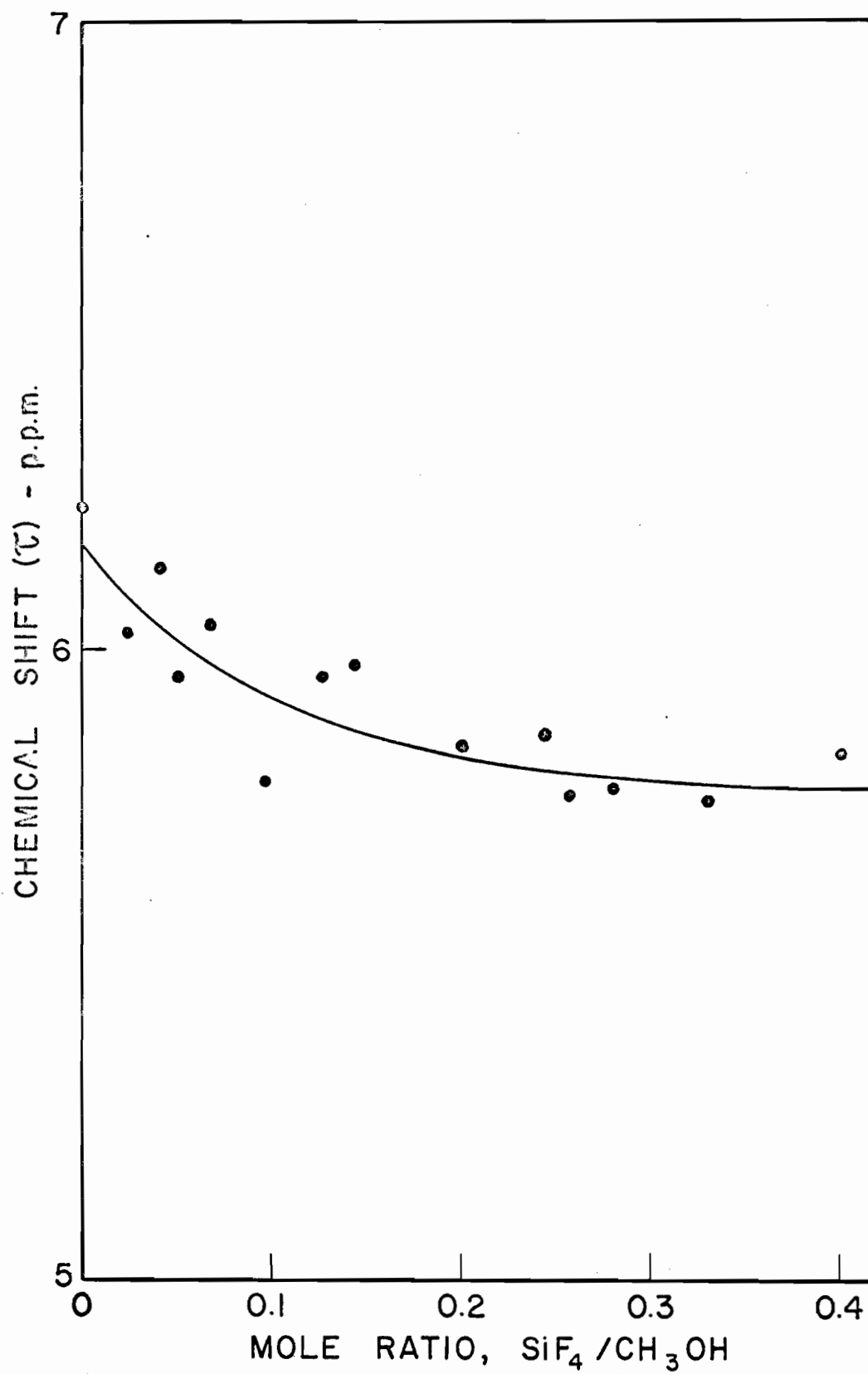


FIG. 14

The variation of the chemical shift of the CH₃ peak
with the mole ratio, SiF₄/CH₃OH



II. Coordination of SiF_4 with Aliphatic Cyclic Ethers and Dimethyl Ether

1. Coordination of SiF_4 with Ethylene Oxide

(i) Preparation of $\text{SiF}_4 \cdot 2(\text{CH}_2)_2\text{O}$

When a mixture of SiF_4 (8.12 mmole) and $(\text{CH}_2)_2\text{O}$ (6.07 mmole) was warmed slowly ($\sim 1^\circ/\text{min.}$) from -195 to -78° a white solid resulted. From the amount of SiF_4 (5.06 mmole) recovered by distillation at -129° it was evident that SiF_4 and $(\text{CH}_2)_2\text{O}$ had combined in a mole ratio of 1:1.99, corresponding to the complex, $\text{SiF}_4 \cdot 2(\text{CH}_2)_2\text{O}$.

The infrared spectrum of the gas phase at 25° in equilibrium with the solid complex at -65° consisted of bands due to SiF_4 superimposed on those of $(\text{CH}_2)_2\text{O}$. The molecular weight of this gaseous mixture was 87.2 which compares favorably with 85.1, calculated on the assumption that complete dissociation had occurred, that the liberated SiF_4 was completely in the gas phase, and that the liberated $(\text{CH}_2)_2\text{O}$ exerted its equilibrium vapor pressure of 10.0 mm at -65° .

When the temperature of the 1:2 complex was raised to 25° all of the remaining SiF_4 (3.04 mmole) was recovered and a colorless non-volatile viscous liquid resulted. The infrared spectrum of this liquid is shown in Fig. 15 and frequency assignments are given in Table 8. There was no evidence of any $(\text{CH}_2)_2\text{O}$ or 1,4-dioxane.

TABLE 8

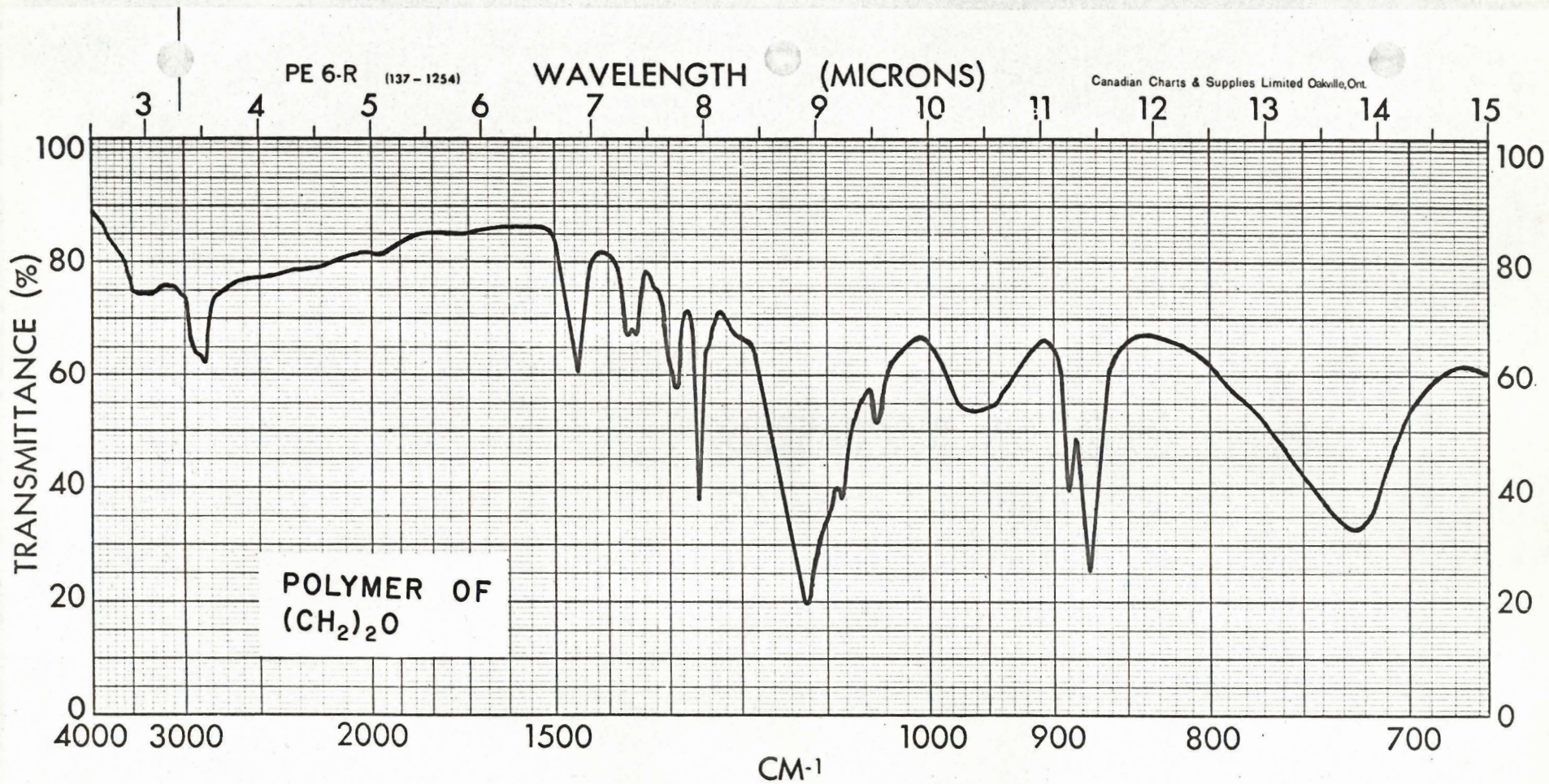
Comparison and assignment of infrared absorption frequencies (cm^{-1})

$(\text{CH}_2)_2\text{O}$ polymer	1,4-dioxane	Assignment	Reference
2950-2900m,b	2950m	$\nu(\text{C-H})$	
	2900m	"	
2850m	2860m	"	
1455m	1460m	$\delta(\text{C-H})$, deformation	
1365m	1365mw	" , twist	
1355m		" , twist	(40)
1290m	1290m	" , wag	
1258ms	1260ms	" , wag	
1123s,b	1125s	$\nu(\text{C-O})$, antisym.	
1085m	1085m	" , antisym.	(41)
1048m	1050m	" , antisym.	
960m,b	-	" , sym.	
890ms	890ms	$\delta(\text{C-H})$, rock	(40,42)
875s	875s	" , rock	
723s,b	-	$\nu(\text{Si-F})$ octahedral for SiF_6^{-2}	(43)

Note: s = strong, m = medium, w = weak, b = broad.

FIG. 15

The infrared spectrum of the polymer produced
in the reaction of $(\text{CH}_2)_2\text{O}$ with excess SiF_4



It was not possible to obtain pure $\text{SiF}_4 \cdot 2(\text{CH}_2)_2\text{O}$ by a direct synthesis using excess $(\text{CH}_2)_2\text{O}$ initially. The unreacted $(\text{CH}_2)_2\text{O}$ could not be distilled from the $(\text{CH}_2)_2\text{O}-\text{SiF}_4 \cdot 2(\text{CH}_2)_2\text{O}$ mixture because the complex has an appreciable dissociation pressure at the temperature at which $(\text{CH}_2)_2\text{O}$ can be distilled. Therefore, the complex was first prepared at -78° by adding an excess of SiF_4 (8.12 mmole) to $(\text{CH}_2)_2\text{O}$ (6.07 mmole) and then an excess of $(\text{CH}_2)_2\text{O}$ (8.32 mmole) was added and the temperature was raised to 25° . After one hour, distillation of the product mixture in the range -78 to 25° yielded the following fractions: (a) a mixture (12.95 mmole. M, 65.0. Calc. for a 1:2 mole mixture of SiF_4 and $(\text{CH}_2)_2\text{O}$: M, 64.0) of SiF_4 and $(\text{CH}_2)_2\text{O}$, inseparable by simple distillation, (b) 1,4-dioxane (1.50 mmole. M, 86.0. Calc. for $\text{C}_4\text{H}_8\text{O}_2$: M, 88.1), (c) a small amount of a dark purple, nonvolatile polymeric material which must contain some SiF_4 (Initial SiF_4 used, 8.12 mmole. Recovered SiF_4 , only $(1/3) \times (12.95) = 4.32$ mmole. Thus 3.80 mmole must be incorporated in the polymer). There was a 21% conversion of $(\text{CH}_2)_2\text{O}$ into 1,4-dioxane and a 9% yield of polymer, the infrared spectrum of which is shown in Fig. 16 and frequency assignments are listed in Table 9.

TABLE 9

Assignment of infrared absorption frequencies (cm^{-1})

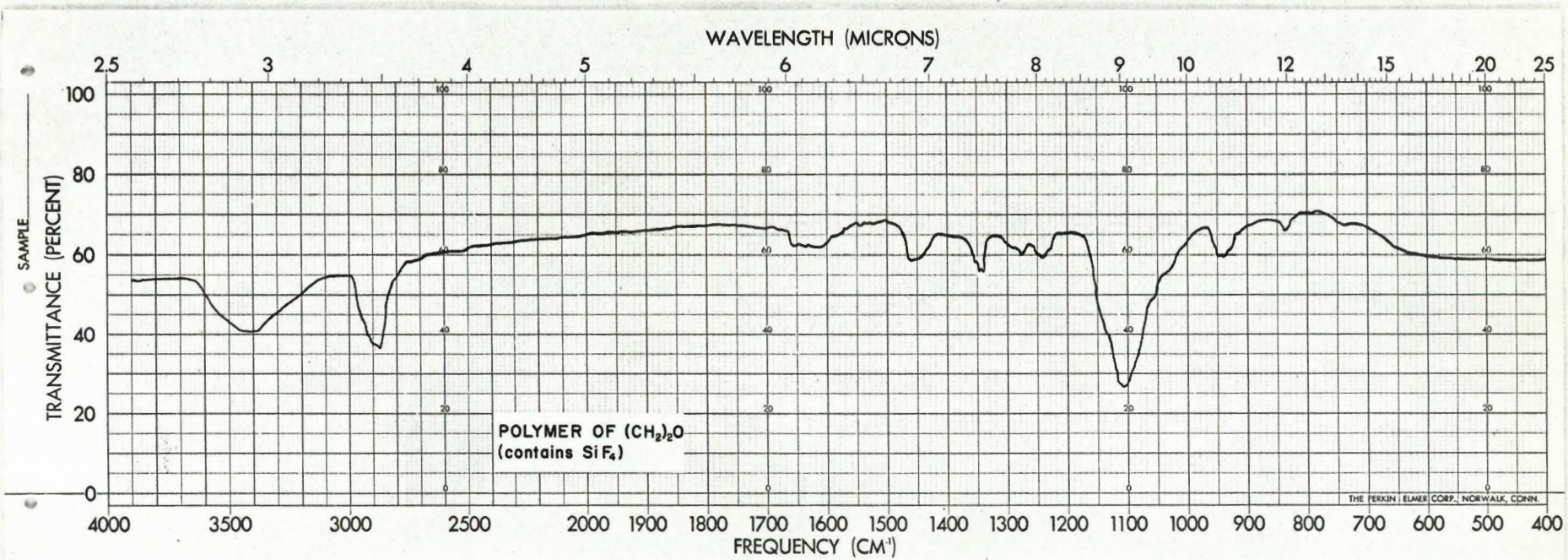
Dark purple polymer of $(\text{CH}_2)_2\text{O}$	Assignment
3420m,b	$\checkmark(\text{O-H})$, due to H_2O
2910m,b	$\checkmark(\text{C-H})$
2870m	"
1630vw,b	due to H_2O
1460w	$\delta(\text{C-H})$
1355w	"
1347w	"
1340w	"
1275w	"
1240w	"
1108s	$\checkmark(\text{Si-F})$ tetrahedral* and perhaps $\checkmark(\text{Si-O})^{**}$
945w,b	$\delta(\text{C-H})$
838w	"

* due to (Si-F) tetrahedral bonds in the polymer

** due to hydrolysis

FIG. 16

The infrared spectrum of the polymer produced in the
reaction of SiF_4 with excess $(\text{CH}_2)_2\text{O}$



(ii) Tensimetric Titration

A tensimetric titration of SiF_4 (12.21 mmole) with $(\text{CH}_2)_2\text{O}$ (Fig. 17, Table 10) showed the formation of only 1:2 complex. After each addition of $(\text{CH}_2)_2\text{O}$ to SiF_4 the mixture was warmed quickly to -78° and kept at this temperature for 15 minutes by which time the pressure became constant. As shown in Fig. 17, the pressure decreased linearly until the mole ratio, $(\text{CH}_2)_2\text{O}/\text{SiF}_4$, had increased to 2.03 (i.e., after the addition of 24.8 mmole $(\text{CH}_2)_2\text{O}$), when the pressure became essentially constant at about 8 mm (\sim the v.p. of $(\text{CH}_2)_2\text{O}$ at -78°), corresponding to the formation of $\text{SiF}_4 \cdot 2(\text{CH}_2)_2\text{O}$.

In the reverse tensimetric titration of $(\text{CH}_2)_2\text{O}$ (20.60 mmole) with SiF_4 (Table 10, Fig. 18) under the conditions used in the preceding titration, the pressure remained at about 5 mm until the mole ratio, $(\text{CH}_2)_2\text{O}/\text{SiF}_4$, decreased to about 2.3, when the pressure increased rapidly as more SiF_4 was added. Extrapolation of the linear portion of the plot to 5 mm pressure gave a mole ratio of 2.00 (corresponding to the addition of 10.3 mmole SiF_4) indicating the formation of only the 1:2 complex.

TABLE 10

Tensimetric titration of SiF_4 with $(\text{CH}_2)_2\text{O}$ and $(\text{CH}_2)_2\text{O}$ with SiF_4

SiF_4 with $(\text{CH}_2)_2\text{O}$ (Fig. 11)		$(\text{CH}_2)_2\text{O}$ with SiF_4 (Fig. 12)	
SiF_4 present initially, 12.21 mmole		$(\text{CH}_2)_2\text{O}$ present initially, 20.60 mmole	
$T_r, -78^\circ; T_p, -78^\circ$		$T_r, -78^\circ; T_p, -78^\circ$	
Total $(\text{CH}_2)_2\text{O}$ added mmole	Pressure mm	Total SiF_4 added mmole	Pressure mm
0	648.8	0	4.0
3.09	572.2	3.10	4.0
6.19	489.0	6.20	5.0
9.29	408.5	9.21	5.0
12.38	327.0	9.96	7.0
15.49	294.4	11.13	38.0
18.59	167.5	14.86	152.0
21.69	88.0	17.50	229.0
24.79	13.3	21.48	354.5
27.88	10.6		
31.00	9.4		
34.10	8.3		

FIG. 17

The tensimetric titration of SiF_4 with $(\text{CH}_2)_2\text{O}$

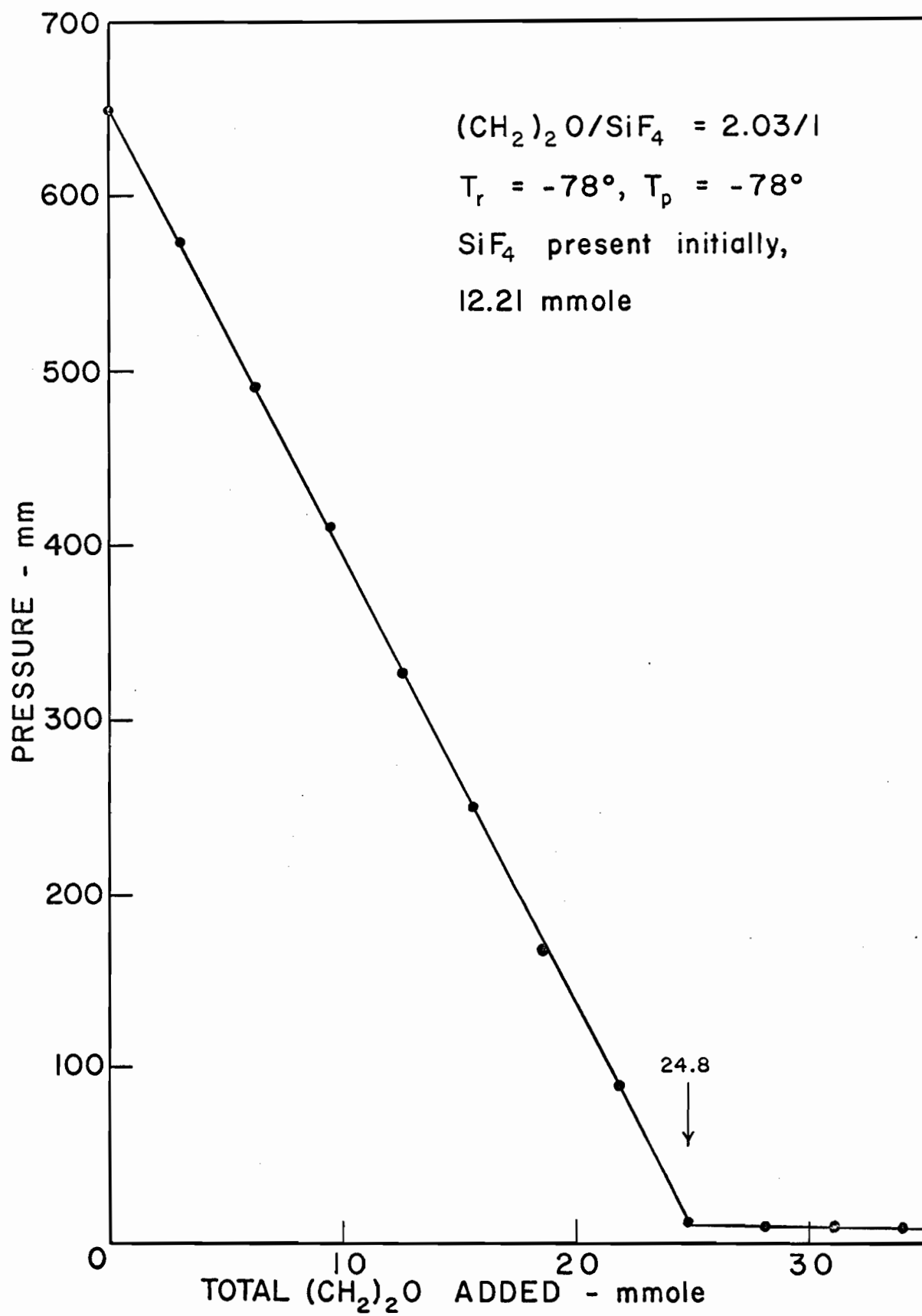
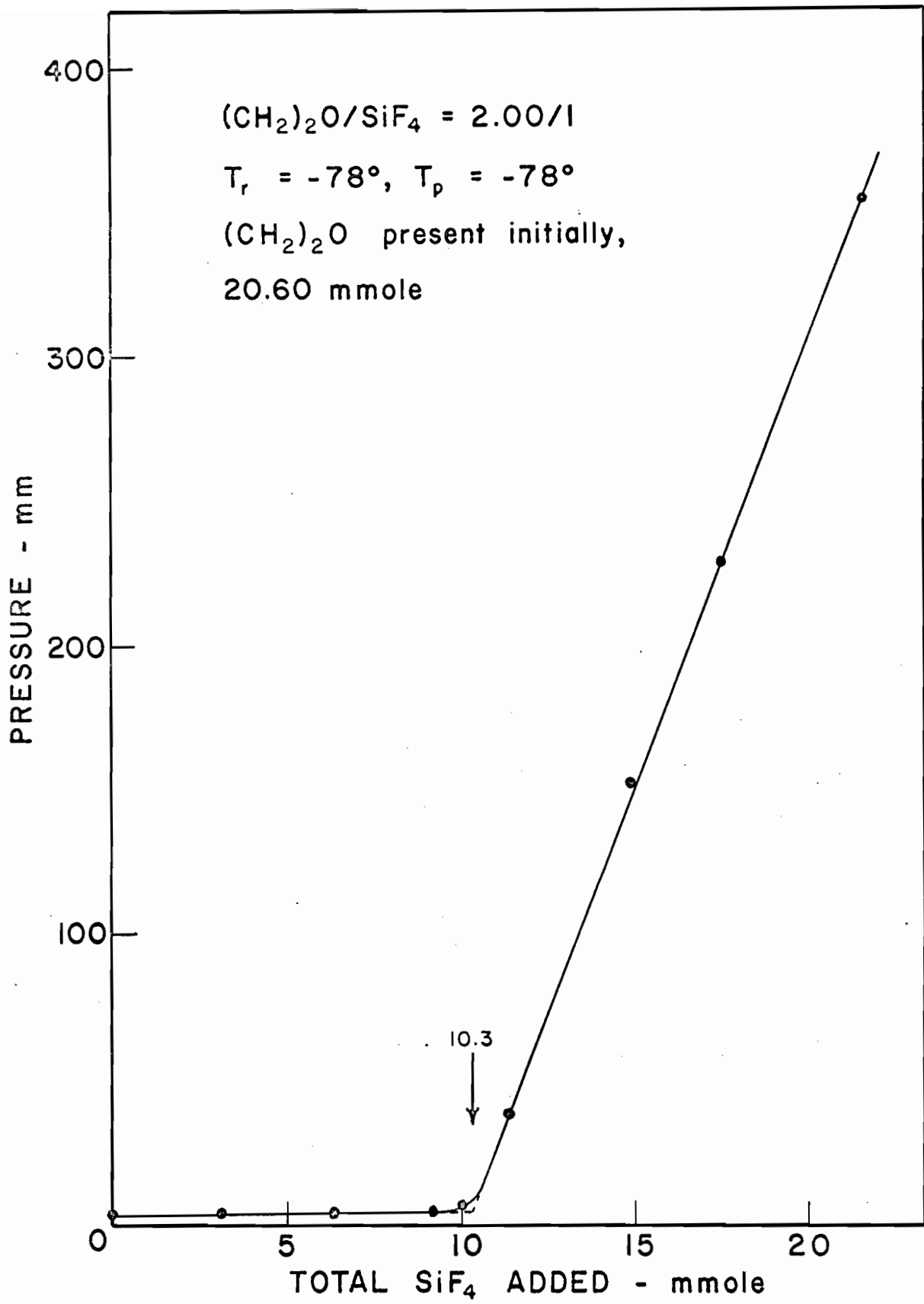


FIG. 18

The tensimetric titration of $(\text{CH}_2)_2\text{O}$ with SiF_4



(iii) Heat of Dissociation

The complex, $\text{SiF}_4 \cdot 2(\text{CH}_2)_2\text{O}$, was prepared as previously described by removal at -116° of excess SiF_4 (10.12 mmole) from a SiF_4 (12.06 mmole)- $(\text{CH}_2)_2\text{O}$ (3.885 mmole) mixture. Pressure-temperature measurements were made from -93.2 to -68.3° and the results (Table 11) are plotted in Fig. 19. A heat of dissociation of 10.6 ± 0.3 kcal mole⁻¹ was calculated from the slope of the linear plot. At a higher temperature than -68.3° (e.g., -63°) there was an abnormally large pressure increase (> 45 mm), the complete disappearance of solid complex, and failure to observe identical pressures before and after the pumping off operation (described in the experimental section). These observations confirmed that a dynamic equilibrium no longer existed.

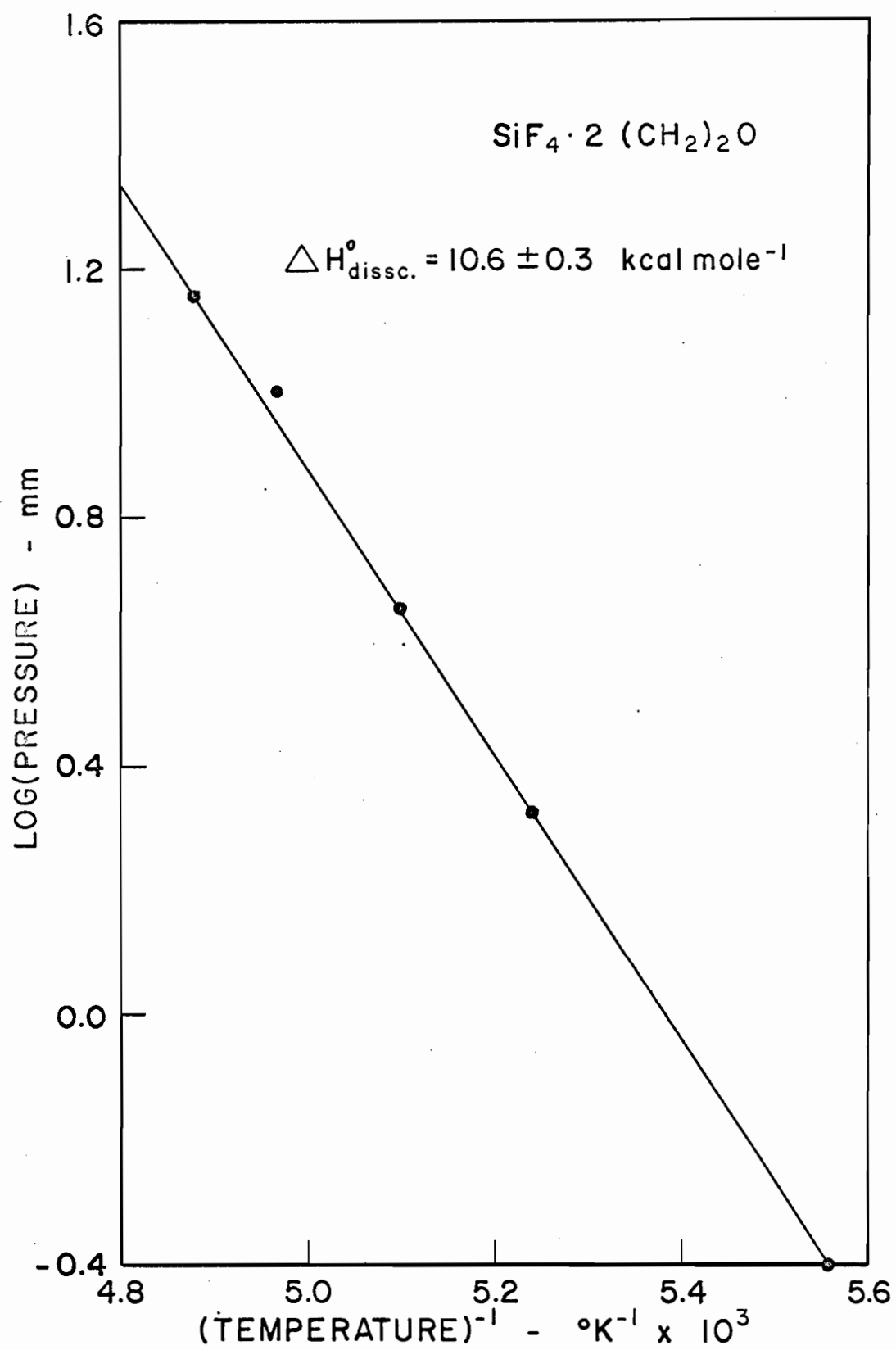
TABLE 11

Data for the heat of dissociation of $\text{SiF}_4 \cdot 2(\text{CH}_2)_2\text{O}$

Temperature			Pressure	Calculations,
$^{\circ}\text{C}$	$^{\circ}\text{K}$	$^{\circ}\text{K}^{-1} \times 10^3$	mm	$\Delta H^{\circ} = \frac{-\log (P_1/P_2)}{T_1^{-1} - T_2^{-1}} \times 2.303 \times 1.987$
				$P_1 = 20.0 \text{ mm}$
-93.2	180.0	5.555	0.4	$P_2 = 0.2 \text{ mm}$
-82.3	190.9	5.240	2.1	$T_1^{-1} = 4.820 \times 10^{-3} \text{ } ^{\circ}\text{K}^{-1}$
-77.2	196.0	5.100	4.5	$T_2^{-1} = 5.685 \times 10^{-3} \text{ } ^{\circ}\text{K}^{-1}$
-71.8	201.4	4.965	10.0	
-68.3	204.9	4.880	14.3	$\Delta H^{\circ} = 10.6 \text{ kcal mole}^{-1}$

FIG. 19

Dissociation pressures of $\text{SiF}_4 \cdot 2(\text{CH}_2)_2\text{O}$



2. Coordination of SiF_4 with Trimethylene Oxide

(i) Preparation of $\text{SiF}_4 \cdot 2(\text{CH}_2)_3\text{O}$

Under experimental conditions identical to those used in the preparation of $\text{SiF}_4 \cdot 2(\text{CH}_2)_2\text{O}$, SiF_4 (11.93 mmole) and $(\text{CH}_2)_3\text{O}$ (3.86 mmole) combined in a 1:2.05 mole ratio as evident from the amount of uncombined SiF_4 (10.05 mmole), producing the white solid, $\text{SiF}_4 \cdot 2(\text{CH}_2)_3\text{O}$. Infrared and molecular weight measurements showed that the gas phase at 25° in equilibrium with the solid complex at 0° consisted of only SiF_4 and $(\text{CH}_2)_3\text{O}$ (Found: M, 75.0. Calc. M, 73.4 assuming complete dissociation of the complex in the gas phase and that the liberated SiF_4 and $(\text{CH}_2)_3\text{O}$ are completely gaseous (the v.p. of $(\text{CH}_2)_3\text{O} = 125 \text{ mm}$ at 0° is not completely established due to the large volume of vessel)).

On raising the temperature of the $\text{SiF}_4 \cdot 2(\text{CH}_2)_3\text{O}$ complex to 25°, the remaining SiF_4 (1.85 mmole) was liberated and polymerization of $(\text{CH}_2)_3\text{O}$ occurred with the formation of a colorless nonvolatile, viscous polymer. The infrared spectrum of this polymer is shown in Fig. 20 and frequency assignments are given in Table 12. Polymerization commenced rapidly above 13.6° but below this temperature the complex could be sublimed unchanged.

When $(\text{CH}_2)_3\text{O}$ (8.00 mmole) was added to previously prepared $\text{SiF}_4 \cdot 2(\text{CH}_2)_3\text{O}$ (1.88 mmole) and the temperature of the mixture was raised to 25° for 12 hours, the products were: SiF_4 (1.86 mmole) and a colorless, viscous, nonvolatile polymer whose infrared spectrum was the same as that of the polymer produced with excess SiF_4 (Fig. 20). Thus SiF_4 had catalyzed the polymerization of $(\text{CH}_2)_3\text{O}$ producing the same polymer whether $(\text{CH}_2)_3\text{O}$ was in excess or not.

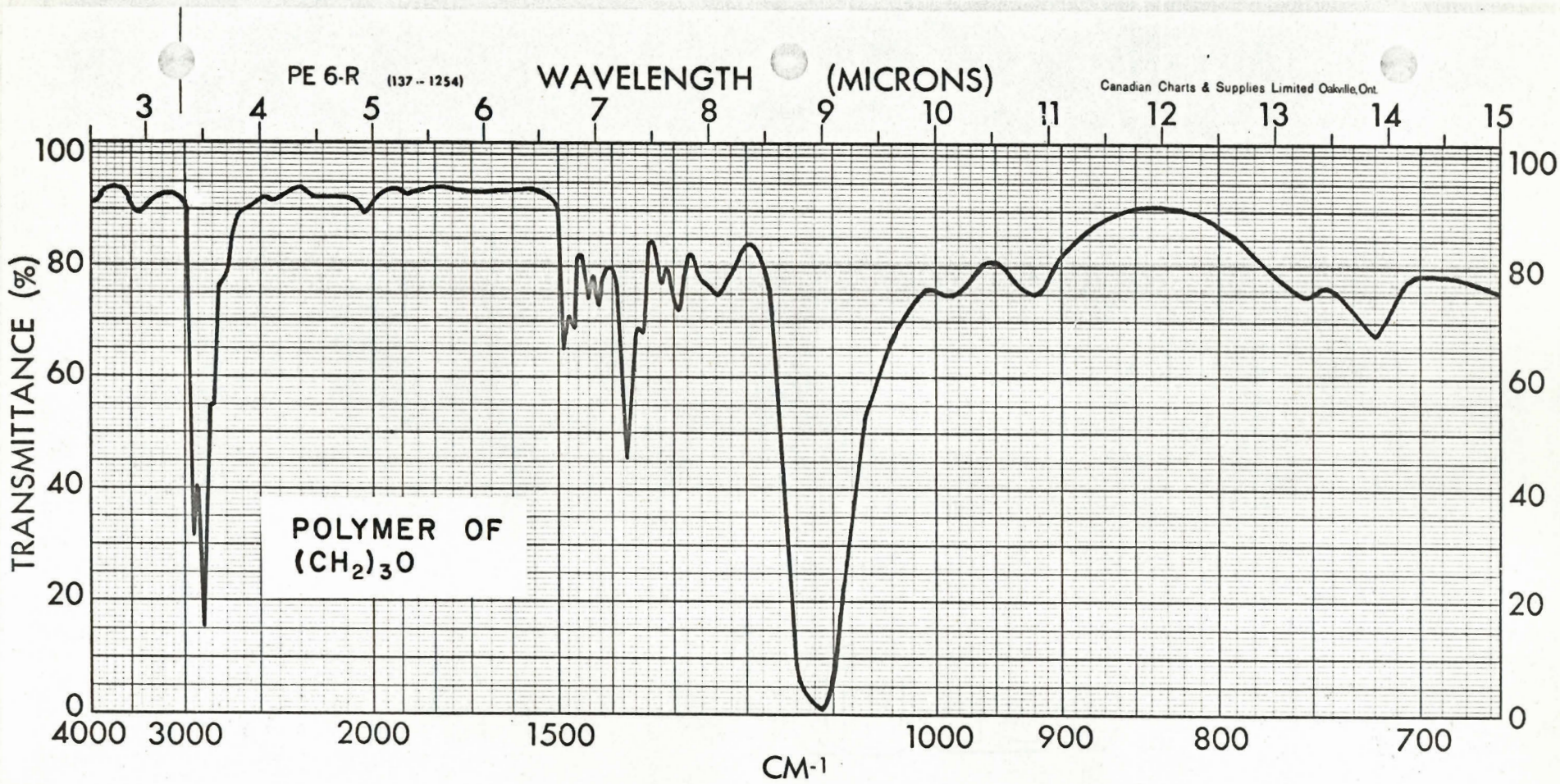
TABLE 12

Assignment of infrared absorption frequencies (cm^{-1})

$(\text{CH}_2)_3\text{O}$ polymer cm^{-1}	Assignments
3460w	\downarrow (O-H)
2930s	\downarrow (C-H)
2860s	"
2780m	"
2040w	combination
1490m	\int (C-H)
1470m	"
1440m	"
1425m	"
1375m	"
1350m	"
1320m	"
1295m	"
1240m	"
1112vs	\downarrow (C-O)
920w	\int (C-H)
755w	unidentified
720w	\downarrow (Si-F) octahedral for SiF_6^{-2} (43)

FIG. 20

The infrared spectrum of the polymer produced in the reaction of SiF_4 with $(\text{CH}_2)_3\text{O}$, either component in excess



(ii) Tensimetric Titration

A tensimetric titration at -95° of SiF_4 (9.38 mmole) with $(\text{CH}_2)_3\text{O}$ showed a combining ratio, $(\text{CH}_2)_3\text{O}/\text{SiF}_4$, of 2.24. As shown in Fig. 21 (Table 13), the pressure decreased linearly until the mole ratio had increased to 2.24, after which the slope of the line began to change and the pressure became zero. Extrapolation of the linear part of the plot to zero pressure gave a mole ratio of 2.27 (corresponding to the addition of 21.3 mmole $(\text{CH}_2)_3\text{O}$), in agreement with the formation of $\text{SiF}_4 \cdot 2(\text{CH}_2)_3\text{O}$.

When the tensimetric titration was done in reverse, i.e., by addition of SiF_4 to $(\text{CH}_2)_3\text{O}$, combining ratios, $(\text{CH}_2)_3\text{O}/\text{SiF}_4$, were always high ($> 4:1$). The data from a typical experiment are shown in Table 13. This suggested that, as with $\text{SiF}_4 \cdot 2(\text{CH}_2)_2\text{O}$, polymerization was enhanced when more $(\text{CH}_2)_3\text{O}$ was present than was necessary to produce the 1:2 complex.

TABLE 13

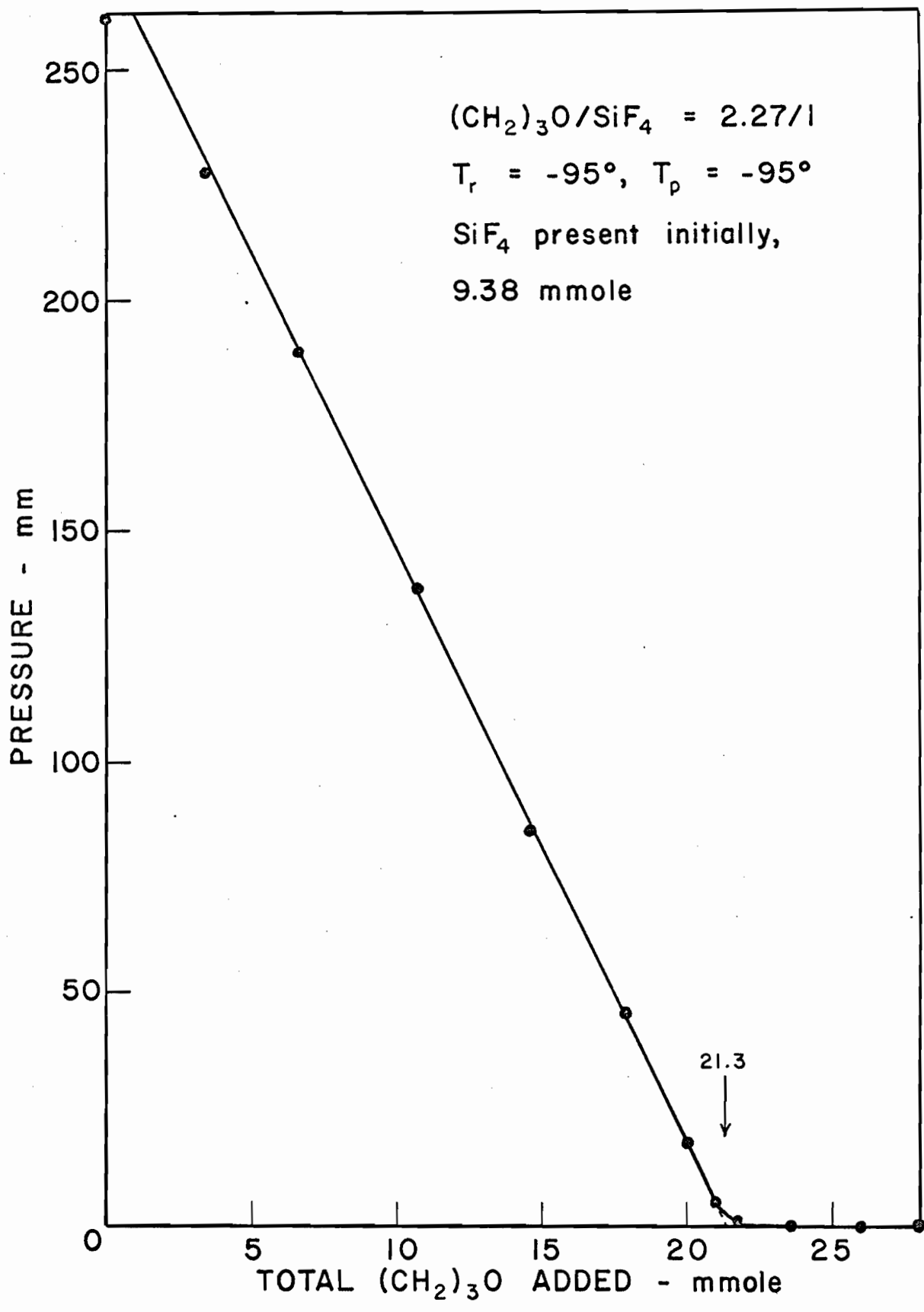
The tensimetric titration of SiF_4 with $(\text{CH}_2)_3\text{O}$ and $(\text{CH}_2)_3\text{O}$ with SiF_4

SiF_4 with $(\text{CH}_2)_3\text{O}$ (Fig. 21)		$(\text{CH}_2)_3\text{O}$ with SiF_4 (*)	
SiF_4 present initially, 9.38 mmole		$(\text{CH}_2)_3\text{O}$ present initially, 27.90 mmole	
$T_r, -95^\circ; T_p, -95^\circ$		$T_r, -95^\circ; T_p, -95^\circ$	
Total $(\text{CH}_2)_3\text{O}$ added mmole	Pressure mm	Total SiF_4 added mmole	Pressure mm
0	260.9	0	0
3.40	227.5	5.02	0
6.47	189.2	10.39	118.0
10.74	137.5	13.71	209.8
14.48	85.0	18.32	335.8
17.88	45.0	23.25	469.8
19.96	17.0	28.16	604.7
21.00	5.0		
21.80	1.0		
23.63	0		
26.00	0		
28.00	0		

* These data were not plotted.

FIG. 21

The tensimetric titration of SiF_4 with $(\text{CH}_2)_3\text{O}$



(iii) Heat of Dissociation

The complex, $\text{SiF}_4 \cdot 2(\text{CH}_2)_3\text{O}$ (1.88 mmole) was prepared as described previously in section 2(i) using identical quantities. Pressure-temperature measurements were made from -23.0 to 13.6° and the results (Table 14) are plotted in Fig. 22. The slope of the straight line gave a heat of dissociation of 13.9 ± 0.3 kcal mole⁻¹. At a higher temperature (e.g., 15°), similar non-equilibrium effects as occurred for $\text{SiF}_4 \cdot 2(\text{CH}_2)_2\text{O}$ were observed.

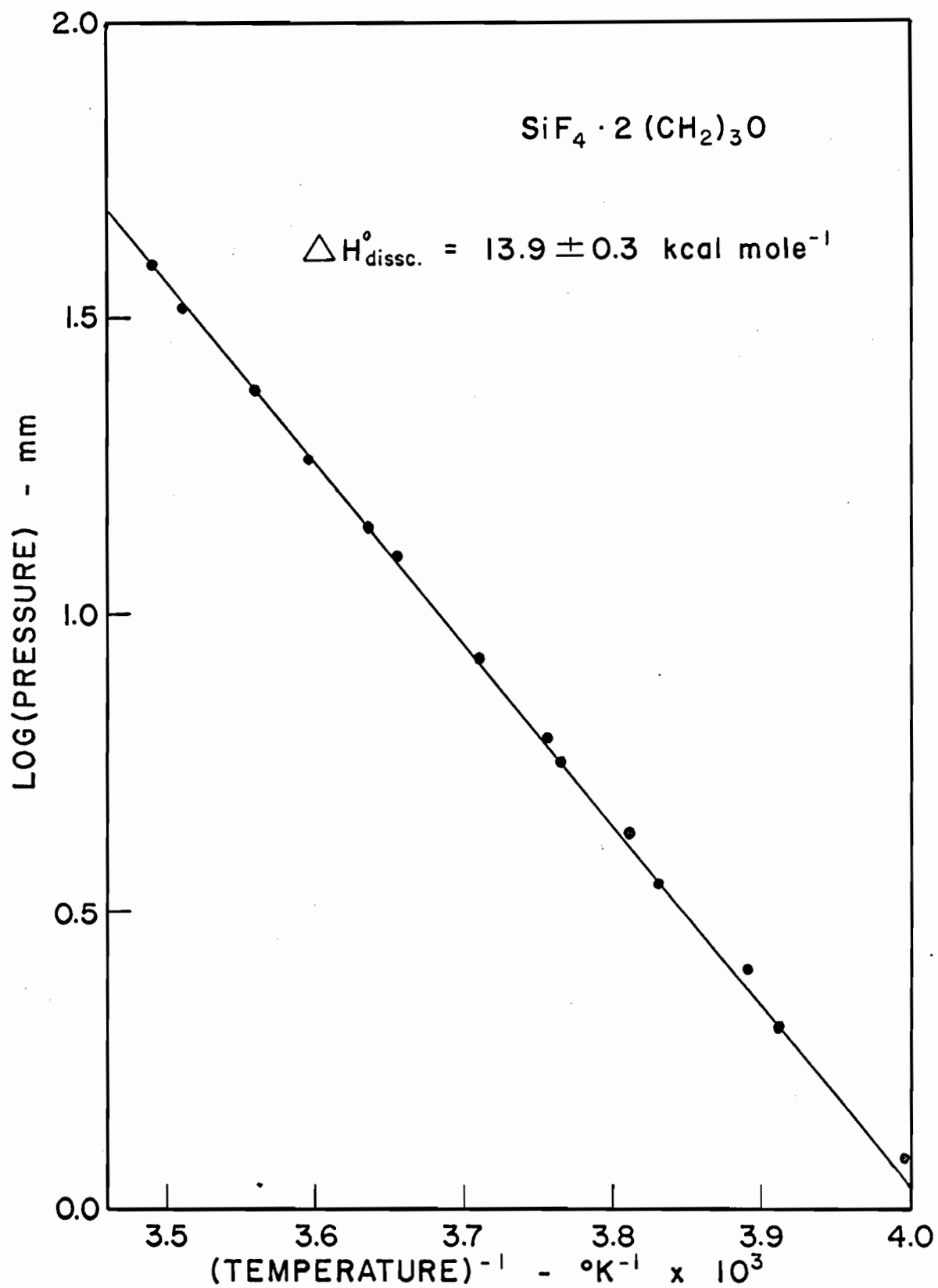
TABLE 14

Data for heat of dissociation of $\text{SiF}_4 \cdot 2(\text{CH}_2)_3\text{O}$

Temperature			Pressure	Calculations,
$^{\circ}\text{C}$	$^{\circ}\text{K}$	$^{\circ}\text{K}^{-1} \times 10^3$	mm	$\Delta H^{\circ} = \frac{-\log (P_1/P_2)}{T_1^{-1} - T_2^{-1}} \times 2.303 \times 1.987$
-23.0	250.2	3.995	1.2	$P_1 = 20.0 \text{ mm}$
-17.7	255.5	3.910	2.0	$P_2 = 2.0 \text{ mm}$
-16.2	257.0	3.890	2.5	$T_1^{-1} = 3.584 \times 10^{-3} \text{ }^{\circ}\text{K}^{-1}$
-12.0	261.2	3.830	3.5	$T_2^{-1} = 3.913 \times 10^{-3} \text{ }^{\circ}\text{K}^{-1}$
-11.0	262.2	3.810	4.3	
- 7.3	265.9	3.765	5.6	$\Delta H^{\circ} = 13.9 \text{ kcal mole}^{-1}$
- 6.8	266.4	3.755	6.2	
- 3.5	269.7	3.710	8.4	
0.3	273.5	3.655	12.4	
2.0	275.2	3.635	14.0	
5.2	278.4	3.595	18.3	
8.1	281.3	3.560	23.9	
11.7	284.9	3.510	32.7	
13.6	286.8	3.490	38.7	

FIG. 22

Dissociation pressures of $\text{SiF}_4 \cdot 2(\text{CH}_2)_3\text{O}$



(iv) Infrared Spectrum of $\text{SiF}_4 \cdot 2(\text{CH}_2)_3\text{O}$

The infrared spectrum of crystalline $\text{SiF}_4 \cdot 2(\text{CH}_2)_3\text{O}$ was taken at -195° using a special low-temperature infrared cell. A sample of the complex was sublimed at 3° in a vacuum onto a NaCl plate cooled to -195° . It was difficult to obtain a good spectrum because the thickness of the crystalline film was not uniform and there was much infrared light scattering by the crystalline deposit. Nevertheless, it was possible to identify most of the absorption bands shown in Fig. 23 (Table 15). The intensity of the 720 cm^{-1} band decreased by about 75% when the sample was removed confirming that the band was due mainly to an absorption of the sample. The remainder was probably due to SiF_6^{-2} formed by an interaction between $\text{SiF}_4 \cdot 2(\text{CH}_2)_3\text{O}$ with the NaCl surface, since such a reaction occurs between gaseous SiF_4 and NaCl plates (43).

TABLE 15

Assignment of infrared frequencies (cm^{-1})

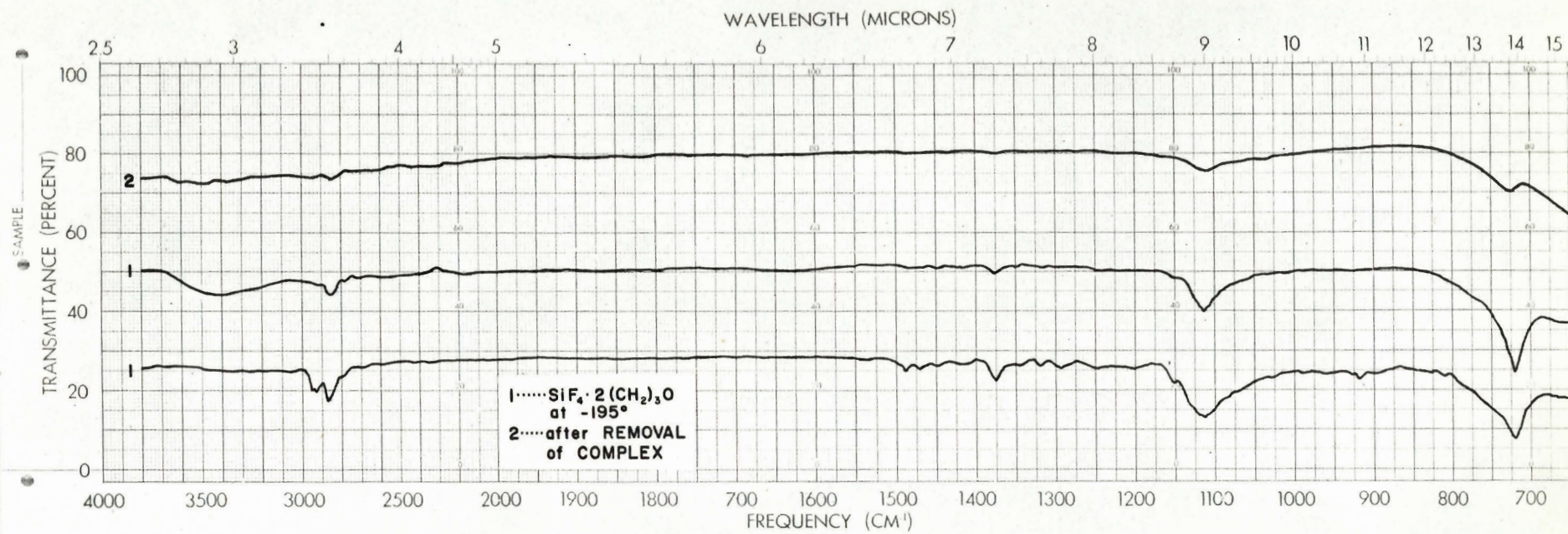
<u>$\text{SiF}_4 \cdot 2(\text{CH}_2)_3\text{O}$ crystalline</u>	<u>Assignment</u>
2955w	$\nu(\text{C-H})$ for CH_2
2935w	"
2870w	"
1500-1450vw	$\delta(\text{C-H})$ for CH_2
1375w	"
1150sh	unidentified
1113m	$\nu(\text{C-O})$
920vw	$\delta(\text{C-H})$, rocking
720s	$\nu(\text{Si-F})$ octahedral for $\text{SiF}_4 \cdot 2(\text{CH}_2)_3\text{O}$ and perhaps some SiF_6^{-2*}

sh = shoulder

* formed by reaction of $\text{SiF}_4 \cdot 2(\text{CH}_2)_3\text{O}$ with NaCl plates

FIG. 23

The infrared spectrum of crystalline $\text{SiF}_4 \cdot 2(\text{CH}_2)_3\text{O}$
at low temperature



3. Coordination of SiF_4 with Tetrahydrofuran

(i) Preparation of $\text{SiF}_4 \cdot 2(\text{CH}_2)_4\text{O}$

Slow cooling of a mixture of SiF_4 (4.94 mmole) and $(\text{CH}_2)_4\text{O}$ (4.01 mmole) from 25 to -78° resulted in a white solid and excess SiF_4 (2.84 mmole). Thus, the white solid contained $(\text{CH}_2)_4\text{O}$ and SiF_4 in a mole ratio of 1.91, corresponding to the complex, $\text{SiF}_4 \cdot 2(\text{CH}_2)_4\text{O}$. Combining ratios in the range 1:1.91 to 1:2.13 were also obtained in several other experiments.

Increasing the temperature of the complex to 25° resulted in the complete dissociation of the complex into SiF_4 and $(\text{CH}_2)_4\text{O}$ as shown by the infrared and molecular weight measurements on the gas phase at 25° in equilibrium with the liquid at 25° (Found: M, 93.9. Calc. M, 98.0 assuming complete dissociation of the complex in the gas phase and establishment of $(\text{CH}_2)_4\text{O}$'s v.p. = 125 mm at 25°). There was no indication of any polymerization since the infrared of the liquid phase at 25° showed only the presence of $(\text{CH}_2)_4\text{O}$.

It was not possible to obtain pure $\text{SiF}_4 \cdot 2(\text{CH}_2)_4\text{O}$ by a direct synthesis using excess $(\text{CH}_2)_4\text{O}$ initially because the unreacted $(\text{CH}_2)_4\text{O}$ could not be removed from the $(\text{CH}_2)_4\text{O}-\text{SiF}_4 \cdot 2(\text{CH}_2)_4\text{O}$ mixture due to the appreciable dissociation pressure of the complex at the temperature at which $(\text{CH}_2)_4\text{O}$ can be removed.

(ii) Tensimetric Titration

After each addition of $(\text{CH}_2)_4\text{O}$ to SiF_4 (9.43 mmole) the mixture was warmed to 25° and then slowly cooled to -78° at which temperature pressure measurements were made. As shown in Fig. 24 (Table 16), the pressure decreased linearly until the mole ratio had increased to 2.07, when the slope of the line began to change and the pressure became zero. A mole ratio of 2.15 (corresponding to the addition of 20.25 mmole $(\text{CH}_2)_4\text{O}$) was indicated by the extrapolation of the linear portion of the plot for the formation of the 1:2 complex, $\text{SiF}_4 \cdot 2(\text{CH}_2)_4\text{O}$.

Fig. 25 (Table 16) shows the results of the reverse tensimetric titration of $(\text{CH}_2)_4\text{O}$ (20.10 mmole) by addition of SiF_4 . The pressure remained zero until the mole ratio had decreased to 2.13 (corresponding to the addition of 9.45 mmole SiF_4), when the pressure increased rapidly as more SiF_4 was added. This confirmed the formation of only $\text{SiF}_4 \cdot 2(\text{CH}_2)_4\text{O}$.

TABLE 16

Tensimetric titration of SiF_4 with $(\text{CH}_2)_4\text{O}$ and $(\text{CH}_2)_4\text{O}$ with SiF_4

SiF_4 with $(\text{CH}_2)_4\text{O}$ (Fig. 24)		$(\text{CH}_2)_4\text{O}$ with SiF_4 (Fig. 25)	
SiF_4 present initially, 9.43 mmole		$(\text{CH}_2)_4\text{O}$ present initially, 20.10 mmole	
$T_r, 25^\circ; T_p, -78^\circ$		$T_r, 25^\circ; T_p, -78^\circ$	
Total $(\text{CH}_2)_4\text{O}$ added mmole	Pressure mm	Total SiF_4 added mmole	Pressure mm
0	283.3	0	0
2.24	253.0	4.38	0.5
5.57	203.0	8.26	1.0
9.23	155.0	9.71	1.2
13.89	94.7	10.81	59.0
17.06	45.0	13.86	162.5
19.20	17.0	16.08	220.6
20.00	8.0	19.03	338.2
20.82	0.8	21.69	420.2
22.50	0		

FIG. 24

The tensimetric titration of SiF_4 with $(\text{CH}_2)_4\text{O}$

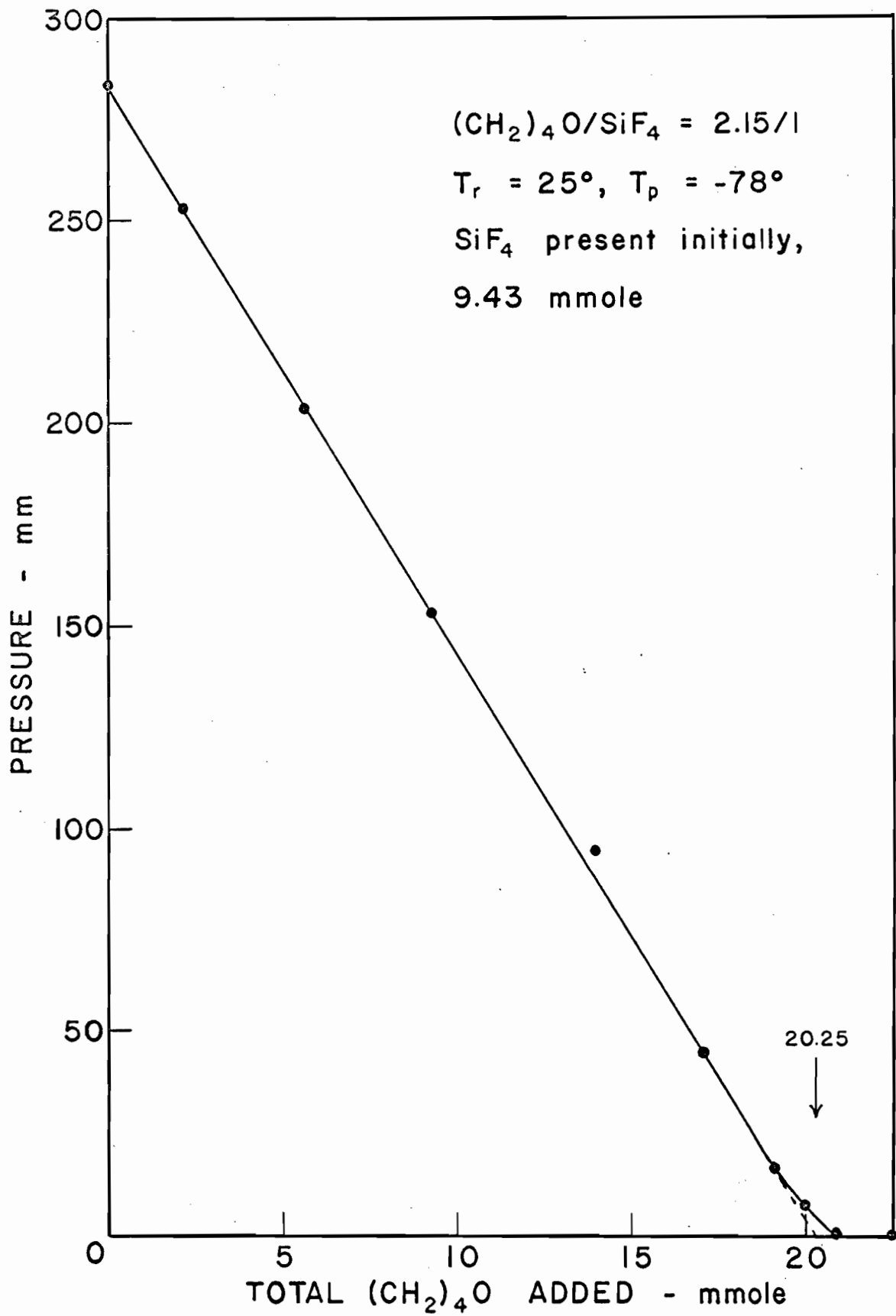
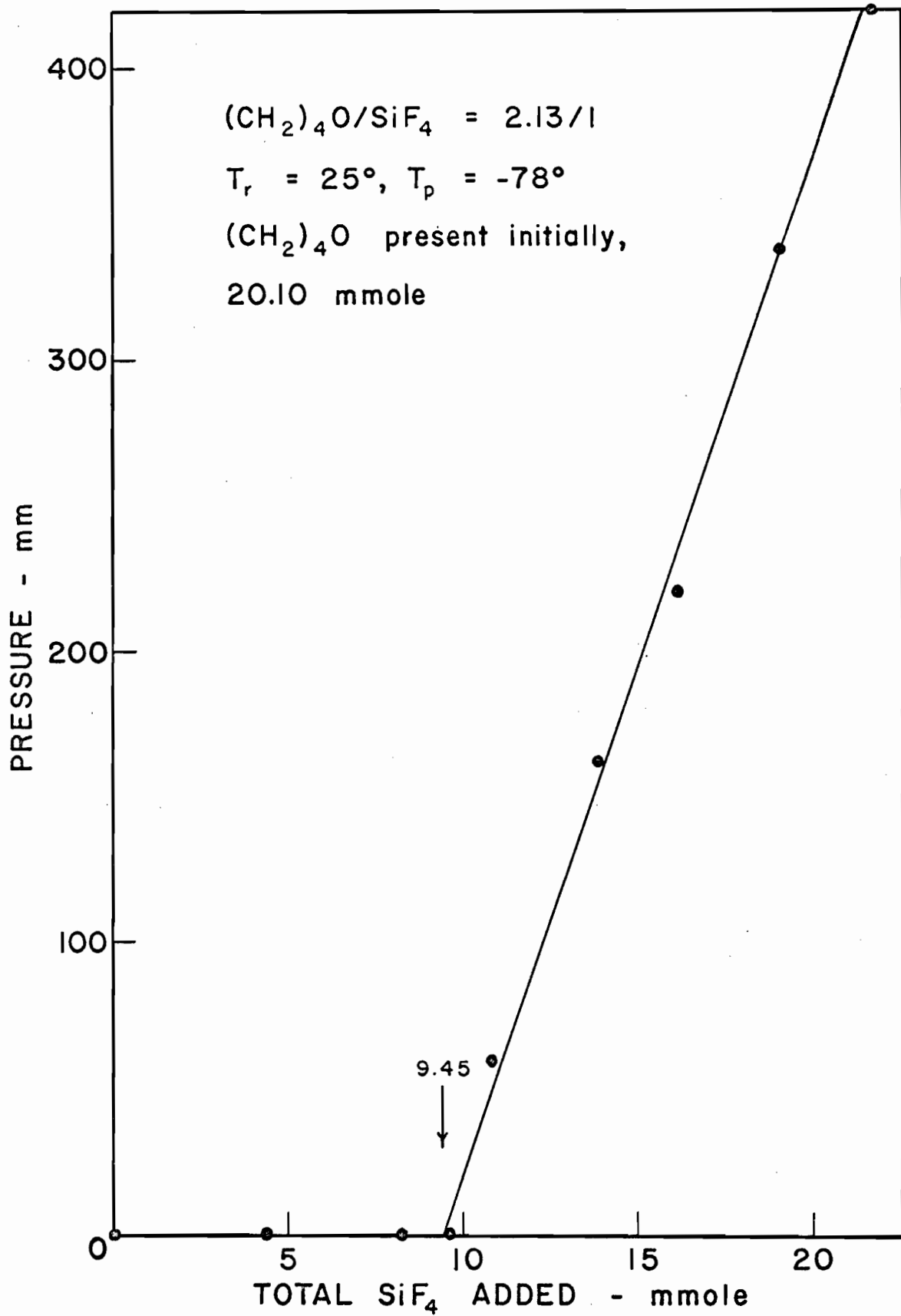


FIG. 25

The tensimetric titration of $(\text{CH}_2)_4\text{O}$ with SiF_4



(iii) Heat of Dissociation

The complex, $\text{SiF}_4 \cdot 2(\text{CH}_2)_4\text{O}$, was prepared as previously described in section 3(i) by removal of unreacted SiF_4 (3.10 mmole) from a mixture of SiF_4 (6.74 mmole) and $(\text{CH}_2)_4\text{O}$ (7.63 mmole). Pressure-temperature measurements were made from -69.0 to -30.8° . The results (Table 17) are plotted in Fig. 26, and a heat of dissociation of 11.3 ± 0.3 kcal mole⁻¹ was calculated from the slope of the straight line.

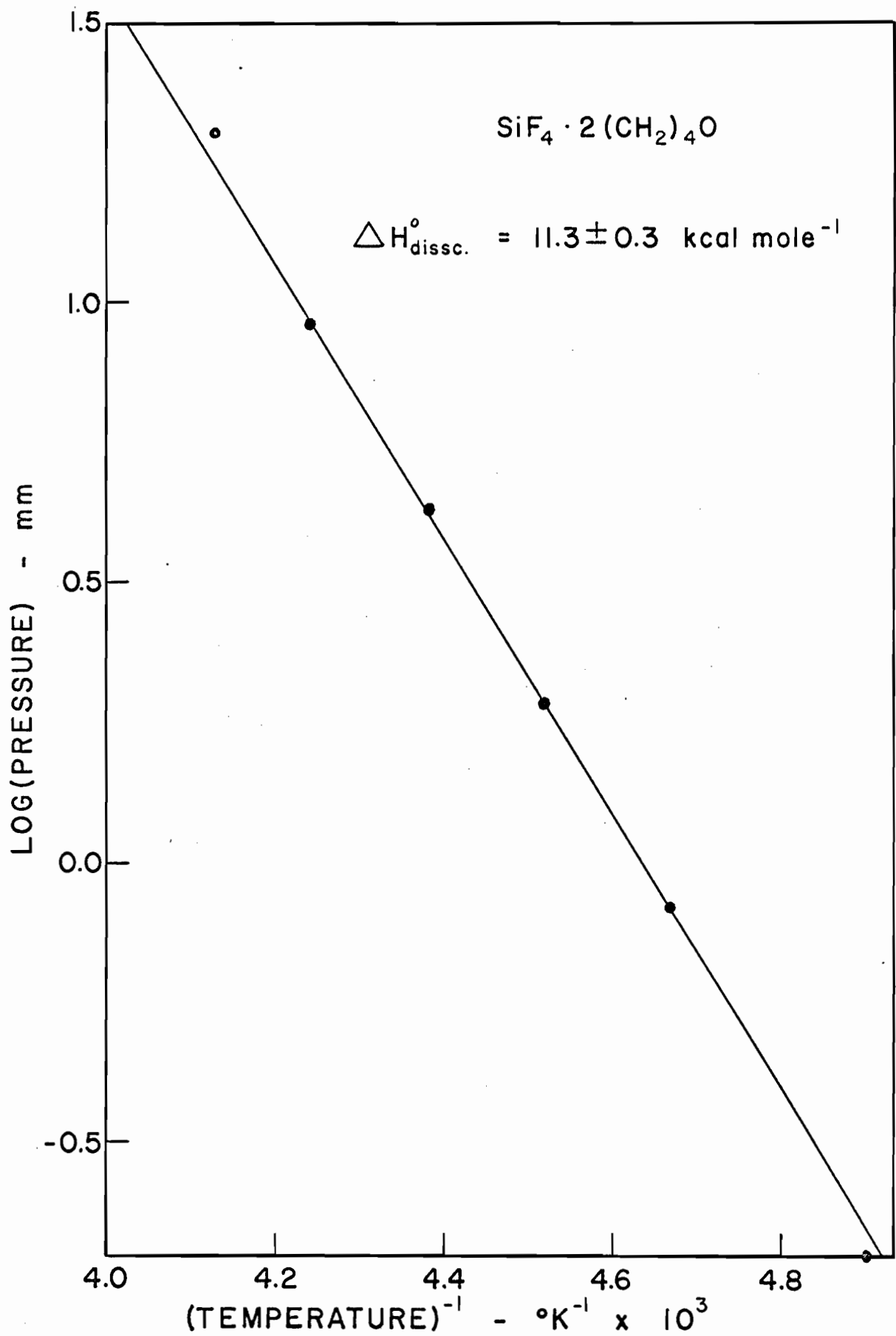
TABLE 17

Data for the heat of dissociation of $\text{SiF}_4 \cdot 2(\text{CH}_2)_4\text{O}$

Temperature			Pressure	Calculations,
$^{\circ}\text{C}$	$^{\circ}\text{K}$	$^{\circ}\text{K}^{-1} \times 10^3$	mm	$\Delta H^{\circ} = \frac{-\log (P_1/P_2)}{T_1^{-1} - T_2^{-1}} \times 2.303 \times 1.987$
-69.0	204.2	4.90	0.20	$P_1 = 20.0 \text{ mm}$
-58.9	214.3	4.67	0.84	$P_2 = 2.0 \text{ mm}$
-51.7	221.5	4.52	1.90	$T_1^{-1} = 4.105 \times 10^{-3} \text{ }^{\circ}\text{K}^{-1}$
-45.0	228.2	4.38	4.28	$T_2^{-1} = 4.512 \times 10^{-3} \text{ }^{\circ}\text{K}^{-1}$
-37.7	235.5	4.24	9.16	
-30.8	242.4	4.13	20.20	$\Delta H^{\circ} = 11.3 \text{ kcal mole}^{-1}$

FIG. 26

Dissociation pressures of $\text{SiF}_4 \cdot 2(\text{CH}_2)_4\text{O}$



4. Coordination of SiF_4 with Tetrahydropyran

(i) Preparation of $\text{SiF}_4 \cdot 2(\text{CH}_2)_5\text{O}$

Unreacted SiF_4 (8.00 mmole) was recovered by distillation at -129° from a mixture of SiF_4 (9.03 mmole) and $(\text{CH}_2)_5\text{O}$ (2.21 mmole) that had been kept at 25° for 30 minutes. These results show that interaction had occurred in a mole ratio 1:2.14, corresponding to the white solid complex, $\text{SiF}_4 \cdot 2(\text{CH}_2)_5\text{O}$. Higher mole ratios resulted when larger quantities of $(\text{CH}_2)_5\text{O}$ were used. These data indicated a surface effect. This problem was not solved until heat of dissociation measurements had been made. From these measurements it was found that no solid complex existed above -54.3° . But at temperatures below -54.3° $(\text{CH}_2)_5\text{O}$ is a solid (m.p. -49°)! Therefore, once the temperature has been sufficiently decreased to freeze the $(\text{CH}_2)_5\text{O}$, further reaction with SiF_4 becomes very difficult. It is obvious that the bulk of the $(\text{CH}_2)_5\text{O}$ could not be reached by the SiF_4 once the surface has become solid. This means that the smaller the bulk of $(\text{CH}_2)_5\text{O}$, the more efficiently SiF_4 can reach all parts of it. The results corroborate this. Undoubtedly this incomplete reaction effect gave the somewhat high mole ratio of 2.14 even when the quantity of $(\text{CH}_2)_5\text{O}$ used was fairly low.

Infrared and molecular weight measurements of the gas at 25° in equilibrium with the liquid at 25° showed that the complex was completely dissociated in the gas phase at 25° (Found: M, 95.0. Calc. M, 97.5, assuming complete dissociation of the complex in the gas phase and establishment of $(\text{CH}_2)_5\text{O}$'s v.p. = 70 mm at 25°). The infrared of the

liquid phase at 25° showed only the presence of $(\text{CH}_2)_5\text{O}$.

As in the case of $\text{SiF}_4 \cdot 2(\text{CH}_2)_4\text{O}$, it was not possible to prepare the pure complex by direct synthesis using excess $(\text{CH}_2)_5\text{O}$ for similar reasons.

(ii) Tensimetric Titration

Attempts at tensimetric titrations at -95° of SiF_4 with $(\text{CH}_2)_5\text{O}$ or vice versa resulted in erratic pressure-composition plots. Invariably the pressure readings were much higher than they should have been assuming the formation of only the 1:2 complex, $\text{SiF}_4 \cdot 2(\text{CH}_2)_5\text{O}$. The change in slope was generally too gradual to read the mole ratio with any degree of accuracy.

The reasons for this phenomenon have been mentioned in the previous section. It is a result of the relatively high melting point of $(\text{CH}_2)_5\text{O}$ (-49°) and the large dissociation pressure of $\text{SiF}_4 \cdot 2(\text{CH}_2)_5\text{O}$ near this temperature.

(iii) Heat of Dissociation

Using identical quantities, the complex, $\text{SiF}_4 \cdot 2(\text{CH}_2)_5\text{O}$ (1.03 mmole), was prepared as described in section 4(i). Dissociation pressure measurements were made over the temperature range -83.0 to -54.3° and the results (Table 18) are plotted in Fig. 27. From the slope of the straight line, the heat of dissociation was found to be 11.1 ± 0.3 kcal mole⁻¹.

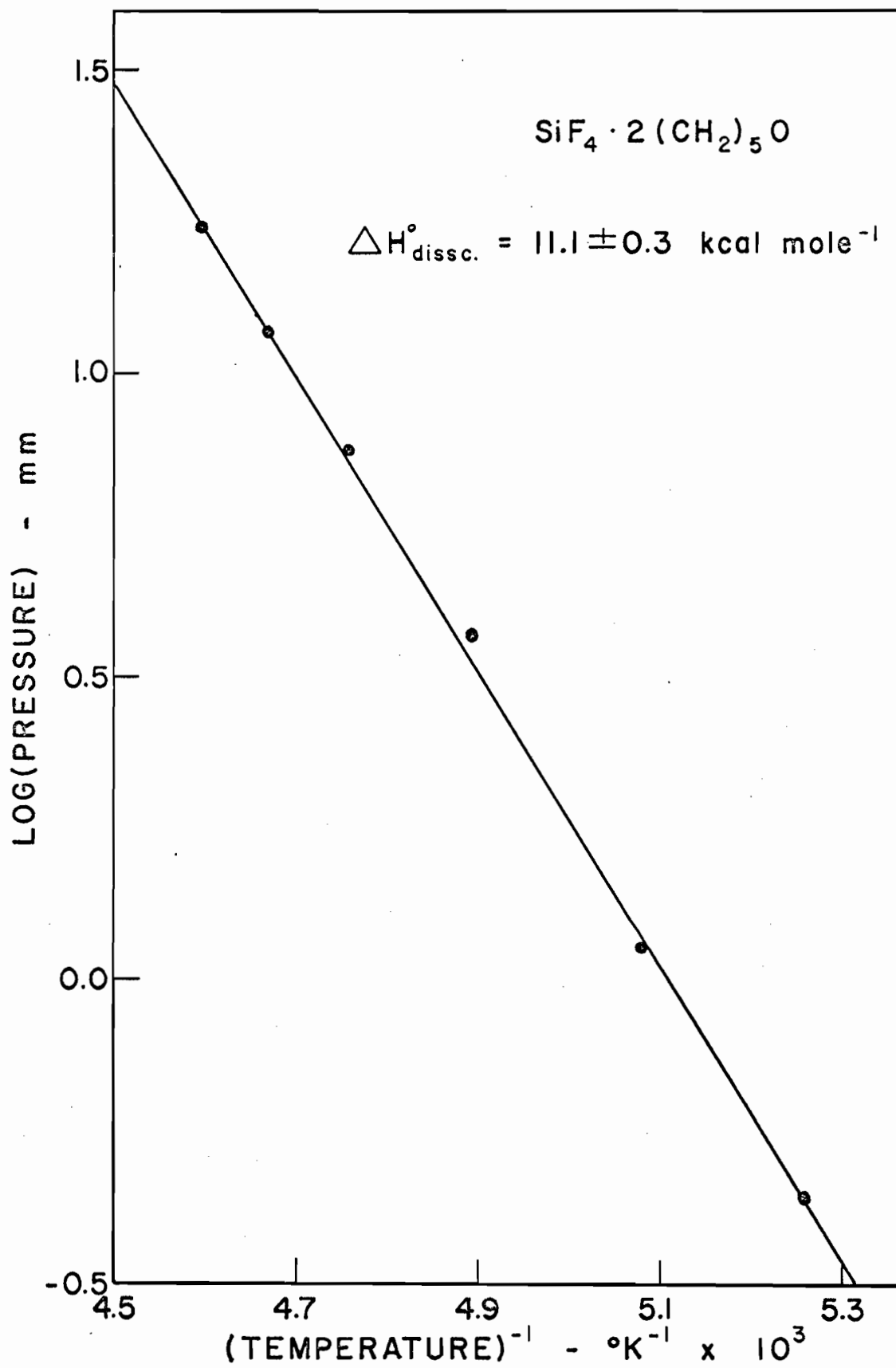
TABLE 18

Data for the heat of dissociation of $\text{SiF}_4 \cdot 2(\text{CH}_2)_5\text{O}$

Temperature			Pressure	Calculations,
$^{\circ}\text{C}$	$^{\circ}\text{K}$	$^{\circ}\text{K}^{-1} \times 10^3$	mm	$\Delta H^{\circ} = \frac{-\log (P_1/P_2)}{T_1^{-1} - T_2^{-1}} \times 2.303 \times 1.987$
-83.0	190.2	5.260	0.44	$P_1 = 20.0 \text{ mm}$
-76.1	197.1	5.080	1.13	$P_2 = 2.0 \text{ mm}$
-68.7	204.5	4.890	3.69	$T_1^{-1} = 4.577 \times 10^{-3} \text{ }^{\circ}\text{K}^{-1}$
-63.0	210.2	4.760	7.40	$T_2^{-1} = 4.988 \times 10^{-3} \text{ }^{\circ}\text{K}^{-1}$
-58.9	214.3	4.670	11.65	
-54.3	218.9	4.570	17.36	$\Delta H^{\circ} = 11.1 \text{ kcal mole}^{-1}$

FIG. 27

Dissociation pressures of $\text{SiF}_4 \cdot 2(\text{CH}_2)_5\text{O}$



5. Coordination of SiF_4 with Dimethyl Ether

(i) Preparation of $\text{SiF}_4 \cdot 2(\text{CH}_3)_2\text{O}$

In a typical experiment, SiF_4 (3.83 mmole) and $(\text{CH}_3)_2\text{O}$ (3.09 mmole) were combined at 25° and the mixture was cooled slowly to -129° . From the amount of SiF_4 (2.29 mmole) recovered by distillation at -129° , it was evident that SiF_4 and $(\text{CH}_3)_2\text{O}$ had reacted in a mole ratio 1:2.01, corresponding to the white solid complex, $\text{SiF}_4 \cdot 2(\text{CH}_3)_2\text{O}$.

Increasing the temperature of the complex to 25° resulted in its complete dissociation into SiF_4 and $(\text{CH}_3)_2\text{O}$ as shown by the infrared and molecular weight measurements on the gas mixture at 25° (Found: M, 65.4. Calc. M, 65.4 for the complete dissociation of the complex into its gaseous products). No liquid or solid remained at 25° .

As in previous cases and for similar reasons, it was not possible to obtain pure $\text{SiF}_4 \cdot 2(\text{CH}_3)_2\text{O}$ by a direct synthesis using an excess of $(\text{CH}_3)_2\text{O}$ initially.

(ii) Tensimetric Titration

Fig. 28 (Table 19) shows the result of the tensimetric titration of SiF_4 (3.65 mmole) with $(\text{CH}_3)_2\text{O}$. Pressure measurements were made at -78° and reaction was allowed to occur at 25° . As shown in Fig. 28, the pressure decreased linearly until the mole ratio, $(\text{CH}_3)_2\text{O}/\text{SiF}_4$, had increased to nearly 2, when the pressure decreased much more rapidly attaining a minimum at a mole ratio of 2.01 (corresponding to the addition of 7.33

mmole $(\text{CH}_3)_2\text{O}$), after which it increased rapidly to 40 mm (the v.p. of $(\text{CH}_3)_2\text{O}$ at -78° is 35 mm) and became constant.

Fig. 29 (Table 19) shows the reverse tensimetric titration of $(\text{CH}_3)_2\text{O}$ (10.04 mmole) by the addition of SiF_4 . In this case, the pressure remained constant at 35 mm until the mole ratio had decreased to nearly 2, when the pressure dropped sharply to a minimum at a mole ratio of 2.01 (corresponding to the addition of 5.00 mmole SiF_4), after which it increased rapidly.

Both of these plots indicated the formation of only the 1:2 complex, $\text{SiF}_4 \cdot 2(\text{CH}_3)_2\text{O}$.

TABLE 19

Tensimetric titration of SiF_4 with $(\text{CH}_3)_2\text{O}$ and $(\text{CH}_3)_2\text{O}$ with SiF_4

SiF_4 with $(\text{CH}_3)_2\text{O}$ (Fig. 22)		$(\text{CH}_3)_2\text{O}$ with SiF_4 (Fig. 23)	
SiF_4 present initially, 3.65 mmole		$(\text{CH}_3)_2\text{O}$ present initially, 10.04 mmole	
$T_r, 25^\circ; T_p, -78^\circ$		$T_r, 25^\circ; T_p, -78^\circ$	
Total $(\text{CH}_3)_2\text{O}$ added mmole	Pressure mm	Total SiF_4 added mmole	Pressure mm
0	194.4	0	35.2
1.83	165.5	1.79	35.2
3.59	139.6	3.71	35.0
5.40	90.0	4.83	35.0
7.14	55.0	5.00	25.0
7.28	27.0	5.14	38.0
7.33	15.0	5.28	50.1
7.50	33.0	5.78	74.9
8.03	40.1	6.17	120.1
9.14	40.2	7.43	168.8
10.00	40.2		

FIG. 28

The tensimetric titration of SiF_4 with $(\text{CH}_3)_2\text{O}$

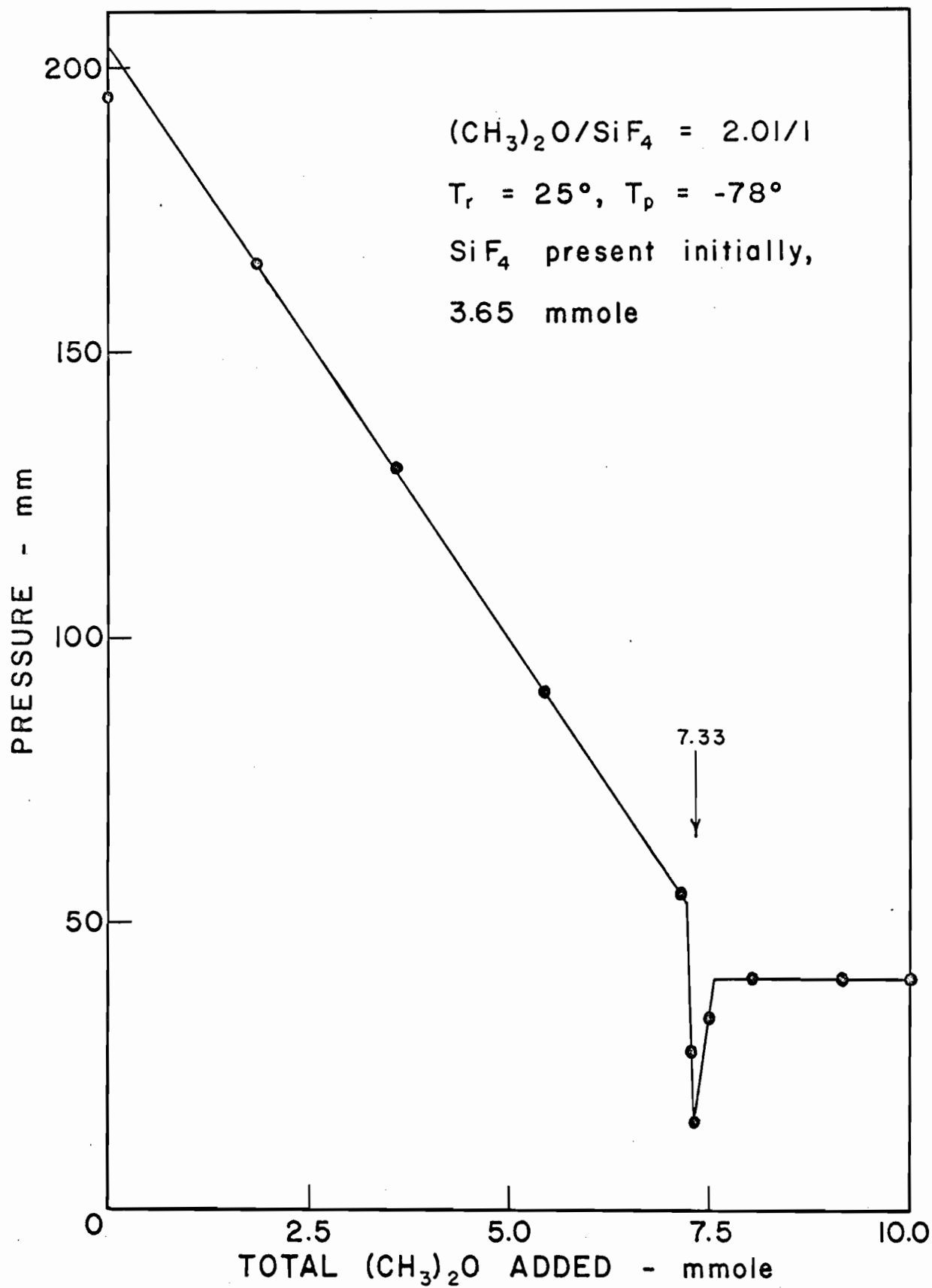
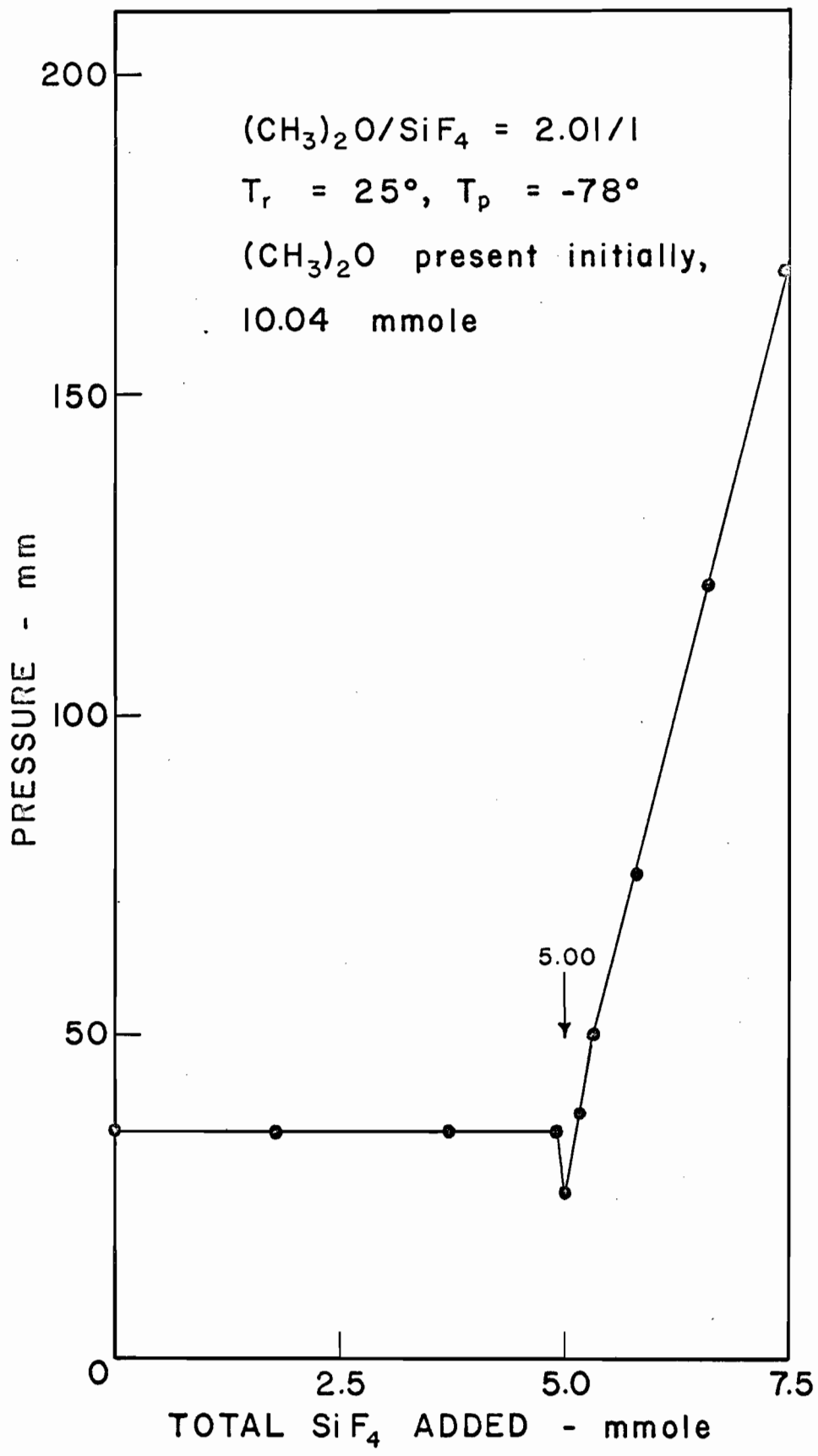


FIG. 29

The tensimetric titration of $(\text{CH}_3)_2\text{O}$ with SiF_4



(iii) Heat of Dissociation

A sample of $\text{SiF}_4 \cdot 2(\text{CH}_3)_2\text{O}$ (1.54 mmole) was prepared as described in section 5(i) using identical quantities. Pressure-temperature measurements were made in the range -94.0 to -56.6° and the results (Table 20) are plotted in Fig. 30. The slope of the straight line over this temperature range indicated a heat of dissociation of 9.0 ± 0.3 kcal mole⁻¹.

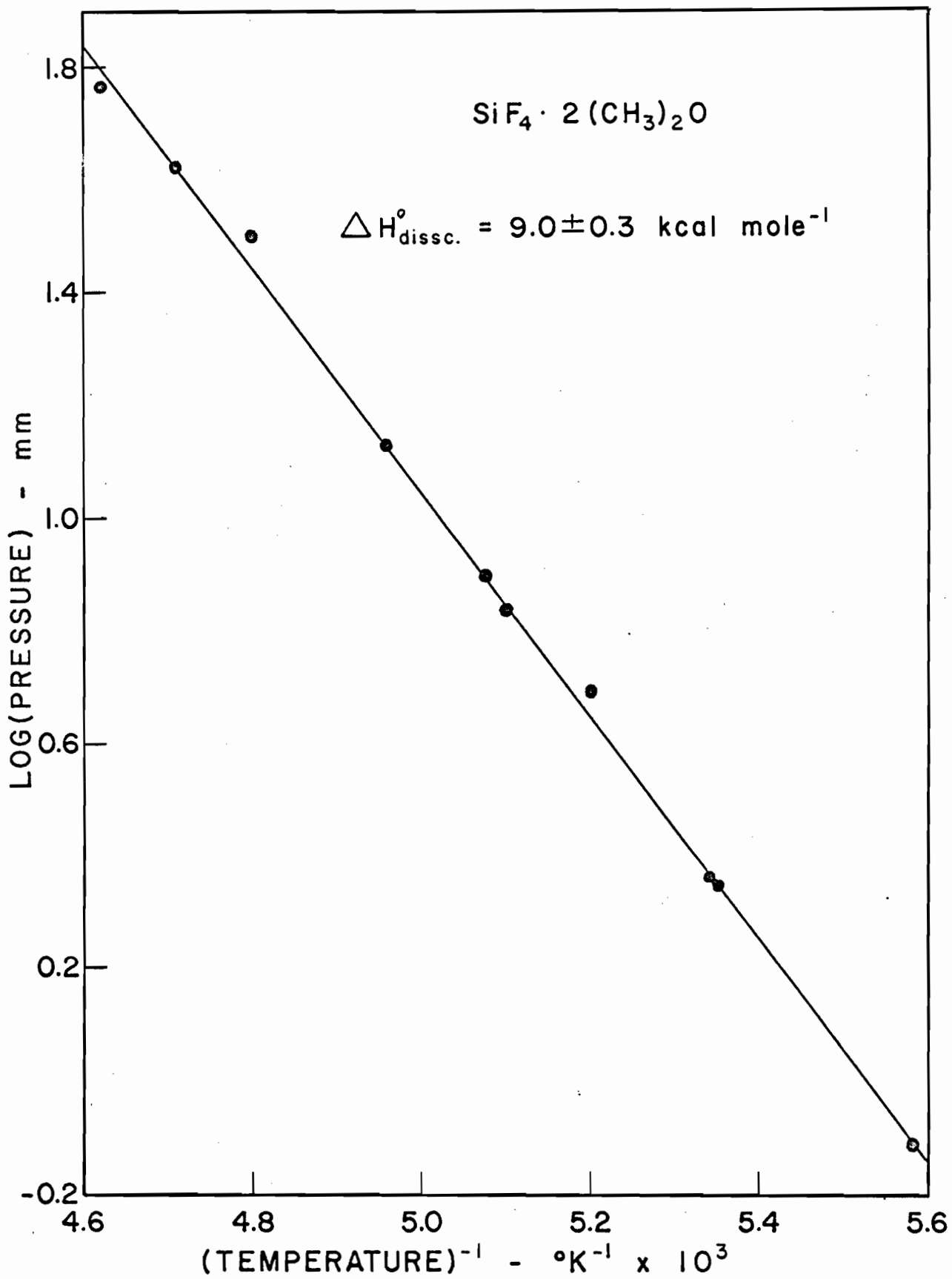
TABLE 20

Data for the heat of dissociation of $\text{SiF}_4 \cdot 2(\text{CH}_3)_2\text{O}$

Temperature			Pressure mm	Calculations, $\Delta H^\circ = \frac{-\log(P_1/P_2)}{T_1^{-1} - T_2^{-1}} \times 2.303 \times 1.987$
$^\circ\text{C}$	$^\circ\text{K}$	$^\circ\text{K}^{-1} \times 10^3$		
-94.0	179.2	5.58	0.77	$P_1 = 20.0 \text{ mm}$
-86.3	186.9	5.35	2.25	$P_2 = 2.0 \text{ mm}$
-85.9	187.3	5.34	2.30	$T_1^{-1} = 4.872 \times 10^{-3} \text{ }^\circ\text{K}^{-1}$
-80.9	192.3	5.20	4.90	$T_2^{-1} = 5.378 \times 10^{-3} \text{ }^\circ\text{K}^{-1}$
-77.2	196.0	5.10	6.81	
-76.3	196.9	5.08	8.00	$\Delta H^\circ = 9.0 \text{ kcal mole}^{-1}$
-71.7	201.5	4.96	13.52	
-64.7	208.5	4.80	31.81	
-60.6	212.5	4.71	41.87	
-56.6	216.6	4.62	57.88	

FIG. 30

Dissociation pressures of $\text{SiF}_4 \cdot 2(\text{CH}_3)_2\text{O}$



6. Attempted Reaction of SiF_4 with 1,4-dioxane

Silicon tetrafluoride (1.96 mmole) and 1,4-dioxane (10.80 mmole) were condensed together and pressures were measured in the temperature range -94 to 25° . These observed pressures were compared with the total pressure calculated assuming no interaction and ideal gaseous behavior (Dalton's Law of Partial Pressures), as shown in Table 21. This comparison reveals that no interaction had occurred in the temperature range -94 to 25° . Distillation at -115 and -129° in both cases yielded all the SiF_4 (1.94 mmole). Infrared measurement on the gas phase at 25° in equilibrium with the liquid at 25° showed only SiF_4 and 1,4-dioxane absorption bands, while measurements on the liquid phase at 25° showed only 1,4-dioxane absorption bands.

TABLE 21

Temperature-pressure data showing no complex formation

<u>Temperature</u> <u>°C</u>	<u>SiF₄</u> <u>pressure</u> <u>mm</u>	<u>1,4-dioxane</u> <u>pressure</u> <u>mm**</u>	<u>Mixture</u> <u>pressure</u> <u>mm (Obs.)</u>	<u>Mixture</u> <u>pressure</u> <u>mm (Calc.)*</u>
-94	100.0	0	101.5	100.0
-78	102.0	0	104.5	102.0
-45	104.9	0.1	106.0	105.0
-23	105.8	2.1	108.0	107.9
0	106.5	8.5	115.0	115.0
25	107.1	30.9	137.1	138.0

* Dalton's Law: $P_{\text{mixture}} = P_{\text{SiF}_4} + P_{1,4\text{-dioxane}}$

** Equilibrium v.p. of 1,4-dioxane at that temperature.

III. Coordination of SiF_4 with Pyridine and Other Nitrogen Electron-Pair Donor Molecules

1. Coordination of SiF_4 with Pyridine

(i) Preparation of $\text{SiF}_4 \cdot 2\text{C}_5\text{H}_5\text{N}$

Various methods of preparation always yielded only the 1:2 complex, $\text{SiF}_4 \cdot 2\text{C}_5\text{H}_5\text{N}$, when SiF_4 was mixed with $\text{C}_5\text{H}_5\text{N}$ at 25° .

In the direct vacuum synthesis, SiF_4 (35.45 mmole) was condensed over $\text{C}_5\text{H}_5\text{N}$ (27.12 mmole) and the mixture slowly warmed to 25° . Distillation at -78° yielded SiF_4 (21.90 mmole), indicating a combining ratio of 1:2.00, which corresponded to the complex, $\text{SiF}_4 \cdot 2\text{C}_5\text{H}_5\text{N}$. Fluorine analysis showed that the complex was pure (Found: %F, 28.60. Calc. %F, 28.95 for $\text{SiF}_4 \cdot 2\text{C}_5\text{H}_5\text{N}$). The white solid complex melted at $170-180^\circ$ (with decomposition), had no measurable vapor pressure at 25° , but could be sublimed in a vacuum at $60-80^\circ$ (without decomposition) into white opaque crystals (Found: %F, 29.01). Its ease of hydrolysis was manifested by the odor of $\text{C}_5\text{H}_5\text{N}$ when it was exposed to moist air.

The same complex resulted when an excess of $\text{C}_5\text{H}_5\text{N}$ was used initially. Thus $\text{C}_5\text{H}_5\text{N}$ (40.40 mmole) when condensed over SiF_4 (15.00 mmole) and slowly warmed to 25° produced unreacted SiF_4 (10.38 mmole) recovered by distillation at 25° , and a white solid which contained SiF_4 and $\text{C}_5\text{H}_5\text{N}$ in a mole ratio 1:2.00, as required for the 1:2 complex, $\text{SiF}_4 \cdot 2\text{C}_5\text{H}_5\text{N}$ (Found: %F, 28.60).

Silicon tetrafluoride (15.10 mmole) was condensed over a 10.5% by weight solution of C_5H_5N (12.10 mmole) in diethyl ether (183.0 mmole) and the mixture was warmed slowly to 25° and stirred magnetically. The resulting insoluble white precipitate was made solvent free by a vacuum distillation at 25° and an analysis for fluorine confirmed that it was pure $SiF_4 \cdot 2C_5H_5N$ (Found: %F, 28.58).

Using the bubbling technique, SiF_4 was bubbled through solutions of C_5H_5N in diethyl ether (1.5, 3.0 and 6.0% by weight) and C_5H_5N in acetonitrile (10% by weight) with the resultant production of copious quantities of white insoluble precipitates which proved also to be the complex, $SiF_4 \cdot 2C_5H_5N$ (Found: %F, 29.40, 29.09, 29.00 for the diethyl ether solution preparation and 28.64 for the acetonitrile solution preparation). Extensive pumping under vacuum did not change the composition of the samples.

(ii) Tensimetric Titration

In the tensimetric titration of SiF_4 (17.52 mmole) with C_5H_5N (Fig. 31, Table 22) pressures were measured after the temperature of the mixture was decreased from 25 to -78° . The pressure decreased linearly to zero at a mole ratio of 1:2.01 (corresponding to the addition of 35.25 mmole C_5H_5N), indicating the formation of only the 1:2 complex, $SiF_4 \cdot 2C_5H_5N$.

In the case of the reverse titration of C_5H_5N (31.02 mmole) with SiF_4 (Fig. 32, Table 22), using the above temperature conditions, the

pressure remained zero until the mole ratio had decreased to 2.01 (corresponding to the addition of 15.45 mmole SiF_4), when it increased rapidly as more SiF_4 was added. This confirmed the formation of only the 1:2 complex.

TABLE 22

Tensimetric titration of SiF_4 with $\text{C}_5\text{H}_5\text{N}$ and $\text{C}_5\text{H}_5\text{N}$ with SiF_4

SiF_4 with $\text{C}_5\text{H}_5\text{N}$ (Fig. 25)		$\text{C}_5\text{H}_5\text{N}$ with SiF_4 (Fig. 26)	
SiF_4 present initially, 17.52 mmole		$\text{C}_5\text{H}_5\text{N}$ present initially, 31.02 mmole	
$T_r, 25^\circ; T_p, -78^\circ$		$T_r, 25^\circ; T_p, -78^\circ$	
Total $\text{C}_5\text{H}_5\text{N}$ added mmole	Pressure mm	Total SiF_4 added mmole	Pressure mm
0	494.9	0	0
3.76	444.4	3.93	0
9.57	361.9	7.98	0
13.52	304.9	11.73	0
17.83	246.8	15.26	0
22.15	185.9	17.25	50.0
26.40	127.9	19.19	106.8
30.53	71.0	22.93	215.3
34.80	2.7	26.90	330.3
39.05	0	30.48	423.6
43.40	0	34.20	539.9
46.50	0	37.91	644.7

FIG. 31

The tensimetric titration of SiF_4 with $\text{C}_5\text{H}_5\text{N}$

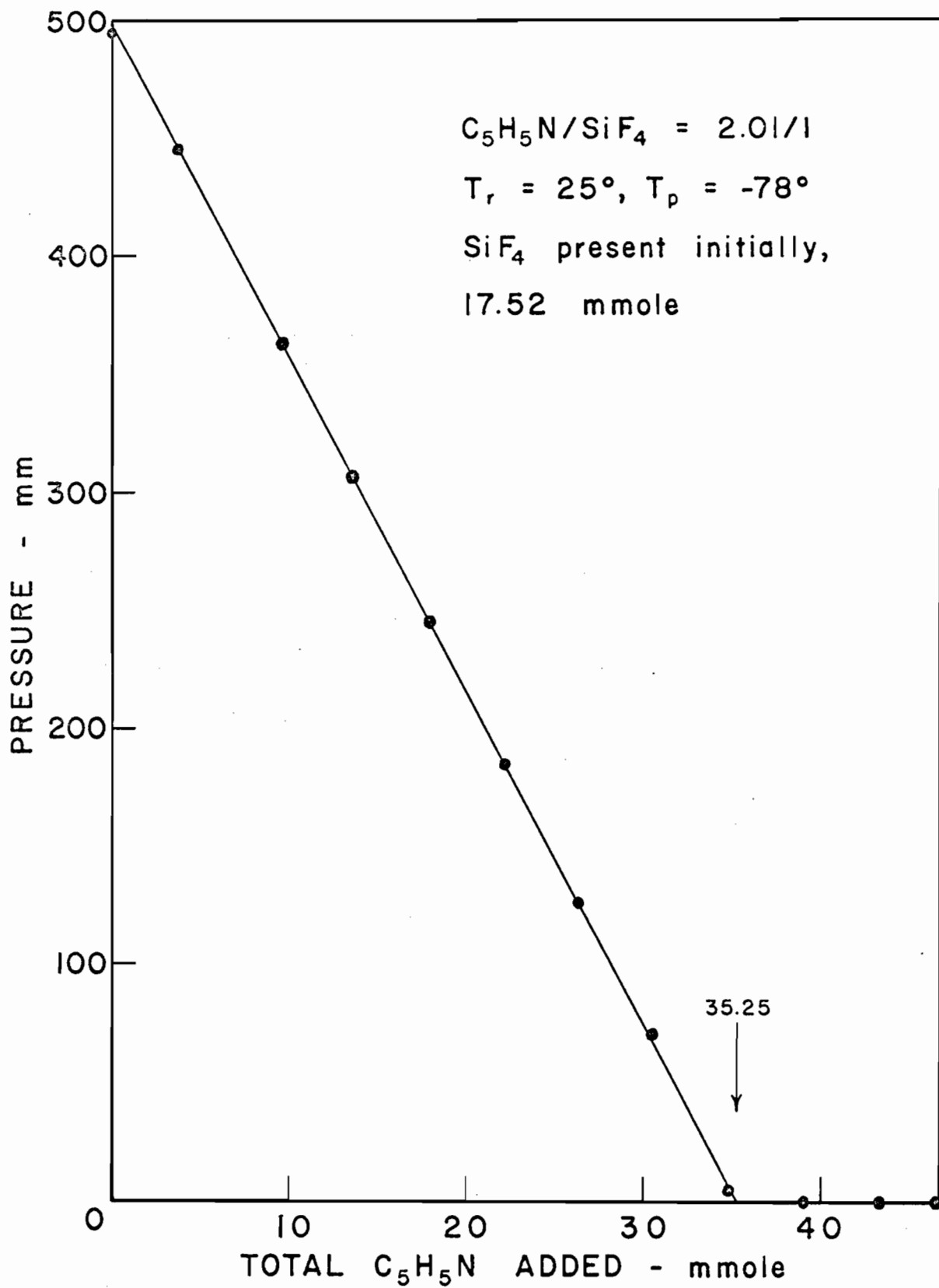
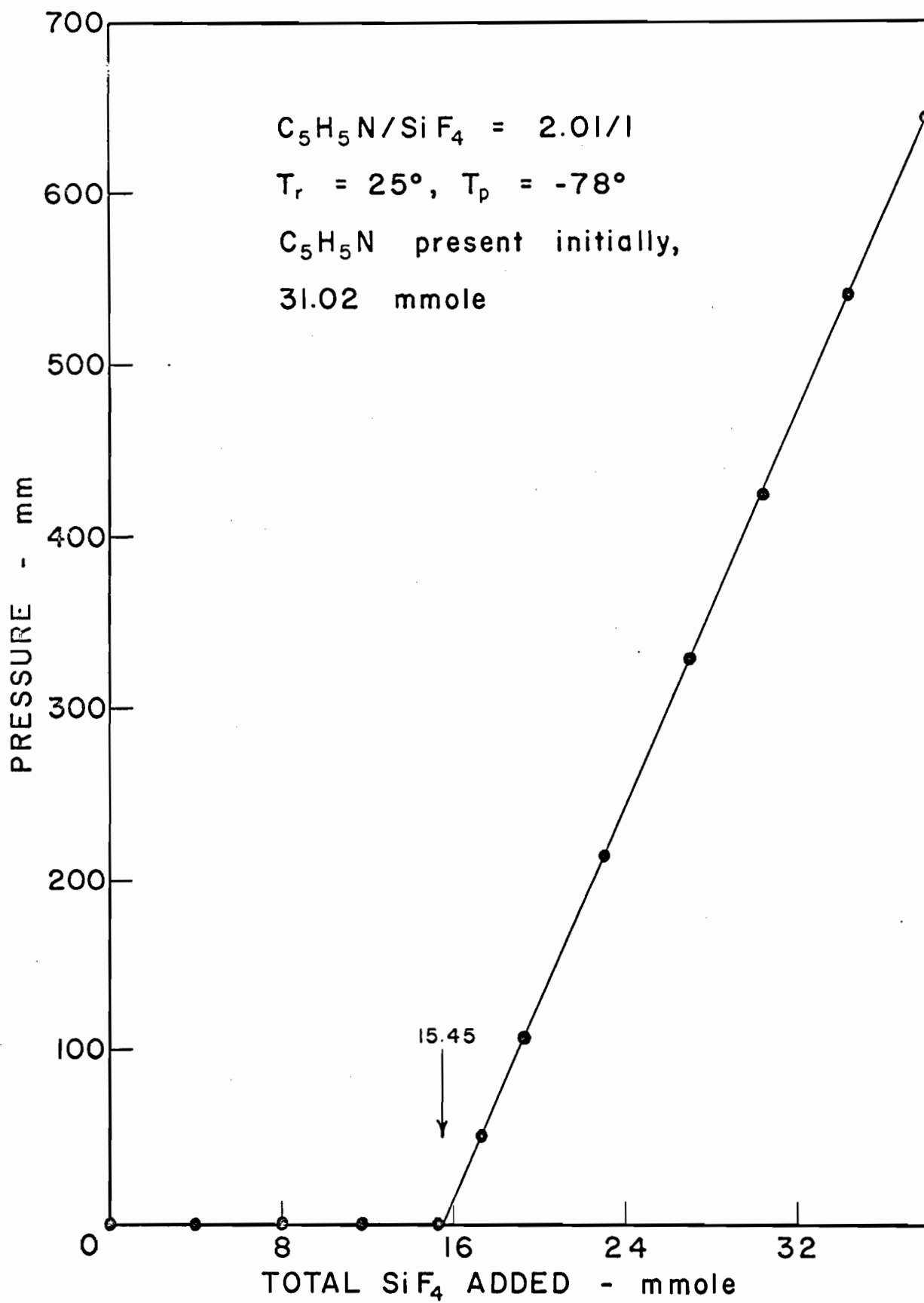


FIG. 32

The tensimetric titration of C_5H_5N with SiF_4



(iii) Displacement Reaction with Ethylenediamine

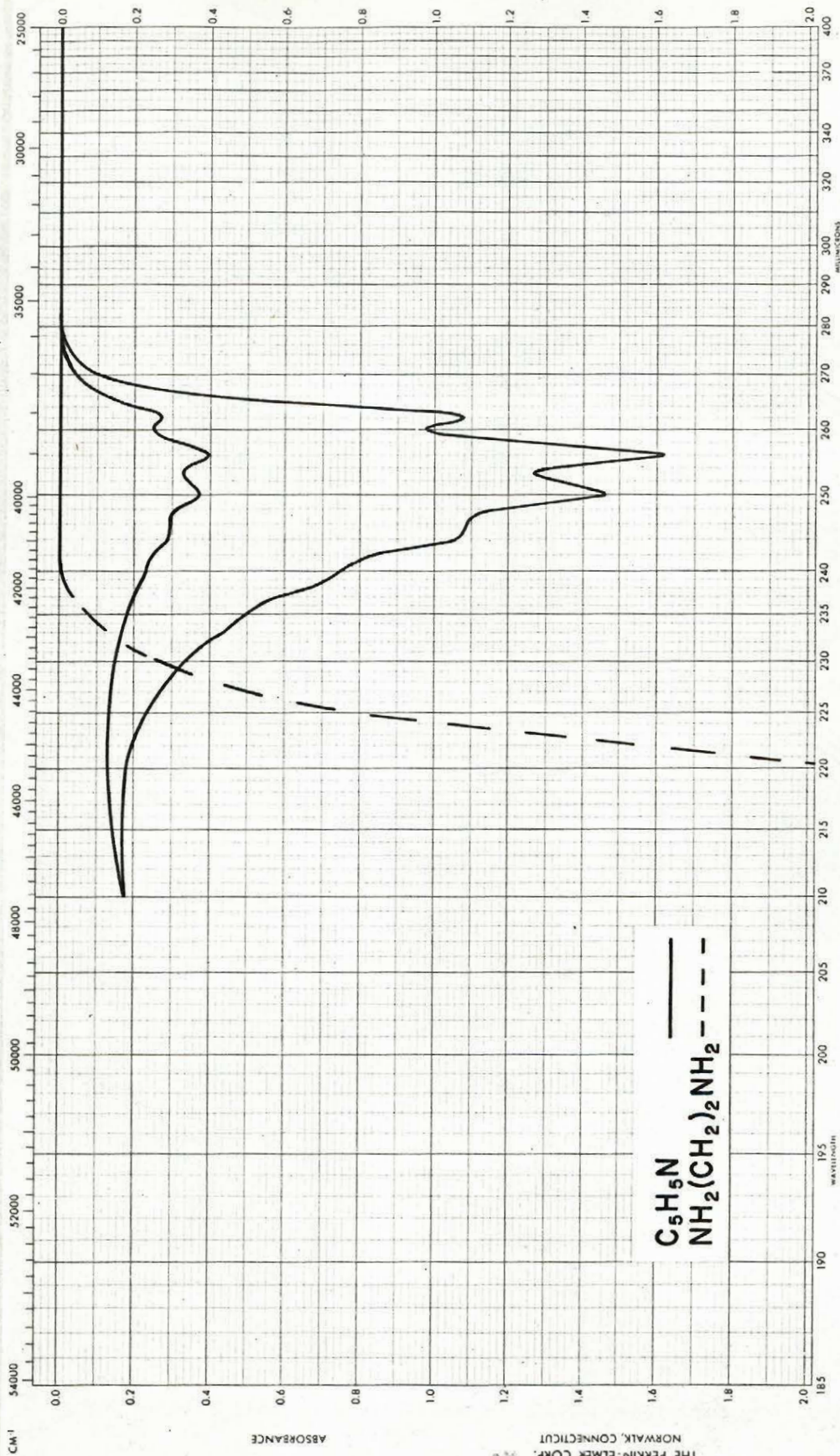
Using the dry box technique, a previously prepared sample of $\text{SiF}_4 \cdot 2\text{C}_5\text{H}_5\text{N}$ (0.9103 g) was mixed with $\text{NH}_2(\text{CH}_2)_2\text{NH}_2$ (1.8198 g) for one hour at 25°. The volatile products (2.0845 g) were then distilled from the remaining yellowish nonvolatile residue. The infrared spectrum of the solid residue showed no $\text{C}_5\text{H}_5\text{N}$ absorption bands and compared well with the infrared spectrum of $\text{SiF}_4 \cdot \text{NH}_2(\text{CH}_2)_2\text{NH}_2$.

Quantitative ultraviolet analysis on the volatile, colorless liquid product showed that it contained $\text{C}_5\text{H}_5\text{N}$ (Found: 0.546 g. Calc. 0.549 g for complete displacement). Calculations on the $\text{NH}_2(\text{CH}_2)_2\text{NH}_2$ consumed resulted in a value larger than theoretical as shown in Table 27 (Found: 0.2808 g. Calc. 0.2085 g for complete displacement). This was probably due to some degradation of the ethylenediamine during the reaction as evidenced by the slight yellowing of the sample. Fig. 33 shows the ultraviolet spectrum of standard $\text{C}_5\text{H}_5\text{N}$ ($4.680 \times 10^{-4} \text{ g.l}^{-1}$) and that of the sample ($4.364 \times 10^{-4} \text{ g.l}^{-1}$) both diluted with absolute ethanol. Also shown in the diagram is the spectrum of a concentrated solution $\text{NH}_2(\text{CH}_2)_2\text{NH}_2$ ($4.028 \times 10^{-2} \text{ g.l}^{-1}$) in absolute ethanol. No interference of absorbances occurred. Table 23 shows how the data were used to calculate the amount of $\text{C}_5\text{H}_5\text{N}$ displaced and of $\text{NH}_2(\text{CH}_2)_2\text{NH}_2$ consumed. The overall reaction may therefore be written as follows,

$$\text{SiF}_4 \cdot 2\text{C}_5\text{H}_5\text{N} + \text{NH}_2(\text{CH}_2)_2\text{NH}_2 \longrightarrow \text{SiF}_4 \cdot \text{NH}_2(\text{CH}_2)_2\text{NH}_2 + 2\text{C}_5\text{H}_5\text{N} + \text{heat.}$$

FIG. 33

Quantitative ultraviolet spectrum in absolute ethanol of the C_5H_5N liberated by $NH_2(CH_2)_2NH_2$ from $SiF_4 \cdot 2C_5H_5N$. Also included are the ultraviolet spectra of standard C_5H_5N and $NH_2(CH_2)_2NH_2$ in absolute ethanol



$\text{C}_5\text{H}_5\text{N}$ ———
 $\text{NH}_2(\text{CH}_2)_2\text{NH}_2$ - - -

TABLE 23

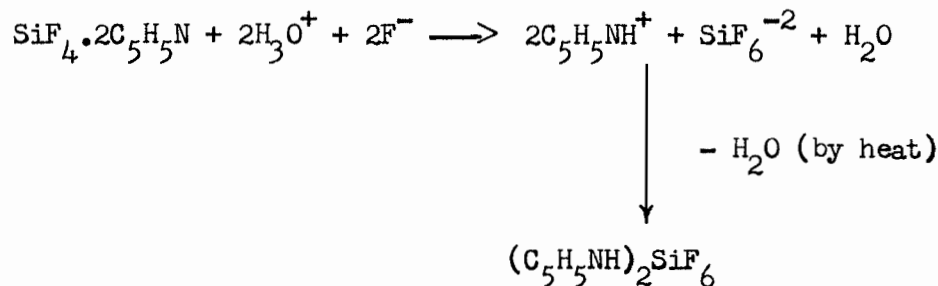
Ultraviolet data for the analysis of the displacement reaction

Given or Observed	Calculated
$A_1 = 1.620$	
$A_2 = 0.395$	$c_2 = 1.142 \times 10^{-4} \text{ g.l}^{-1}$
$c_1 = 4.680 \times 10^{-4} \text{ g.l}^{-1}$	
Sample concentration = $4.364 \times 10^{-4} \text{ g.l}^{-1}$	% $C_5H_5N = 26.20$
Total weight of liquid = 2.0845 g	weight of $C_5H_5N = \underline{0.546 \text{ g}}$
	weight of $NH_2(CH_2)_2NH_2 = 1.539 \text{ g}$
Initial weight of $NH_2(CH_2)_2NH_2 = 1.8198 \text{ g}$	weight of $NH_2(CH_2)_2NH_2$ consumed = $\underline{0.2808 \text{ g}}$

(iv) Reaction of $\text{SiF}_4 \cdot 2\text{C}_5\text{H}_5\text{N}$ with aqueous HF

Mixing $\text{SiF}_4 \cdot 2\text{C}_5\text{H}_5\text{N}$ (3.21 mmole) with excess 48% HF (~ 15 ml) in a platinum crucible and gently boiling the resultant colorless solution to dryness produced a white solid. Heating the solid in an oven at 105° for two hours did not remove all the unreacted HF as evident by the analysis (Found: %F, 39.2. Calc. %F, 37.7 for $(\text{C}_5\text{H}_5\text{NH})_2\text{SiF}_6$) and by the fact that the solid evolved HF (shown by the etching of the sample vial). Finally, vacuum sublimation of this solid at 165° resulted in pure pyridinium hexafluorosilicate, $(\text{C}_5\text{H}_5\text{NH})_2\text{SiF}_6$ (Found: %F, 37.3), in 100% yield (3.21 mmole). The hydrolysis product, $(\text{C}_5\text{H}_5\text{NH})_2\text{SiF}_6$, was not hygroscopic and melted without decomposition at 154-157°, some sublimation occurring.

The overall reaction may be written as follows,



(v) Infrared Spectrum of $\text{SiF}_4 \cdot 2\text{C}_5\text{H}_5\text{N}$ and $(\text{C}_5\text{H}_5\text{NH})_2\text{SiF}_6$

Figs. 34 and 35 show the infrared spectrum of $\text{SiF}_4 \cdot 2\text{C}_5\text{H}_5\text{N}$ and $(\text{C}_5\text{H}_5\text{NH})_2\text{SiF}_6$, respectively; frequency assignments are given in Table 24. Most of the frequency assignments were made by comparison of their infrared spectra with that of pure liquid $\text{C}_5\text{H}_5\text{N}$ (44, 49-53) and gaseous SiF_4 .

TABLE 24

Comparisons and assignment of infrared absorption frequencies (cm^{-1})

$\text{SiF}_4 \cdot 2\text{C}_5\text{H}_5\text{N}$		$(\text{C}_5\text{H}_5\text{NH})_2\text{SiF}_6$		$\text{C}_5\text{H}_5\text{N}$	SiF_4	Assignment
solid (Fig. 29)		solid (Fig. 28)		liquid	gas	
Nujol	KBr	Nujol	KBr			
				3400w		unidentified (44)
3140w	3130w	3220m	3200m	3080s		$\nu(\text{C-H})$, py
3125w	3120w	3130m	3140m	3050s		"
3090w	3080w	3080m	3120m	3030s		"
3070w	3060w	3070m	3045s	3022s		"
3050w	3040w		2920s	3000s		"
			2850s			"
		2720w,b	2770s,b			$\nu(\text{N}^+-\text{H})$, H-bonded (45)
					2060vw	SiF_4 , combination
1992w	1982w	2100w	2030w	1975w		overtones and
1945w	1940w	1990w	1940w	1910w		combinations, py
1865w	1860w	1875w	1870vw	1860w		
					1830vw	SiF_4 , combination
				1672w		$\nu(\text{C}=\text{C})$ and $\nu(\text{C}=\text{N})$, py
		1630m	1630s			$\delta(\text{N}^+-\text{H})$, H-bonded
1615s	1612s	1610m	1610s	1622m		$\nu(\text{C}=\text{C})$ and $\nu(\text{C}=\text{N})$, py
1575s	1568s	1590m		1585s		"
				1570s		"
		1530m	1530s	1565s		"
1483m	1477s	1480m	1480s	1472s		"
nujol	1443s	nujol		1430s		$\delta(\text{C-H})$, i.p.py ring vibration
					1390vw	SiF_4 , combination
nujol		nujol	1367w	1365w		$\delta(\text{C-H})$, i.p.py ring vibration
			1330w			"
1250w	1245w	1245w	1245m			"
			1238m			"
1204m	1200m	1190w	1190mw	1210s		"
					1192vw	SiF_4 , combination
1158m	1152m	1160w	1153mw	1139s		$\delta(\text{C-H})$, i.p.py ring vibration
		1090w	1085mw			"
1071s	1067s	1055m	1055m	1062s		$\delta(\text{C-H})$, o.p.py ring vibration
1049m	1045m		1035mw			$\delta(\text{C-H})$, i.p.py ring vibration
					1035vs	$\nu(\text{Si-F})$ tetrahedral
					1032vs	"

.....

TABLE 24 (cont'd.)

$\text{SiF}_4 \cdot 2\text{C}_5\text{H}_5\text{N}$		$(\text{C}_5\text{H}_5\text{NH})_2\text{SiF}_6$		$\text{C}_5\text{H}_5\text{N}$	SiF_4	Assignment
solid (Fig.29)		solid (Fig.28)		liquid	gas	
Nujol	KBr	Nujol	KBr			
102lm	1018w		995mw	1023s		$\delta(\text{C-H})$, i.p.py ring vibration
957w	950w	950m	912w,b	985s		$\delta(\text{C-H})$, o.p.py ring vibration
874w		875w,b	880w	875w		$\delta(\text{C-H})$, i.p.py ring vibration
798vs	792s					$\nu(\text{Si-F})$ octahedral for $\text{SiF}_4 \cdot 2 \text{ py}$
762s	754s	750s	750vs	743s		$\delta(\text{C-H})$, o.p.py ring vibration
683s	679s	735s 720s	740vs	705s		" $\nu(\text{Si-F})$ octahedral for SiF_6^{-2}
656s	653s	674s	674s	693s		$\delta(\text{C-H})$, o.p.py ring vibration
		598m	600mw	598s		$\delta(\text{C-H})$, i.p.py ring vibration
484s	488s	485s	487s			? (Si-F) octahedral (mixed** (46) fundamental)
476s	481s	467s	480s			py coordinated to Si (47,48)
387w	389vw	380vw	390vw	402m		$\delta(\text{C-H})$, o.p.py ring vibration

Note: Nujol absorption bands, 2920 (vs), 2855 (vs), 1460 (s), 1370 (m), 720 (w).

** A mixed or coupled vibration is one that is neither a stretching nor a deformation vibration but a combination of the two.

FIG. 34

The infrared spectrum of $\text{SiF}_4 \cdot 2\text{C}_5\text{H}_5\text{N}$

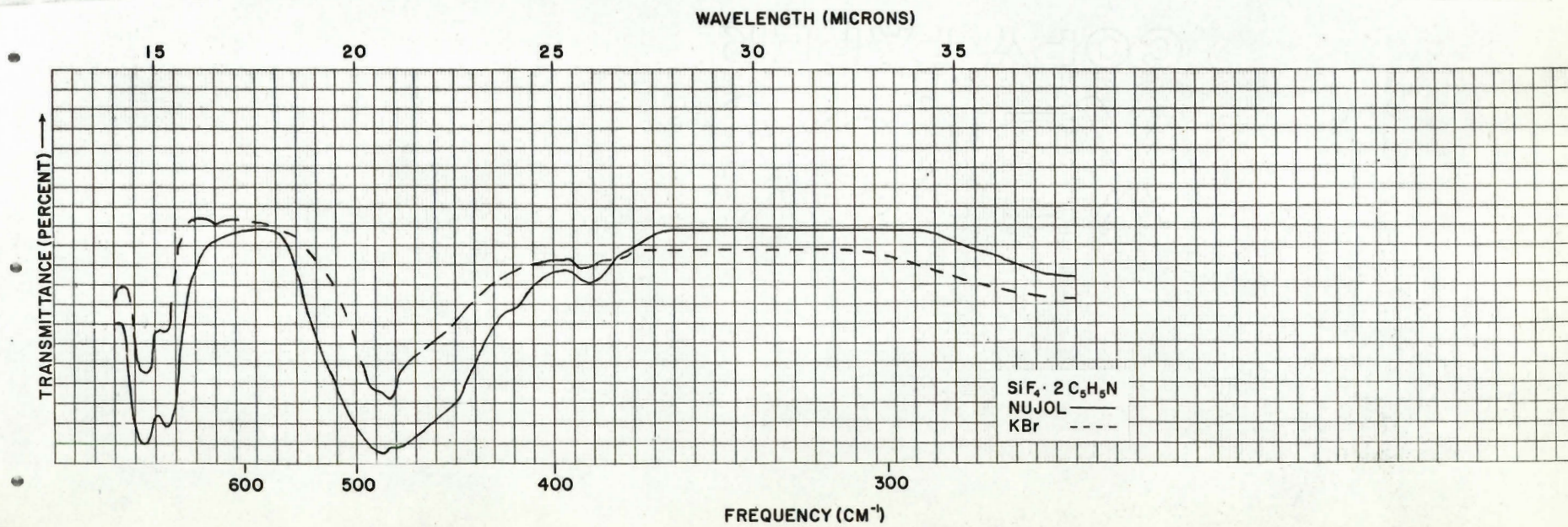
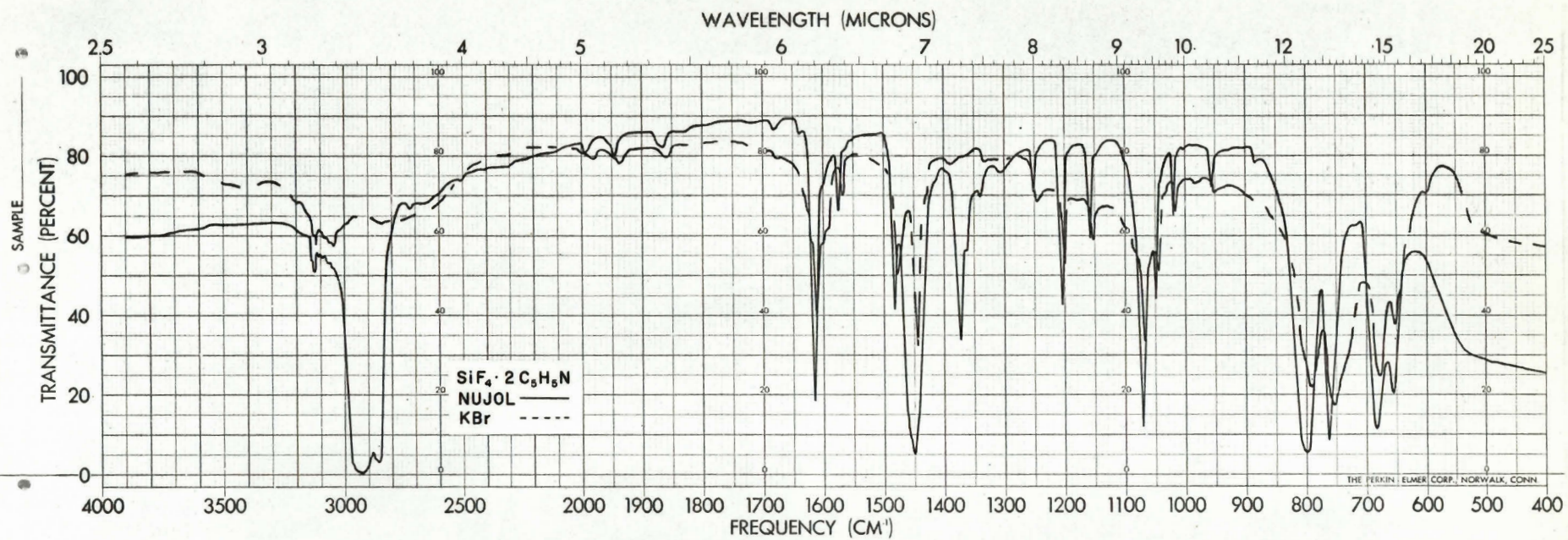
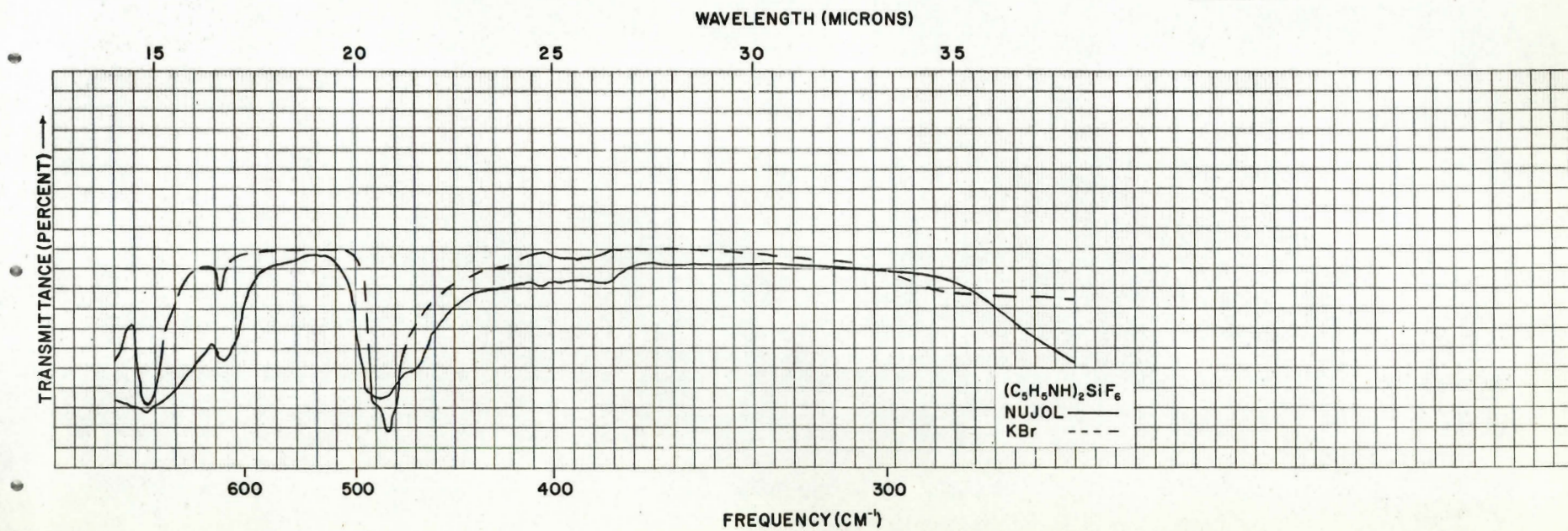
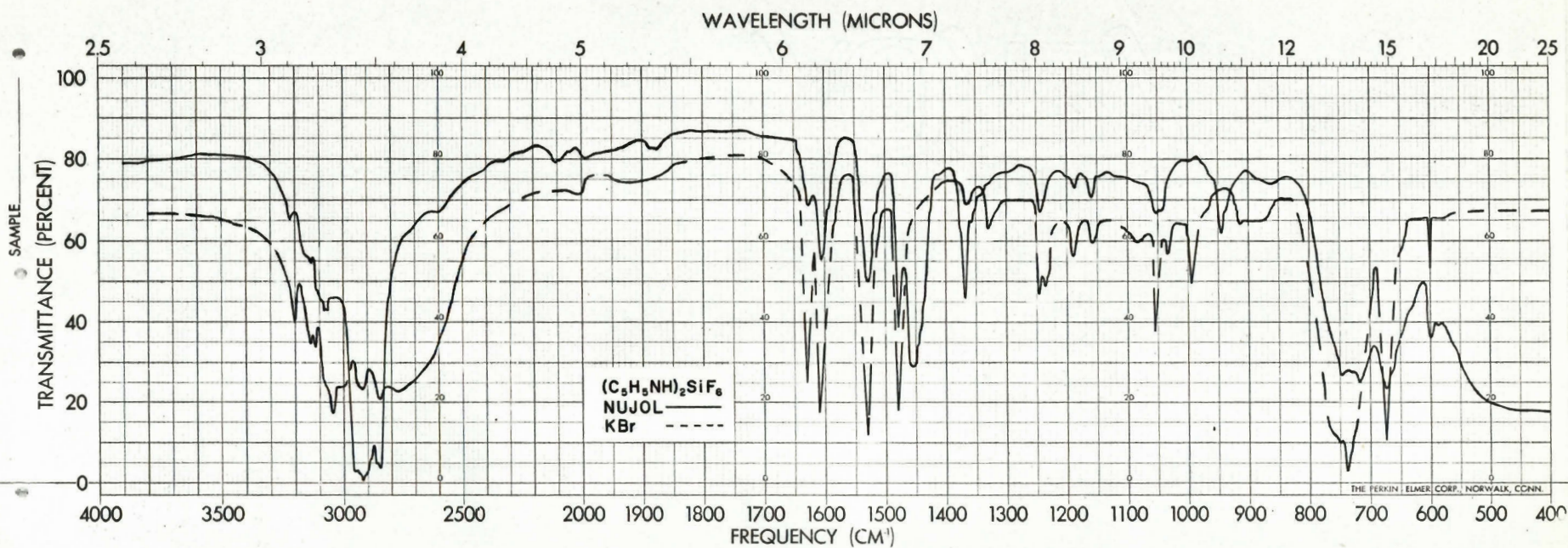


FIG. 35

The infrared spectrum of $(C_5H_5NH)_2SiF_6$



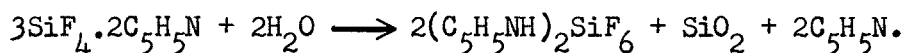
(vi) Solubility of $\text{SiF}_4 \cdot 2\text{C}_5\text{H}_5\text{N}$

The complex, $\text{SiF}_4 \cdot 2\text{C}_5\text{H}_5\text{N}$, was found to be insoluble in the following solvents: methanol, carbon tetrachloride, benzonitrile, pyridine, benzene, nitrobenzene, monochlorobenzene, chloroform, methyl iodide, thiophene, methylene chloride, methylene bromide, mesitylene, acetonitrile, and a few fluorinated aromatic solvents such as perfluorodecalin, 2-chloro-5-nitrobenzotrifluoride, trichlorobenzotrifluoride, dichlorobenzotrifluoride, meta-nitrobenzotrifluoride and benzotrifluoride. It appeared to be soluble to the extent of about 5 g.l^{-1} in nitromethane and bis-(2-methoxyethyl)ether. Due to the low volatility of this ether at 25° , it was not possible to evaporate the solvent in order to examine whether the complex would precipitate from solution unchanged; moreover heating the solution above 25° resulted in the decomposition of the complex. Therefore, the solubility of the complex in this ether was not further investigated.

(vii) "Solubility" of $\text{SiF}_4 \cdot 2\text{C}_5\text{H}_5\text{N}$ in Nitromethane

A colorless solution and a little insoluble, grey, jelly-like material resulted when $\text{SiF}_4 \cdot 2\text{C}_5\text{H}_5\text{N}$ (0.5 g, 19.05 mmole) was mixed with nitromethane (100 ml). After filtering the insoluble material, the infrared spectrum of which showed that it was SiO_2 (0.02 g) (broad $\nu(\text{Si-O})$ at 1095 cm^{-1}) the solution was evaporated to dryness at 25° and a white solid remained. Infrared measurement and elemental analysis showed that it was $(\text{C}_5\text{H}_5\text{NH})_2\text{SiF}_6$ (0.36 g, 11.88 mmole) containing a trace of $\text{SiF}_4 \cdot 2\text{C}_5\text{H}_5\text{N}$ and/or SiO_2 (Found: %F, 36.9. %Si, 10.3. %N, 8.2. %C, 39.1.

%H, 4.1. Calc. for $(C_5H_5NH)_2SiF_6$: %F, 37.7. %Si, 9.3. %N, 9.25. %C, 39.7.
%H, 4.0). Therefore, the mole ratio of $(C_5H_5NH)_2SiF_6$ formed to SiF_4 .
 $2C_5H_5N$ used was 1:1.60. After considering various possible mechanisms
(see Discussion section of thesis) the most satisfactory representation
of the overall reaction was,



(viii) Cryoscopic Molecular Weight Determination of $SiF_4 \cdot 2C_5H_5N$ in
Nitromethane

Table 25 contains the data which are plotted in Fig. 36 and
Table 26 shows the results calculated from the slopes of the linear plots
of Fig. 36. The molecular weight result, 130, supports the preceding
evidence that $SiF_4 \cdot 2C_5H_5N$ had reacted with nitromethane to form mainly
 $(C_5H_5NH)_2SiF_6$.

TABLE 25

Cryoscopic data for molecular weight plots in Fig. 36

Sample, line 1		Calibration, line 2		Calibration check, line 3	
SiF ₄ .2C ₅ H ₅ N		naphthalene		anthracene	
total wt. added	freezing pt. reading	total wt. added	freezing pt. reading	total wt. added	freezing pt. reading
g X 10 ³	v X 10 ⁶	g X 10 ³	v X 10 ⁶	g X 10 ³	v X 10 ⁶
0	440	0	480	0	480
36.6	410	71.3	418	71.3	438
75.8	376	135.4	358	217.8	356
-	-	208.3	298	293.0	312

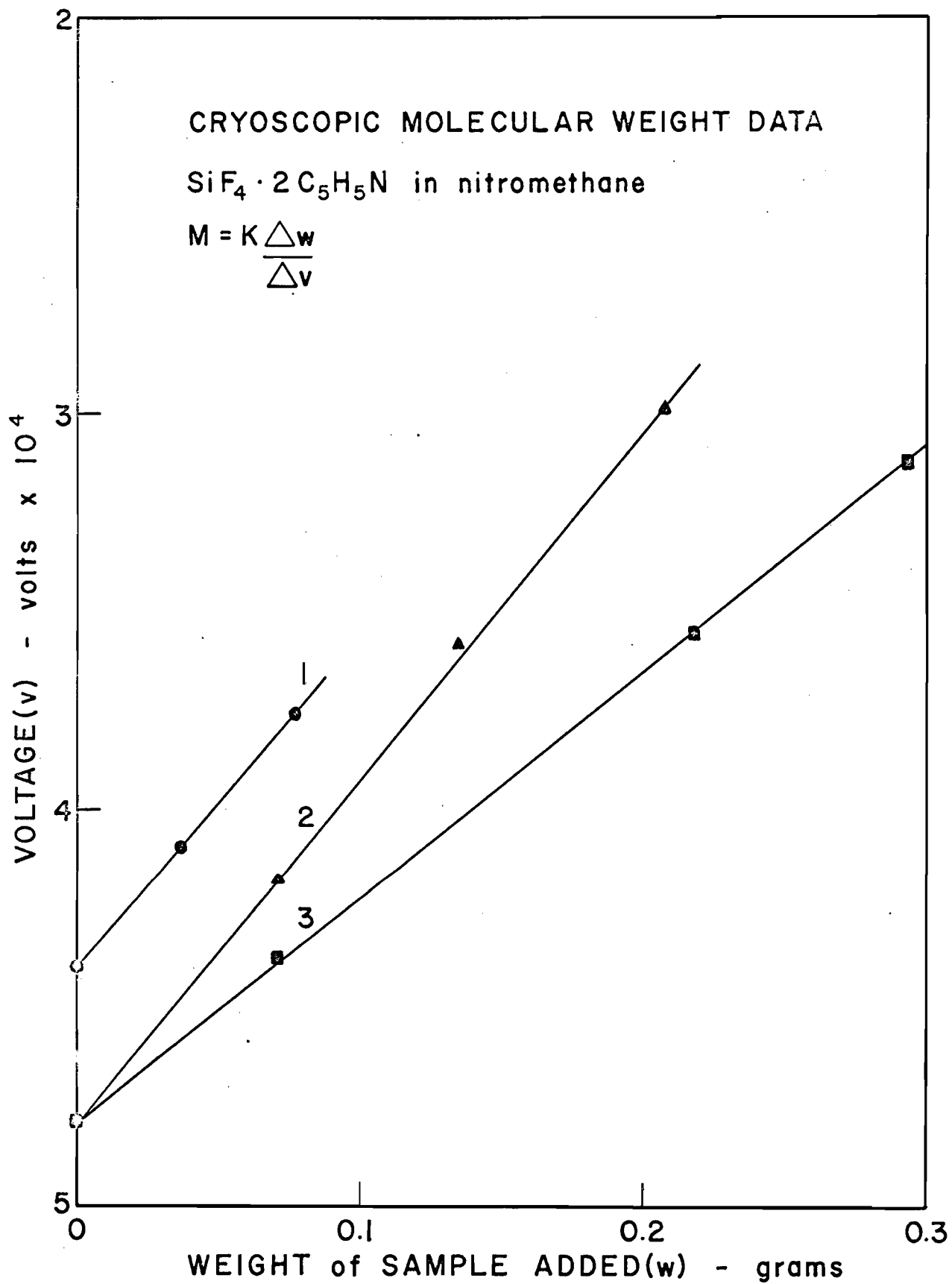
TABLE 26

Cryoscopic data obtained from plots of Fig. 36

$K_{\text{CH}_3\text{NO}_2}$, from line 2	0.11 v.g^{-1}
$M_{\text{C}_{14}\text{H}_{10}}$, from line 3	192
M_{sample} , from line 1	130
<hr/>	
$M_{\text{C}_{14}\text{H}_{10}}$, Calc.	178.2
$M_{\text{SiF}_4 \cdot 2\text{C}_5\text{H}_5\text{N}}$, Calc.	262.3
$M_{(\text{C}_5\text{H}_5\text{NH})_2\text{SiF}_6}$, Calc. (3 particles)	100.8
<hr/>	

FIG. 36

Cryscopic data for $\text{SiF}_4 \cdot 2\text{C}_5\text{H}_5\text{N}$ in nitromethane



(ix) Conductivity of $\text{SiF}_4 \cdot 2\text{C}_5\text{H}_5\text{N}$ in Nitromethane

A plot (Fig. 37) of the conductivity data (Table 27) for $\text{SiF}_4 \cdot 2\text{C}_5\text{H}_5\text{N}$ in nitromethane revealed that the sample was a strong electrolyte, again confirming the previous solubility data which had indicated the formation of the ionic salt, $(\text{C}_5\text{H}_5\text{NH})_2\text{SiF}_6$. The molar conductance decreased linearly until the square root of the concentration had increased to more than $0.054 \text{ mole}^{1/2} \text{ l}^{-1/2}$, corresponding to $0.0029 \text{ mole l}^{-1}$, when linearity ceased, marked by an abnormally large decrease in the molar conductance. Extrapolation of the linear part of the plot to infinite dilution ($c^{1/2} = 0$) gave an estimated molar conductance of $98.0 \text{ mho cm}^2 (\text{g-mole})^{-1} \text{ l}^{-1}$.

TABLE 27

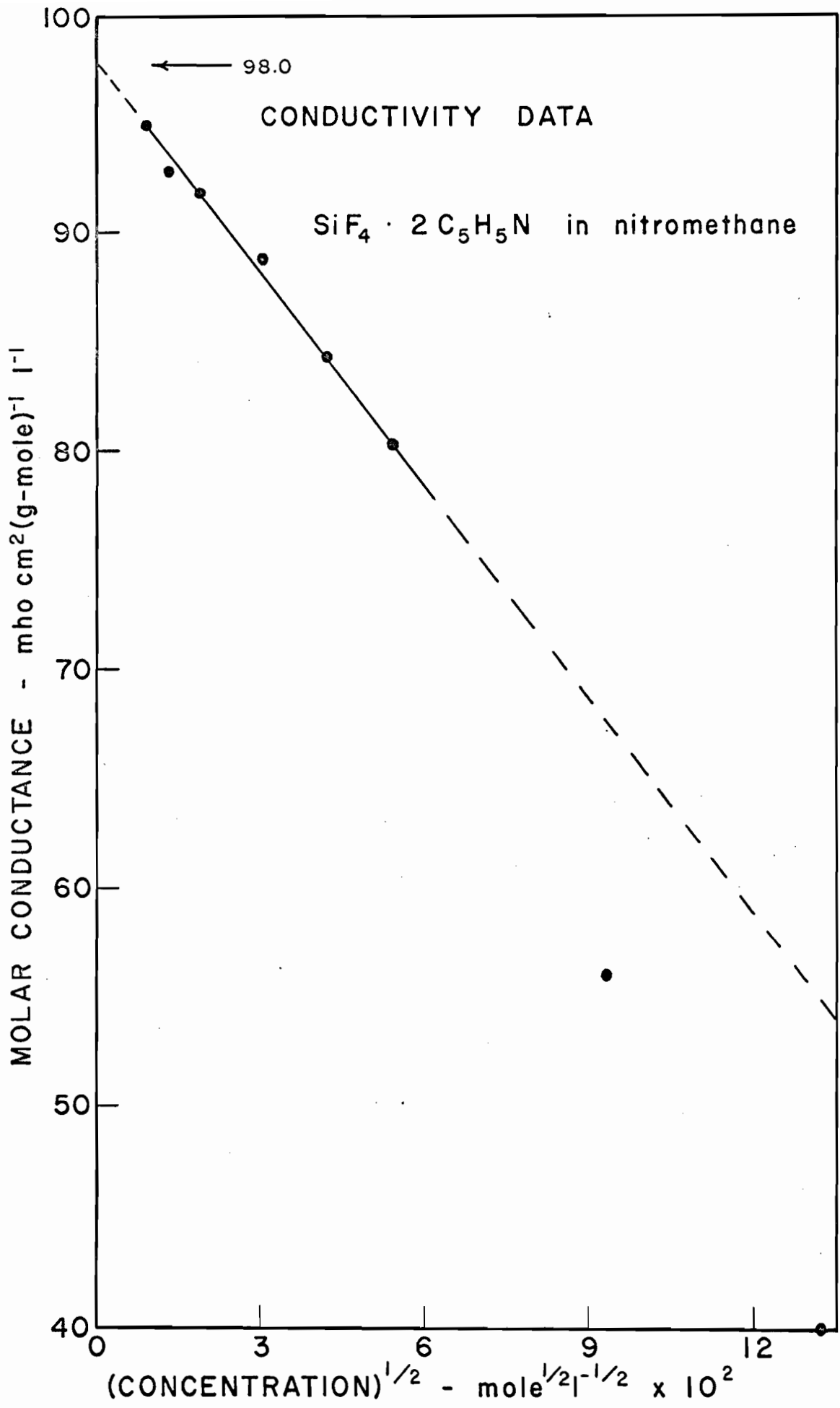
Conductivities of $\text{SiF}_4 \cdot 2\text{C}_5\text{H}_5\text{N}$ in nitromethane

$\text{SiF}_4 \cdot 2\text{C}_5\text{H}_5\text{N}$ concentration c , mole l^{-1}	Specific conductance k , mho cm^{-1}	Molar conductance $\text{mho cm}^2 (\text{g-mole})^{-1} \text{l}^{-1}$	$c^{1/2}$ $\text{mole}^{1/2} \text{l}^{-1/2}$
0.01745	7.00×10^{-4}	40.1	0.1322
0.008725	4.90×10^{-4}	56.1	0.0935
0.002920	2.34×10^{-4}	80.2	0.0540
0.001745	1.47×10^{-4}	84.3	0.0418
0.0008725	7.75×10^{-5}	88.8	0.0295
0.0003490	3.20×10^{-5}	91.7	0.0187
0.0001745	1.62×10^{-5}	92.8	0.0132
0.00008725	8.29×10^{-6}	95.0	0.00935
0*	2.50×10^{-6}	-	-

* pure nitromethane (lit. (54) value: $1 \times 10^{-8} \text{ mho cm}^{-1}$).

FIG. 37

The molar conductance of $\text{SiF}_4 \cdot 2\text{C}_5\text{H}_5\text{N}$ in nitromethane



2. Coordination of SiF_4 with Ethylenediamine

(i) Preparation of $\text{SiF}_4 \cdot \text{NH}_2(\text{CH}_2)_2\text{NH}_2$

Slow warming of a mixture of SiF_4 (64.20 mmole) and $\text{NH}_2(\text{CH}_2)_2\text{NH}_2$ (60.20 mmole) from -195 to 25° produced a pale yellow solid. Distillation of the unreacted SiF_4 (5.36 mmole) at -78° indicated that the reaction had occurred in a mole ratio 1:1.02, corresponding to the 1:1 complex, $\text{SiF}_4 \cdot \text{NH}_2(\text{CH}_2)_2\text{NH}_2$.

The complex was further purified by vacuum sublimation at 120° . Analysis indicated that the white solid was now pure (Found: %F, 46.0. Calc. for $\text{SiF}_4 \cdot \text{NH}_2(\text{CH}_2)_2\text{NH}_2$: %F, 46.2). Since $\text{NH}_2(\text{CH}_2)_2\text{NH}_2$ was found to react with stopcock grease, it was measured and introduced using the syringe technique (29). The complex was involatile at 25° , very hygroscopic, and decomposed without melting at about 300° .

(ii) Infrared Measurements

The infrared spectrum of $\text{SiF}_4 \cdot \text{NH}_2(\text{CH}_2)_2\text{NH}_2$ is shown in Fig. 38, and frequency assignments are given in Table 28 together with the corresponding data for $\text{NH}_2(\text{CH}_2)_2\text{NH}_2$ (55).

TABLE 28

Comparisons and assignments of infrared vibration frequencies (cm^{-1})

$\text{SiF}_4 \cdot \text{NH}_2(\text{CH}_2)_2\text{NH}_2$ solid		$\text{NH}_2(\text{CH}_2)_2\text{NH}_2$		Assignment
Nujol cm^{-1}	KBr cm^{-1}	liquid cm^{-1}	gas* cm^{-1}	
3320s	3322s	3355s	3335w	ν (N-H), free
3283s	3283s	3280s		"
3160w	3180w, b	3200m, sh		ν (N-H), H-bonded
nujol	3010vw, b	2920s	2930m	ν (C-H), antisym.
"		2850s	2860m	ν (C-H), sym.
1620m, b	1610m, b	1590s	1619m	δ (N-H), bending
1577m	1577m			"
1520w	1520w			"
nujol	1470w	1453m		δ (C-H), bending
1333m	1333m	1347m		δ (C-H), twisting
1307s	1308s	1302m		δ (C-H), wagging
1292m, sh	1290vw			"
1225m	1225w	1248vw		δ (N-H), twisting
1160s	1160s	1090m		ν (C-N)
1122mw	1122w			"
1050s	1050s	1046m		"
1010w	1030w			unidentified
896m	896m	875s, b	960s	δ (N-H), wagging
863s	865s	812s, b	927s	unidentified
			765m, b	δ (C-H), rocking
730vs	730vs			ν (Si-F) octahedral
715vs	720vs			"
700vs	708vs			"
600m	602m			? (Si-F) octahedral (46)
568vw		595vw		due to $\text{NH}_2(\text{CH}_2)_2\text{NH}_2$

.....

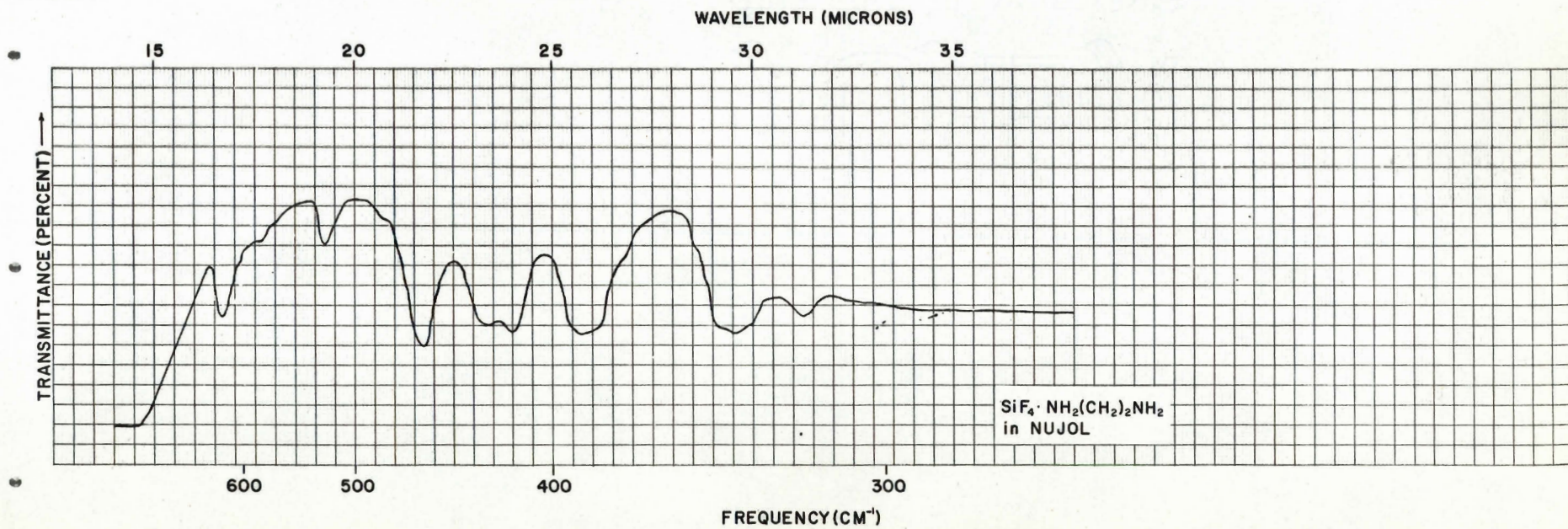
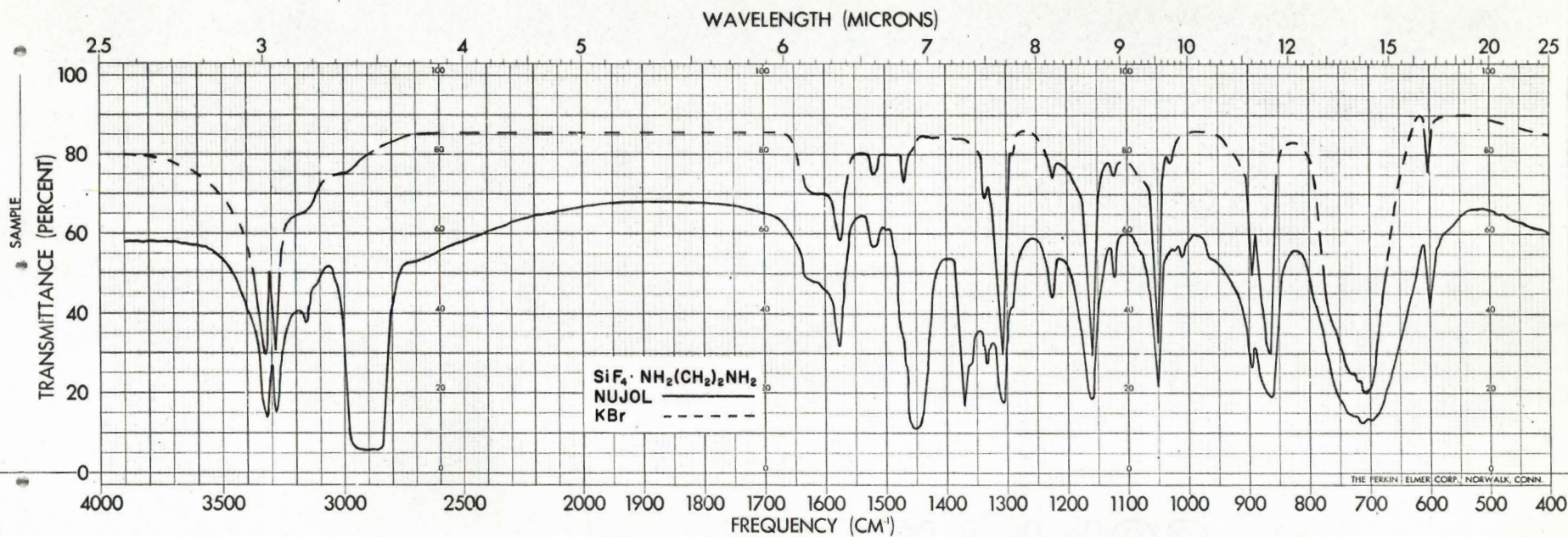
TABLE 28 (cont'd.)

$\text{SiF}_4 \cdot \text{NH}_2(\text{CH}_2)_2\text{NH}_2$ solid		$\text{NH}_2(\text{CH}_2)_2\text{NH}_2$ liquid gas*		Assignment
Nujol -1 cm	KBr -1 cm	-1 cm	-1 cm	
519m		506s		due to $\text{NH}_2(\text{CH}_2)_2\text{NH}_2$
483vw		474m		"
460s				? (Si-F) octahedral (46)
429m				"
417m				"
388s		365- 280b		"
338s				"
326m				"

* The infrared spectrum was not taken below 650 cm^{-1} .

FIG. 38

The infrared spectrum of $\text{SiF}_4 \cdot \text{NH}_2(\text{CH}_2)_2\text{NH}_2$



3. Coordination of SiF_4 with Pyrrolidine

(i) Preparation of $\text{SiF}_4 \cdot 2(\text{CH}_2)_4\text{NH}$

When SiF_4 (5.99 mmole) was condensed over $(\text{CH}_2)_4\text{NH}$ (8.63 mmole) and the mixture was slowly warmed from -195 to 25° , a yellow-white solid formed. It was apparent from the amount of unreacted SiF_4 (1.72 mmole) distilled at -78° that SiF_4 and $(\text{CH}_2)_4\text{NH}$ had reacted in a mole ratio of 1:2.02 to form the complex, $\text{SiF}_4 \cdot 2(\text{CH}_2)_4\text{NH}$.

Further purification by vacuum sublimation at 80° gave a white solid for which analysis confirmed that it was the pure 1:2 complex (Found: %F, 30.86. Calc. for $\text{SiF}_4 \cdot 2(\text{CH}_2)_4\text{NH}$: %F, 30.85). The complex was involatile at 25° , hygroscopic, and melted with some decomposition at $205-210^\circ$.

Using the same bubbling technique as that used to prepare $\text{SiF}_4 \cdot 2\text{C}_5\text{H}_5\text{N}$ (section III, 1.(i)), SiF_4 was bubbled through a 10% solution of $(\text{CH}_2)_4\text{NH}$ in acetonitrile kept at 0° . In this case the product was perfectly white and analyzed as pure $\text{SiF}_4 \cdot 2(\text{CH}_2)_4\text{NH}$ without further purification (Found: %F, 30.85). The impurities must have dissolved in the solvent as indicated by its slight yellow tinge.

(ii) Tensimetric Titration

Fig. 39 (Table 29) shows the tensimetric titration of SiF_4 (12.10 mmole) with $(\text{CH}_2)_4\text{NH}$ while the reverse titration of $(\text{CH}_2)_4\text{NH}$ (8.73 mmole) by the addition of SiF_4 (Table 30) is shown in Fig. 40. As shown in Fig.

39, the **pressure** decreased linearly until the mole ratio, $(\text{CH}_2)_4\text{NH}/\text{SiF}_4$, had increased to 2.01 (i.e., after the addition of 24.5 mmole of $(\text{CH}_2)_4\text{NH}$), when it became zero, corresponding to the formation of only the 1:2 complex, $\text{SiF}_4 \cdot 2(\text{CH}_2)_4\text{NH}$. Similarly, Fig. 40 confirmed the formation of the 1:2 complex. In this case, the pressure remained zero until the mole ratio had increased to 2.03 (corresponding to the addition of 4.3 mmole of SiF_4), when it increased rapidly as more SiF_4 was added.

TABLE 29

Tensimetric titration of SiF_4 with $(\text{CH}_2)_4\text{NH}$ and $(\text{CH}_2)_4\text{NH}$ with SiF_4

SiF_4 with $(\text{CH}_2)_4\text{NH}$ (Fig. 33)		$(\text{CH}_2)_4\text{NH}$ with SiF_4 (Fig. 34)	
SiF_4 present initially, 12.10 mmole		$(\text{CH}_2)_4\text{NH}$ present initially, 8.73 mmole	
$T_r, 25^\circ; T_p, -78^\circ$		$T_r, 25^\circ; T_p, -78^\circ$	
Total $(\text{CH}_2)_4\text{NH}$ added mmole	Pressure mm	Total SiF_4 added mmole	Pressure mm
0	312.0	0	0
2.92	276.2	1.02	0
5.93	238.0	2.07	0
9.14	196.7	3.30	0
11.98	160.5	4.25	0
14.91	123.2	4.58	8.3
18.20	81.9	5.12	24.6
20.86	47.5	6.06	50.2
23.04	20.0	7.89	102.2
24.06	6.0	9.74	153.6
24.43	1.0	11.62	205.5
26.70	0	13.60	262.8
29.00	0	15.00	302.0

FIG. 39

The tensimetric titration of SiF_4 with $(\text{CH}_2)_4\text{NH}$

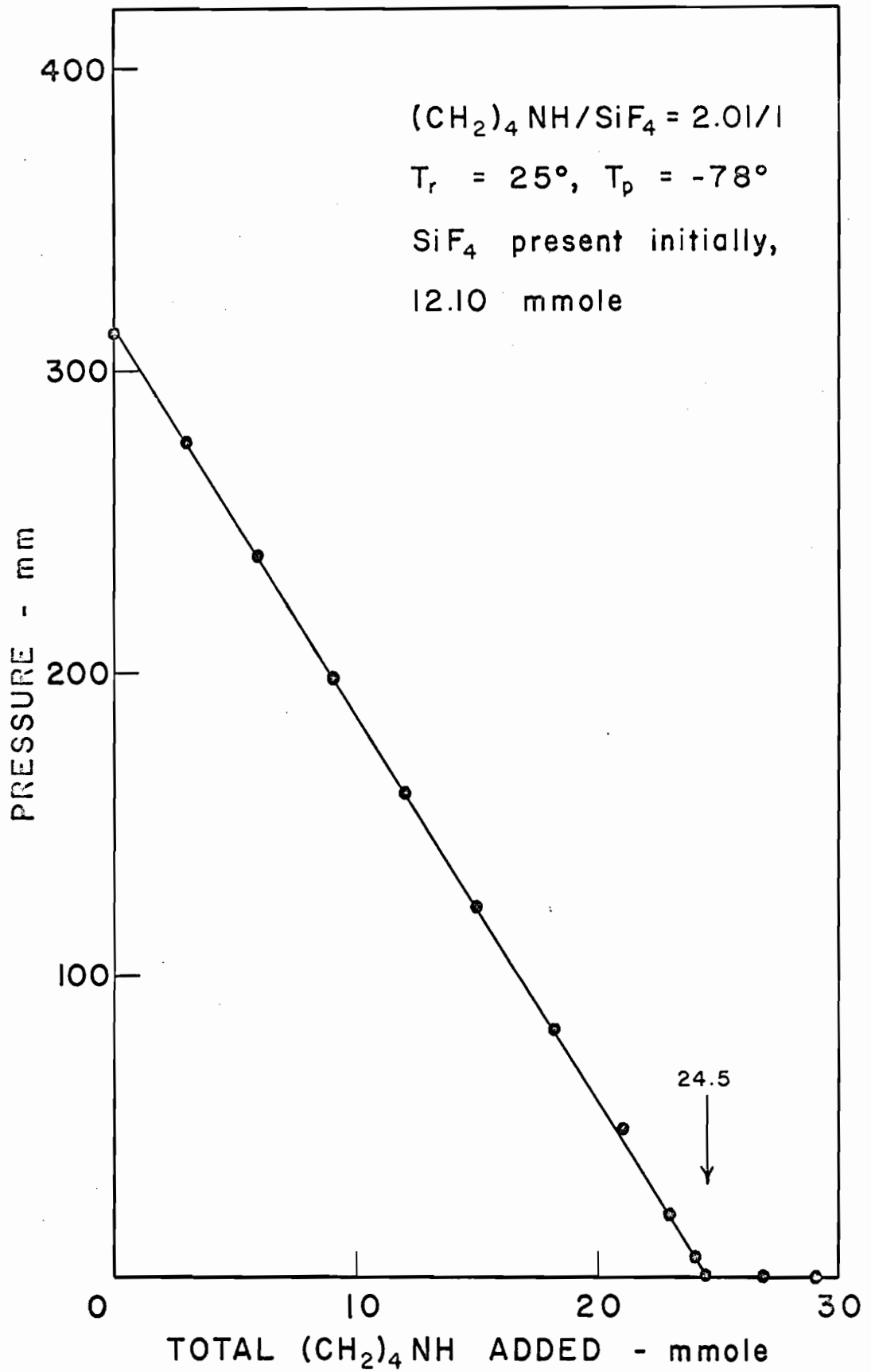
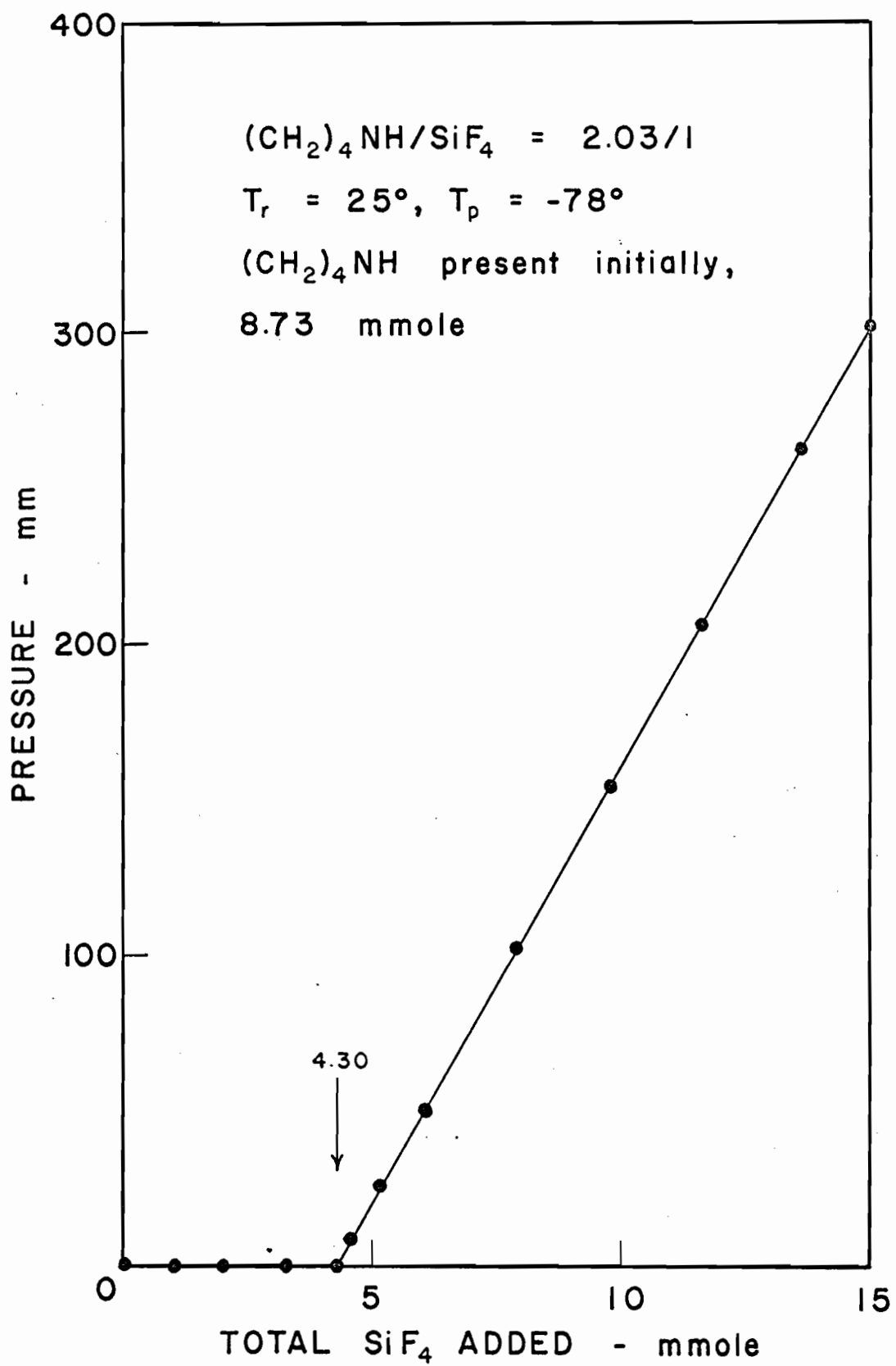


FIG. 40

The tensimetric titration of $(\text{CH}_2)_4\text{NH}$ with SiF_4



(iii) Infrared Measurements

Fig. 41 shows the infrared spectrum of $\text{SiF}_4 \cdot 2(\text{CH}_2)_4\text{NH}$ and frequency assignments are given in Table 30. Assignments were made by comparison of the infrared spectra of the complex with that of pure liquid $(\text{CH}_2)_4\text{NH}$.

TABLE 30

Comparisons and assignments of infrared absorption frequencies (cm^{-1})

$\text{SiF}_4 \cdot 2(\text{CH}_2)_4\text{NH}$ solid		$(\text{CH}_2)_4\text{NH}$ liquid	Assignment
Nujol cm^{-1}	KBr cm^{-1}	cm^{-1}	
3219s	3219s	3275s	ν (N-H), free
3030m	3030m, sh		ν (C-H)
3015m	3013m		"
nujol	2980m	2995s	ν (C-H), antisym.
"	2880m	2880s	ν (C-H), sym.
1590w	1610w	1650w	\int (N-H)
nujol	1465w, sh	1460m	\int (C-H), with combinations
"	1452m		"
	1446m		"
1410m	1408m	1420m	"
1355m	1350m	1340w	"
1324m	1323m		"
1314m, sh	1314m, sh		"
1270w	1270w	1285m	"
1226m	1225m	1200m	ν (C-N)
1169m	1169m	1112m	"
1050m	1049m	1082s	"
1035m, sh	1033m, sh		"
955w	954w	987m	\int (N-H)

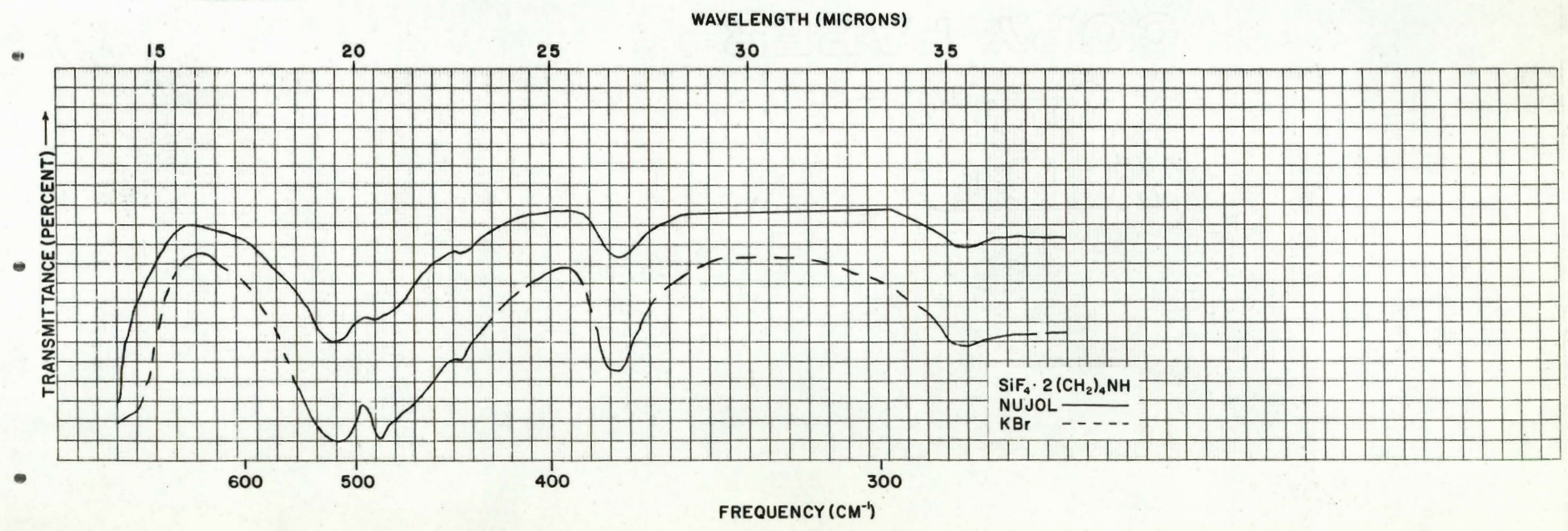
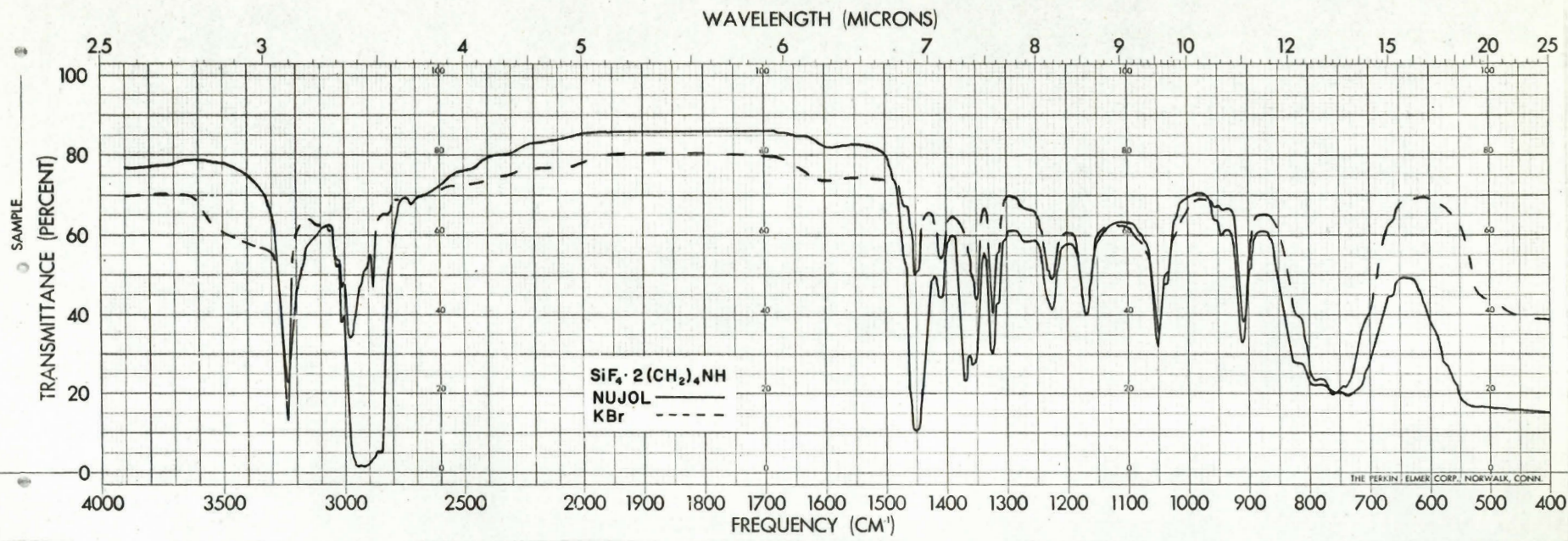
.....

TABLE 30 (cont'd.)

$\text{SiF}_4 \cdot 2(\text{CH}_2)_4\text{NH}$ solid		$(\text{CH}_2)_4\text{NH}$ liquid	Assignment
Nujol cm ⁻¹	KBr cm ⁻¹	cm ⁻¹	
945w	943w	890s,b	∫(N-H)
911m	909m	860s,b	"
825m	822m	810s,b	"
785s	790s		∨(Si-F) octahedral ?
760s,b	765s		"
740s,b	740s		"
515s	513s	568s,b	due to $(\text{CH}_2)_4\text{NH}$
488s	484s		? (Si-F) octahedral (46)
441m,sh	443w,sh		"
373m	375m	365w	due to $(\text{CH}_2)_4\text{NH}$
282m,b	281m,b	293m,b	"

FIG. 41

The infrared spectrum of $\text{SiF}_4 \cdot 2(\text{CH}_2)_4\text{NH}$



4. Coordination of SiF_4 with Piperidine

(i) Preparation of $\text{SiF}_4 \cdot 2(\text{CH}_2)_5\text{NH}$

Using the bubbling technique and identical conditions as those used for the preparation of $\text{SiF}_4 \cdot 2(\text{CH}_2)_4\text{NH}$, the white solid complex, $\text{SiF}_4 \cdot 2(\text{CH}_2)_5\text{NH}$, was prepared and needed no further purification (Found: %F, 27.56. Calc. for $\text{SiF}_4 \cdot 2(\text{CH}_2)_5\text{NH}$: %F, 27.65). The solvent also had a similar yellow tinge after the interaction had occurred.

The complex was hygroscopic, involatile at 25°, sublimed in a vacuum at 80° without decomposition (Found: %F, 27.60), and melted with decomposition at 185-190°.

(ii) Infrared Measurements

The infrared spectrum of $\text{SiF}_4 \cdot 2(\text{CH}_2)_5\text{NH}$ is shown in Fig. 42 and frequency assignments are given in Table 31. Assignments were made on the basis of the comparison between the infrared spectra of the complex and that of the pure liquid and gaseous $(\text{CH}_2)_5\text{NH}$ (56-59).

TABLE 31

$\text{SiF}_4 \cdot 2(\text{CH}_2)_5\text{NH}$ solid		$(\text{CH}_2)_5\text{NH}$		Assignment
Nujol cm^{-1}	KBr cm^{-1}	liquid cm^{-1}	gas cm^{-1}	
3218s	3222s	3270s	3160vw	\checkmark (N-H), free
2998m	3000m			\checkmark (C-H)
nujol	2965s,sh			"
"	2960s			"
"	2945s	2940s	2940s	"
"	2935s			"
"	2865m	2860s	2860s	"
	2805w	2800s	2800s	"
	2735w	2730s	2730m	\checkmark (N-H), H-bonded (45)
		2670m,sh		unidentified
1590w,b	1610w,b	1630vw	1630vw	\int (N-H)
	1577w			"
nujol	1460m,sh	1470m,sh	1450m	\int (C-H), with combinations
"	1442m	1448s		"
	1417m			"
nujol	1372m	1387w	1395w	"
1357m	1357m	1365w		"
1345w,sh	1345vw,sh	1345w,sh		"
1325m	1325m	1335m	1335m	"
1320m,sh	1320m,sh	1321s		"

• • • •

TABLE 31 (cont'd.)

$\text{SiF}_4 \cdot 2(\text{CH}_2)_5\text{NH}$ solid		$(\text{CH}_2)_5\text{NH}$		Assignment
Nujol cm^{-1}	KBr cm^{-1}	liquid cm^{-1}	gas cm^{-1}	
1283m	1284m	1285w		$\int(\text{C-H})$, with combinations
		1270m, sh		"
		1260m	1260w	"
1222m	1223m	1192m		$\vee(\text{C-N})$
1187m	1188m	1168m	1160m	"
	1155w, sh			"
1135m	1136m	1149m		"
1120w, sh	1120w, sh	1119s	1120m	"
1079m	1080m			"
1065w, sh		1070w, sh	1068w	"
1037m	1037m	1053m	1055m	"
1029m	1030m	1038m	1045m	"
1012m	1013m	1008m	1037m	"
		964w	967m	$\int(\text{N-H})$
944m	943m	939m	932m	"
	925w, sh			"
890w, sh	890w, sh	900m, b		"
880m	881m	860s	861m	"
857m	858m	855s	852m	"
812m, sh	813m, sh	822m		$\int(\text{C-H})$, rocking

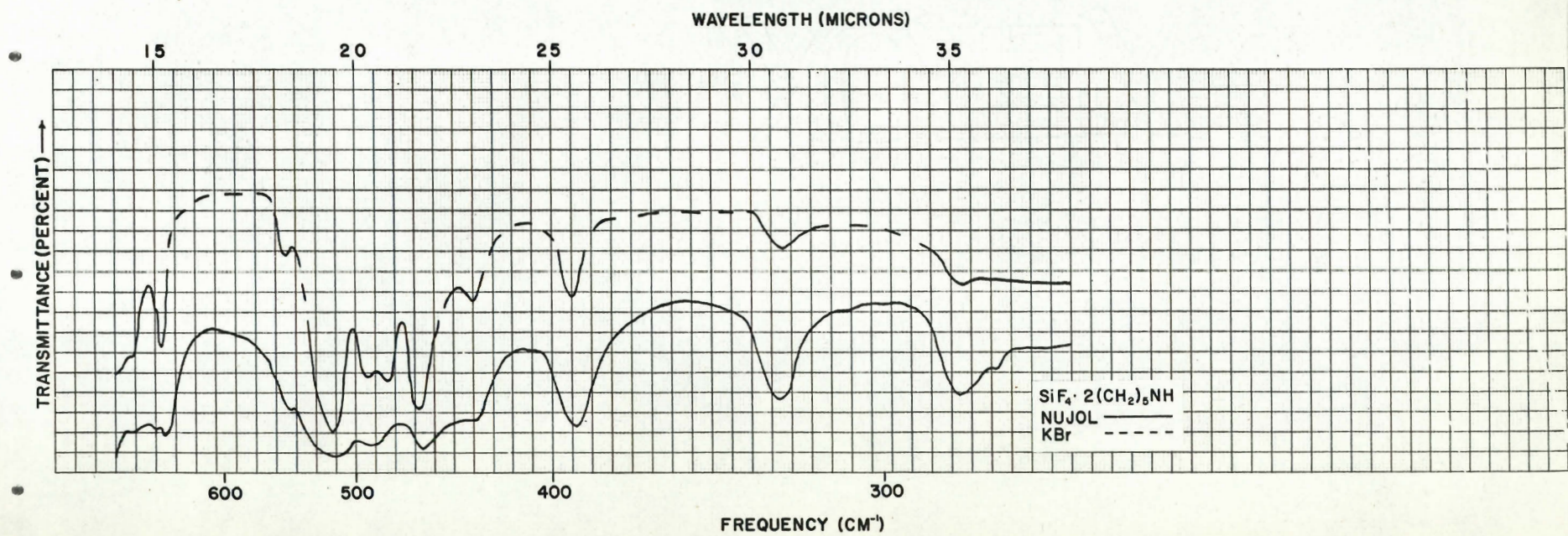
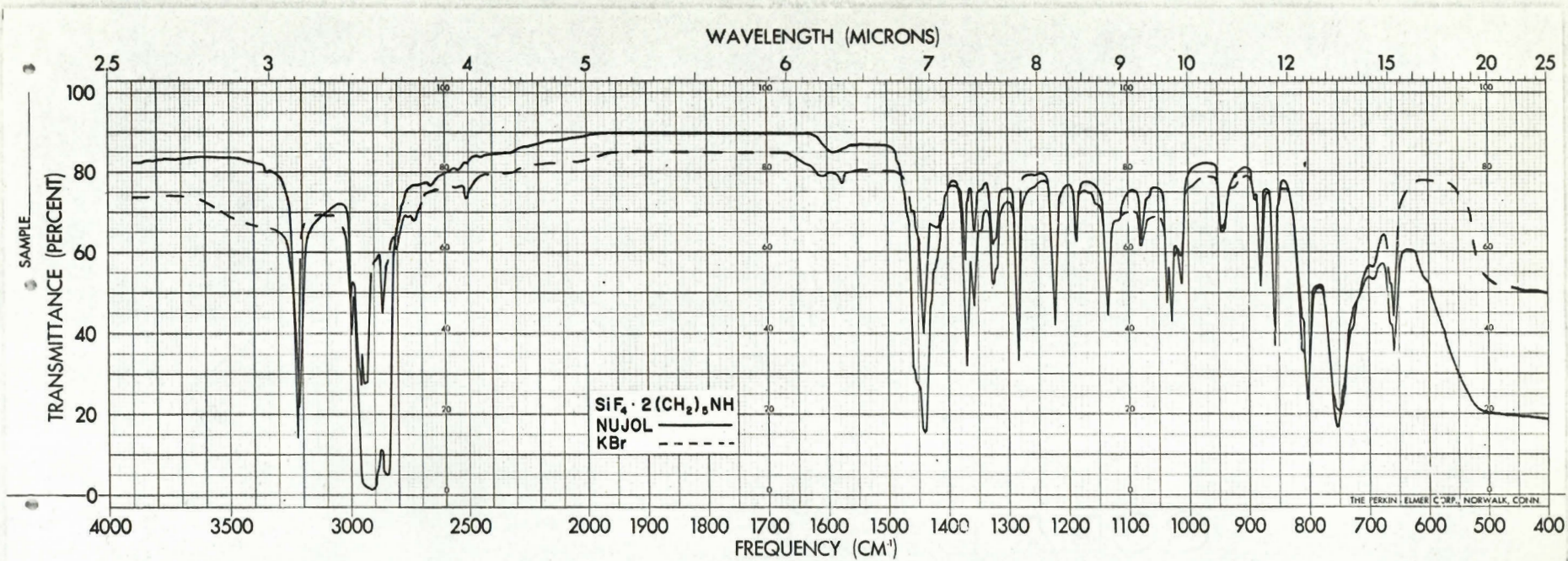
.....

TABLE 31 (cont'd.)

$\text{SiF}_4 \cdot 2(\text{CH}_2)_5\text{NH}$ solid		$(\text{CH}_2)_5\text{NH}$		Assignment
Nujol cm^{-1}	KBr cm^{-1}	liquid cm^{-1}	gas cm^{-1}	
803s	804s	790m	747s	$\delta(\text{C-H})$, rocking
760s, sh		760s	738s	"
		744s	727s	"
750s	755s			$\nu(\text{Si-F})$ octahedral
694w, sh	695w, sh			? (Si-F) octahedral (46)
665m, sh	666m, sh			"
659m	660m			"
543m, sh	549m	555s, sh		"
512s	516s	544s	541m	due to $(\text{CH}_2)_5\text{NH}$
493m	493m			? (Si-F) octahedral (46)
	481s			"
461m	463s	442m, sh		due to $(\text{CH}_2)_5\text{NH}$
435m, b	435m	429s	423w	"
391m	392m	396m, b		"
326m	325m			? (Si-F) octahedral (46)
284m				"
277w, sh				"

FIG. 42

The infrared spectrum of $\text{SiF}_4 \cdot 2(\text{CH}_2)_5\text{NH}$



IV. Attempted Preparation of SiF_4 Complexes with Hydrogen Sulfide, Dimethyl Sulfide, Phosphine, and Nitromethane

1. SiF_4 -Hydrogen Sulfide System

The results of the pressure-temperature measurements in the range -95 to 25° on pure SiF_4 (5.29 mmole) and pure H_2S (3.95 mmole) as well as on the mixture of the two compounds are shown in Table 32. Comparison of the observed pressure of the gaseous mixture with the total pressure calculated assuming no interaction and ideal gaseous behavior (Dalton's Law of Partial Pressures) revealed that an ideal gaseous mixture existed and that no observable interaction had occurred between SiF_4 and H_2S in the range -95 to 25° . Vacuum distillation at -129° yielded the original mixture (9.23 mmole) indicating that no stable involatile complex had been formed at this temperature.

2. SiF_4 -Dimethyl Sulfide System

Table 32 also includes the pressure-temperature data for pure SiF_4 (5.08 mmole) and pure $(\text{CH}_3)_2\text{S}$ (4.00 mmole) as well as for the mixture of the two compounds. Similar comparisons as done on the SiF_4 - H_2S system (section IV, 1.) indicated no reaction in the range -95 to 25° . Since the original SiF_4 (5.08 mmole) was recovered by vacuum distillation at -129° it was concluded that no stable involatile complex existed at this temperature.

3. SiF₄-Phosphine System

The pressure-temperature data shown in the latter part of Table 32 shows the absence of interaction between SiF₄ (5.99 mmole) and PH₃ (3.47 mmole) in the range -95 to 25°. Again, no stable involatile complex could be formed at even -129° as evident from the amount of the SiF₄-PH₃ mixture (9.45 mmole) that was recovered by vacuum distillation at -129°.

4. SiF₄-Nitromethane System

The data in Table 32, also shows that no observable interaction had occurred between SiF₄ (17.50 mmole) and CH₃NO₂ (18.20 mmole) in the range -95 to 25°. Vacuum distillation at -129° yielded the original SiF₄ (17.48 mmole), thus no stable involatile SiF₄-CH₃NO₂ complex had been formed at that temperature, although the formation of a complex volatile at -129° could not be excluded.

TABLE 32

Temperature-pressure data showing no complex formation

Temperature °C	SiF ₄ pressure mm	<u>SiF₄-H₂S</u>	<u>Donor = H₂S</u>	
		<u>Donor</u> pressure mm	Mixture pressure mm (Obs.)	Mixture pressure mm (Calc.)*
25	290.6	216.7	506.3	507.3
0	289.0	215.0	503.1	504.0
-23	287.5	214.0	500.0	501.5
-45	286.0	212.0	496.2	498.0
-78	283.0	209.9	491.0	492.9
-95	280.6	73.3**	350.6	355.9

Temperature °C	SiF ₄ pressure mm	<u>SiF₄-(CH₃)₂S</u>	<u>Donor = (CH₃)₂S</u>	
		<u>Donor</u> pressure mm	Mixture pressure mm (Obs.)	Mixture pressure mm (Calc.)*
25	267.0	219.5	478.8	486.5
0	265.4	181.2**	442.1	446.6
-23	263.8	54.1**	312.3	317.9
-45	262.6	13.0**	270.5	275.6
-78	260.5	0.8**	259.7	261.3
-95	259.3	0.1**	259.8	259.4

.....

TABLE 32 (cont'd.)

Temperature °C	SiF ₄ pressure mm	<u>SiF₄-PH₃</u>	<u>Donor = PH₃</u>	Mixture pressure mm (Obs.)	Mixture pressure mm (Calc.)*
		<u>Donor</u> pressure mm			
25	324.1	190.7		518.8	514.8
0	323.0	189.9		515.6	512.9
-23	320.9	189.0		512.4	509.9
-45	319.7	188.0		509.4	507.7
-78	318.8	187.0		505.3	505.8
-95	314.5	184.0		501.2	498.5

Temperature °C	SiF ₄ pressure mm	<u>SiF₄-CH₃NO₂</u>	<u>Donor = CH₃NO₂</u>	Mixture pressure mm (Obs.) [‡]	Mixture pressure mm (Calc.)*
		<u>Donor</u> pressure mm			
25	506.4	35.0		(512.7) [‡]	541.4
0	503.7	9.4		509.4	513.1
-23	500.6	2.0		506.4	502.6
-45	499.0	0.4		503.9	499.4
-78	494.4	0		498.1	494.4
-95	491.3	0		496.4	491.3

[‡] pressure was not constant

* Dalton's Law: $P_{\text{mixture}} = P_{\text{SiF}_4} + P_{\text{donor}}$

** Equilibrium vapor pressure of donor at that temperature

DISCUSSION

I. The Interaction of SiF_4 with Methanol

1. Preparation of $\text{SiF}_4 \cdot 4\text{CH}_3\text{OH}$

The direct combination of SiF_4 (excess) with CH_3OH gave better combining ratios, $\text{CH}_3\text{OH}/\text{SiF}_4$, than that of the tensimetric titrations. Values in the range 3.75 to 4.20 were obtained. Ratios lower than 4:1 are attributed to the formation of some $(\text{CH}_3)_2\text{O}$ by the SiF_4 catalyzed dehydration of CH_3OH (21); higher ratios are probably due to incomplete reaction of CH_3OH with SiF_4 .

The 1:4 complex, $\text{SiF}_4 \cdot 4\text{CH}_3\text{OH}$, could not be isolated by reacting SiF_4 with an excess of CH_3OH because the complex had an appreciable dissociation pressure at the temperature at which the excess CH_3OH could be removed. Incomplete reaction probably accounts for the somewhat higher mole ratios obtained by the tensimetric titration method, using either excess SiF_4 or excess CH_3OH .

The 4:1 stoichiometry found for the complex has been previously reported by Gierut et al. (13) and confirmed by Topchiev and Bogomolova (21). However, Holzapfel et al. (22) reported 6:1 and 8:1 complexes only. These higher ratios were not observed either in this work or in any other previous work.

2. Properties of $\text{SiF}_4 \cdot 4\text{CH}_3\text{OH}$

(a) Stability

The solid $\text{SiF}_4 \cdot 4\text{CH}_3\text{OH}$ complex is stable below -45° as evident from the fact that it has no measurable vapor pressure or dissociation pressure below this temperature. The infrared spectrum of the liquid complex indicates that it is probably only slightly dissociated in the liquid state at 25° , i.e., it does not simply show the superimposition of SiF_4 and CH_3OH absorption frequencies. This statement is made with the reservation that slight dissociation might not be detected because the dissociation products would likely have similar absorption frequencies as that of the complex. The infrared spectrum of the gaseous products in equilibrium with the liquid complex at 0° showed that the complex is completely dissociated in the gas phase at 25° . The infrared apparatus available did not permit the investigation of the gaseous products at lower temperatures.

By comparison, $\text{GeF}_4 \cdot 2\text{CH}_3\text{OH}$ is a stable white solid at 25° (24), liquid $\text{BF}_3 \cdot \text{CH}_3\text{OH}$ at 25° loses only 0.03% BF_3 on standing for six months (60), and liquid $\text{BF}_3 \cdot 2\text{CH}_3\text{OH}$ can be distilled at $58-59^\circ/4$ mm without decomposition (61). The fact that the bonding between SiF_4 and CH_3OH is somewhat weak is in agreement with a structure involving hydrogen bonding postulated in section 3 of the discussion (p. 145).

(b) Conductivity of $\text{SiF}_4 \cdot 4\text{CH}_3\text{OH}$

Comparisons of plots of molar conductance against square root of concentration for sodium chloride (39), acetic acid (38), and $\text{SiF}_4 \cdot 4\text{CH}_3\text{OH}$ in methanol showed that the complex is a very weak electrolyte in methanol.

Such plots are linear (at least in the dilute concentration range, i.e., less than 0.1 mole l^{-1}) for ionic compounds such as sodium chloride in methanol, the molar conductance rapidly increasing as the square root of the concentration decreases, approaching the limiting value (μ_0) even at concentrations as high as $0.001 \text{ mole l}^{-1}$. They are nonlinear (similar to an exponential behavior in the very dilute concentration range, i.e., less than $0.001 \text{ mole l}^{-1}$) for weak electrolytes such as acetic acid in methanol, the molar conductance starting at much lower values in concentrated solutions (greater than 1.0 mole l^{-1}) and increasing much more gradually as the square root of the concentration decreases. It is not until a dilution of less than $0.001 \text{ mole l}^{-1}$ that the molar conductance begins to increase very rapidly, approaching a limiting value (μ_0) which is considerably higher than that of the ionic compound in methanol. Since the conductivity plot for $\text{SiF}_4 \cdot 4\text{CH}_3\text{OH}$ in methanol had the characteristics of the acetic acid in methanol conductivity plot it was concluded that $\text{SiF}_4 \cdot 4\text{CH}_3\text{OH}$ was a weak electrolyte in methanol at 25° and that any proposed ionic structure for the liquid complex would contribute only slightly to the total structure.

(c) Infrared Spectrum of $\text{SiF}_4 \cdot 4\text{CH}_3\text{OH}$

The infrared spectra of liquid $\text{SiF}_4 \cdot 4\text{CH}_3\text{OH}$ and its gaseous products do not contain a strong band in the Si-O stretching vibration region. This band is usually very strong and occurs at $1085\text{--}1105 \text{ cm}^{-1}$ in methoxysilanes (62) and alkyldisiloxanes (63). Therefore, the complex is not octahedrally bonded and any structure containing an Si-O bond is not valid. It is possible that the octahedral Si-O bond stretching

vibration (as opposed to the tetrahedral Si-O bond stretching vibration) can be shifted to lower wave number as in the case of the octahedral Si-F bond stretching vibration which is shifted to 720 cm^{-1} from 1035 cm^{-1} in gaseous SiF_4 (the tetrahedral Si-F bond stretching vibration), and that this octahedral Si-O stretching vibration be hidden by the somewhat broad and strong absorption band at 1025 cm^{-1} . Therefore, the conclusion that the complex does not contain an Si-O bond is not unequivocal.

As shown in Table 6 the infrared spectrum of the gaseous products of $\text{SiF}_4 \cdot 4\text{CH}_3\text{OH}$ contains the bands characteristic of gaseous CH_3OH and SiF_4 , together with bands of medium intensity at 1220, 1170, and 930 cm^{-1} . These bands are characteristic of $(\text{CH}_3)_2\text{O}$ (64), which is formed in small amounts by the dehydration of CH_3OH with SiF_4 as catalyst. The fact that the 3680 cm^{-1} band, identified as the bond stretching vibration of the free O-H group, occurs in the same position as in gaseous CH_3OH indicates that there was little or no hydrogen bonding between CH_3OH and SiF_4 in the gaseous phase at 10 mm pressure.

A comparison of the infrared absorption bands of liquid $\text{SiF}_4 \cdot 4\text{CH}_3\text{OH}$ with those of liquid CH_3OH and gaseous SiF_4 , also given in Table 6, shows the following noteworthy features. (i) The band at 3340 cm^{-1} in CH_3OH is shifted 40 cm^{-1} lower in $\text{SiF}_4 \cdot 4\text{CH}_3\text{OH}$, indicating that there is stronger hydrogen bonding in the complex than in pure CH_3OH . (ii) The strong and broad band at 1025 cm^{-1} in $\text{SiF}_4 \cdot 4\text{CH}_3\text{OH}$ undoubtedly includes the C-O and Si-F bond stretching vibrations. (iii) The band at 720 cm^{-1} also occurs in the gaseous spectrum. This band appeared with almost the same intensity after the liquid sample was washed from the NaCl plates,

and after the gaseous sample was removed from the NaCl gas cell. Moreover, the intensity of this band in the gas phase spectrum did not change when the sample pressure was doubled. These observations strongly suggest a surface effect involving the formation of a species which absorbs at 720 cm^{-1} . This species must be SiF_6^{-2} formed by the interaction of SiF_4 with the NaCl plates, as previously described by Heslop et al. (43).

(d) Proton Magnetic Resonance Measurements

The indication by the infrared data that hydrogen bonding in liquid $\text{SiF}_4 \cdot 4\text{CH}_3\text{OH}$ is greater than in pure CH_3OH was confirmed by the proton magnetic resonance measurements. Hydrogen bonding between CH_3OH and the fluorine atoms of SiF_4 should change the electron density and magnetic polarizability of the electrons around the hydrogen atom of the OH group and, to a lesser extent, the hydrogen atoms of the CH_3 group of CH_3OH . These effects were observed (Fig. 12) as large and small changes in the chemical shifts (τ) of the OH and CH_3 peaks, respectively.

A comparison (Fig. 13) of the magnitude and direction (from high to low field) of the observed chemical shifts with those of the $\text{CH}_3\text{OH}-\text{CCl}_4$ and $\text{CH}_3\text{OH}-\text{CHCl}_3$ systems (65) reveals that (i) hydrogen bonding occurs to a greater extent between SiF_4 and CH_3OH ($\Delta\tau \sim 3.5$ p.p.m.) than in CH_3OH alone ($\Delta\tau \sim 3.0$ p.p.m.); (ii) successive addition of SiF_4 does not simply dilute the CH_3OH ; if it did, the chemical shift would be towards higher magnetic field strength.

The interpretation of Fig. 13 is as follows. The chemical shift

of the OH peak of pure CH_3OH decreases upon the successive addition of small amounts of SiF_4 because of the immediate formation of $\text{SiF}_4 \cdot 4\text{CH}_3\text{OH}$ molecular species and rapid exchange between solvent CH_3OH and CH_3OH hydrogen bonded to SiF_4 . It is interesting to note that only one OH peak is present in the n.m.r. spectrum of $\text{SiF}_4 \cdot 4\text{CH}_3\text{OH}$, no doubt because of rapid exchange between solvent CH_3OH and CH_3OH hydrogen bonded to SiF_4 . In order to observe the OH peaks of both types of CH_3OH simultaneously the lifetime of each state must be longer than the reciprocal of the chemical shift (in cycles sec^{-1}) between the two states (66). Thus, the single OH peak observed at each mole ratio was an average value. These values decreased as the mole ratio, $\text{SiF}_4/\text{CH}_3\text{OH}$, increased, indicating that proportionately more CH_3OH was hydrogen bonded to SiF_4 . When the ratio became 0.25 all of the CH_3OH was used in the formation of the $\text{SiF}_4 \cdot 4\text{CH}_3\text{OH}$ complex. Further addition of SiF_4 produced secondary concentration effects which were directly proportional to the mole ratio, $\text{SiF}_4/\text{CH}_3\text{OH}$.

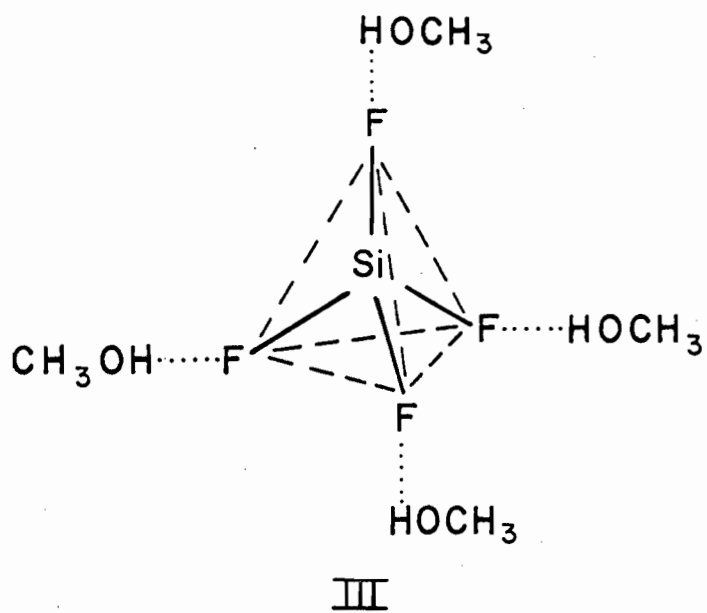
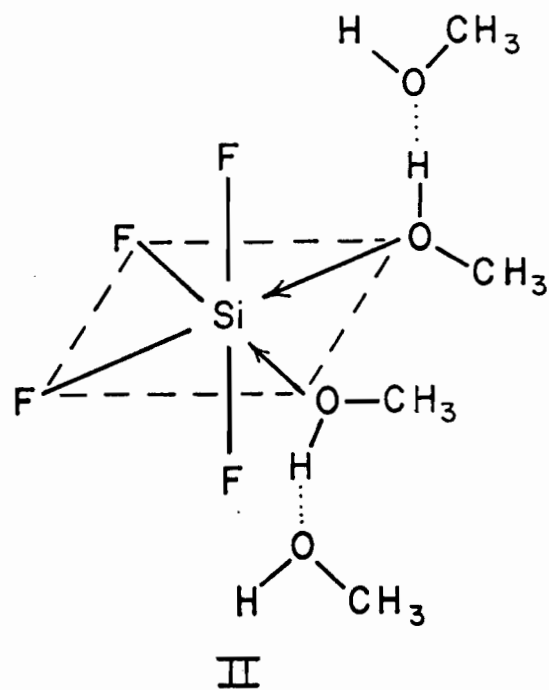
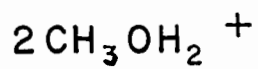
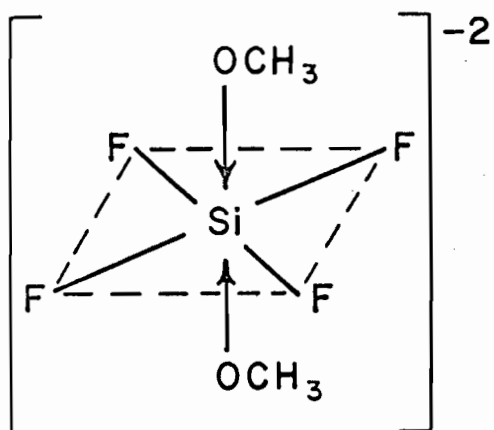
The decrease in τ -values (Fig. 14) of the CH_3 peak was not large because the protons of the CH_3 group were observing only secondary effects. For the previously mentioned reasons only one kind of CH_3 peak was observed.

3. Structure of $\text{SiF}_4 \cdot 4\text{CH}_3\text{OH}$

Fig. 43 shows structures I, II, and III representing three possibilities for the structure of liquid $\text{SiF}_4 \cdot 4\text{CH}_3\text{OH}$. The ionic structure I in which methoxy groups may be in either cis or trans

FIG. 43

Possible structures of liquid $\text{SiF}_4 \cdot 4\text{CH}_3\text{OH}$



arrangement would require (i) a straight line plot for the molar conductance against the square root of the concentration (similar to the one obtained for NaCl in methanol) barring excessive ion-pair formation which seems unlikely in the dilute concentration range; (ii) an octahedral Si-O and Si-F bond stretching vibration in the infrared spectrum; (iii) a probable solid physical state at 25° with perhaps a high melting point although these are not reliable criteria. The liquid complex does not possess any of these properties and therefore structure I is not valid or at least only contributes slightly to the true structure.

Structure II involves octahedral bonding of silicon and hydrogen bonding between CH_3OH and each of the coordinated CH_3OH molecules. The infrared spectrum of such a species should contain an octahedral Si-O bond stretching absorption band and both infrared and proton n.m.r. measurements should indicate only the hydrogen bonding between CH_3OH molecules. Again these properties are not borne out experimentally and therefore structure II is unlikely.

The presence of two peaks in F^{19} magnetic resonance measurements would be evidence for a cis octahedral structure, possibly I or II, but if only one peak results then no new information is obtained. These measurements have not been done for lack of the proper equipment.

In summary, the experimental data reveal that the complex in the liquid state (i) has the composition represented by $\text{SiF}_4 \cdot 4\text{CH}_3\text{OH}$, (ii) is only very slightly dissociated into ions in methanol (conductivity data), (iii) probably does not contain Si-O bonds (infrared data), (iv) contains weak bonding between CH_3OH and SiF_4 such as hydrogen bonds

(compatible with the difficulty in obtaining precise combining ratios), (v) contains strong hydrogen bonds (infrared and n.m.r. data). The most reasonable explanation of these data is that the complex is tetrahedral with strong hydrogen bonds between CH_3OH and each of the four fluorine atoms as shown by structure III.

II. Coordination of SiF_4 with Aliphatic Cyclic Ethers and Dimethyl Ether

1. Preparation of $\text{SiF}_4 \cdot 2(\text{ether})$ Complexes

The $\text{SiF}_4 \cdot 2(\text{ether})$ complexes cannot be prepared by simply bubbling SiF_4 through the ethers at 25° since they are stable only at low temperatures. Muetterties (10) has described some SiF_4 complexes with oxygen electron-pair donor molecules such as, $\text{SiF}_4 \cdot 2(\text{CH}_3)_2\text{SO}$, $\text{SiF}_4 \cdot 2(\text{CH}_3)_2\text{NCHO}$, and $\text{SiF}_4 \cdot x\text{CH}_3\text{COCH}_2\text{COCH}_3$ (where x is uncertain), but his bubbling technique would not have allowed him to detect any complexes which did not precipitate as solids at 25° , and therefore he did not report any complexes between SiF_4 and ethers.

Reaction conditions were generally best when the temperature was such that SiF_4 was gaseous and the ether was either a liquid or a gas. For the preparations of $\text{SiF}_4 \cdot 2(\text{CH}_2)_2\text{O}$ and $\text{SiF}_4 \cdot 2(\text{CH}_2)_3\text{O}$ it was necessary to warm the appropriate SiF_4 -ether mixture slowly from -195° (thus providing a good "heat sink" for the heat of reaction) to a temperature at which reaction would just occur and to prevent any further increase in the temperature. In this way polymerization of the ethers was minimized. For the other $\text{SiF}_4 \cdot 2(\text{ether})$ complexes (where no polymerization occurs) it was best to cool the appropriate SiF_4 -ether mixture slowly from 25° to a temperature sufficiently low to stabilize the complex.

Table 33 summarizes the mole ratios, ether/ SiF_4 , obtained experimentally.

TABLE 33

Combining ratios obtained for $\text{SiF}_4 \cdot 2(\text{ether})$ complexes

Complex prepared	Mole ratio obtained, ether/ SiF_4		
	Direct synthesis	Tensimetric titration	
	Excess SiF_4	Excess SiF_4	Excess ether
$\text{SiF}_4 \cdot 2(\text{CH}_2)_2\text{O}$	1.99	2.03	2.00
$\text{SiF}_4 \cdot 2(\text{CH}_2)_3\text{O}$	2.05	2.27	> 4
$\text{SiF}_4 \cdot 2(\text{CH}_2)_4\text{O}$	1.91	2.15	2.13
$\text{SiF}_4 \cdot 2(\text{CH}_2)_5\text{O}$	2.14	erratic, > 2	erratic, > 2
$\text{SiF}_4 \cdot 2(\text{CH}_3)_2\text{O}$	2.01	2.01	2.01

The results section explains the difficulty in preparing the pure complexes by direct synthesis using excess ether.

In general, SiF_4 combined with an ether in a 1:2 mole ratio (or very nearly so). The high values obtained for the preparation of $\text{SiF}_4 \cdot 2(\text{CH}_2)_3\text{O}$ by tensimetric titration can be explained in terms of polymerization effect particularly in the titration using excess $(\text{CH}_2)_3\text{O}$ in which the polymerization is no doubt enhanced. The case of $\text{SiF}_4 \cdot 2(\text{CH}_2)_5\text{O}$ has been briefly discussed in the results section (p.82). The erratic and somewhat high mole ratios obtained were attributed to the relatively high melting point of $(\text{CH}_2)_5\text{O}$ (m.p. -49°) and the instability of the complex, $\text{SiF}_4 \cdot 2(\text{CH}_2)_5\text{O}$.

2. Properties of the $\text{SiF}_4 \cdot 2$ (ether) Complexes

(a) General Properties and Comparisons

All the $\text{SiF}_4 \cdot 2$ (ether) complexes are white solids stable only at low temperatures ($<<25^\circ$). They did not appear to have any stable liquid state and were completely dissociated in the gas phase at 25° . Only $\text{SiF}_4 \cdot 2(\text{CH}_2)_3\text{O}$ could be sublimed into colorless crystals which were stable only below 13.6° . Table 3 shows quantitative data on the stability of $\text{SiF}_4 \cdot 2$ (ether) complexes and this will be discussed in detail in the next section, "Heats of Dissociation".

Ether complexes of GeF_4 (24) and BF_3 (67-71) are all much more stable than those of SiF_4 . The complexes, $\text{GeF}_4 \cdot 2$ (ether), where ether is $(\text{CH}_3)_2\text{O}$, $(\text{CH}_2)_4\text{O}$, and $(\text{CH}_2)_5\text{O}$, are stable solids at 25° , but

$\text{GeF}_4 \cdot 2(\text{CH}_2)_2\text{O}$ decomposes above -78° . The complexes $\text{BF}_3 \cdot (\text{ether})$, where ether is $(\text{CH}_3)_2\text{O}$, $(\text{CH}_2)_4\text{O}$, and $(\text{CH}_2)_5\text{O}$, are stable liquids at 25° , and $\text{BF}_3 \cdot (\text{CH}_3)_2\text{O}$ and $\text{BF}_3 \cdot (\text{CH}_2)_4\text{O}$ boil without decomposition (67). Both 1:1 and 1:2 complexes of BF_3 with 1,4-dioxane are stable at 25° , the former a solid and the latter a liquid. Only a stable 1:1 complex is formed between GeF_4 and 1,4-dioxane. In contrast, SiF_4 does not interact with 1,4-dioxane even at temperatures as low as -94° .

However, there is a strong similarity between complexes containing $(\text{CH}_2)_2\text{O}$. Thus, $\text{GeF}_4 \cdot 2(\text{CH}_2)_2\text{O}$ (72) and $\text{SiF}_4 \cdot 2(\text{CH}_2)_2\text{O}$ (with excess $(\text{CH}_2)_2\text{O}$) decompose yielding 1,4-dioxane. Ethylene oxide complexes of BF_3 (70,71) and SiF_4 , prepared using excess Lewis acid, decompose at 25° into polymeric nonvolatile material with the evolution of the Lewis acid. Using excess $(\text{CH}_2)_2\text{O}$ no complex was obtained with BF_3 , but on warming such a mixture to 25° , 1,4-dioxane and a purple polymer resulted. Similarly, the addition of excess $(\text{CH}_2)_2\text{O}$ to $\text{SiF}_4 \cdot 2(\text{CH}_2)_2\text{O}$ and subsequent warming to 25° resulted in the formation of a purple polymer.

The products of dissociation have not yet been investigated for the GeF_4 -ether complexes and only superficially for the BF_3 -ether complexes. In the $\text{SiF}_4 \cdot 2(\text{ether})$ complexes dissociation yields only the starting components except when conditions are such that simultaneous polymerization occurs. Under proper experimental conditions, solid $\text{SiF}_4 \cdot 2(\text{CH}_2)_2\text{O}$ and $\text{SiF}_4 \cdot 2(\text{CH}_2)_3\text{O}$ can dissociate partially without polymerization.

A plausible mechanism, similar to the one previously proposed for the $\text{BCl}_3 - (\text{CH}_2)_2\text{O}$ system (73), is suggested for the catalytic dimeriz-

ation of $(\text{CH}_2)_2\text{O}$ by SiF_4 , and is shown in Fig. 44.

Comparison of the infrared spectra of the viscous liquid formed from the decomposition of $\text{SiF}_4 \cdot 2(\text{CH}_2)_2\text{O}$ (prepared using excess SiF_4) with that of liquid 1,4-dioxane (Table 8) indicates strong similarities. The only absorption bands which do not correspond are the 960 and 723 cm^{-1} bands. The 723 cm^{-1} absorption band is probably due to an interaction with the NaCl plates forming SiF_6^{-2} (32,43). The viscous liquid shows a poorly resolved 2950-2850 cm^{-1} region and a broadening of the 1125-1045 cm^{-1} region. Broadening of absorption bands in the C-O bond stretching vibration region has been observed in polyethyleneglycol polymers and ethylene oxide-acrylonitrile copolymers (74).

The almost identical position of the absorption bands for the viscous liquid and 1,4-dioxane indicates the presence of only O-C-C-O linkages in the viscous liquid. The broadening of the C-O bond stretching vibration region, together with the physical characteristics observed, show that the viscous, nonvolatile colorless liquid is polymeric.

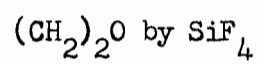
The decomposition of $\text{SiF}_4 \cdot 2(\text{CH}_2)_3\text{O}$ yielded only a colorless polymer and SiF_4 (quantitatively) whether $(\text{CH}_2)_3\text{O}$ was in excess or not. Its infrared spectrum (Fig. 20) is much more complicated than that of the $(\text{CH}_2)_2\text{O}$ polymer.

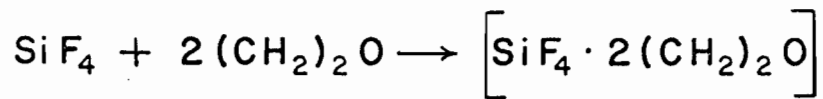
(b) Heats of Dissociation

Table 34 summarizes the general stability of the $\text{SiF}_4 \cdot 2(\text{ether})$ complexes including their heats of dissociation. It is interesting to

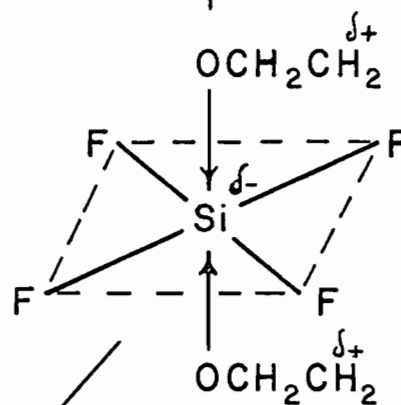
FIG. 44

A proposed mechanism for the catalytic dimerization of

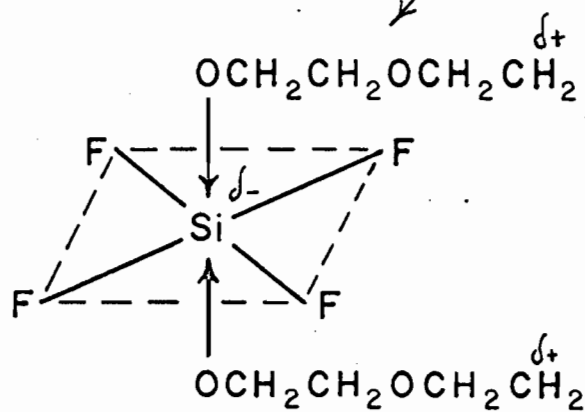




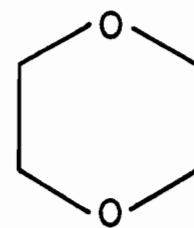
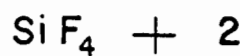
ring fission



addition of (CH₂)₂O



weak Si-O bond broken



1,4-dioxane

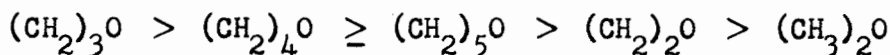
TABLE 34

General stability and heat of dissociation of the
 $\text{SiF}_4 \cdot 2$ (ether) complexes

Complex	$\Delta H_{\text{dissc.}}^\circ$	Decomposition and/or Dissociation	
	± 0.3 kcal mole ⁻¹	Minimum Temperature # , Temperature Range of Reversible Dissociation °C	Products
$\text{SiF}_4 \cdot 2(\text{CH}_2)_2\text{O}$	10.6	-100, -93.2 to -68.3	a) with excess SiF_4 : SiF_4 , polymer b) with excess $(\text{CH}_2)_2\text{O}$: SiF_4 , $(\text{CH}_2)_2\text{O}$, polymer and 1,4-dioxane
$\text{SiF}_4 \cdot 2(\text{CH}_2)_3\text{O}$	13.9	- 30, -23.0 to +13.6	SiF_4 , polymer
$\text{SiF}_4 \cdot 2(\text{CH}_2)_4\text{O}$	11.3	- 80, -69.0 to -30.8	SiF_4 , $(\text{CH}_2)_4\text{O}$
$\text{SiF}_4 \cdot 2(\text{CH}_2)_5\text{O}$	11.1	- 95, -83.0 to -54.3	SiF_4 , $(\text{CH}_2)_5\text{O}$
$\text{SiF}_4 \cdot 2(\text{CH}_3)_2\text{O}$	9.0	-105, -94.0 to -56.6	SiF_4 , $(\text{CH}_3)_2\text{O}$

The temperature at which a pressure of about 0.1 mm is observed above the solid complex.

note that the minimum dissociation temperatures are in the same order as the heats of dissociation of the complexes, i.e., a low minimum dissociation temperature corresponds to a low heat of dissociation. The heat of dissociation of the complexes follows the order:



indicating that this is the relative order of basicities of the ethers towards SiF_4 .

In general, for heterogeneous equilibria the Clausius-Clapeyron equation cannot be used but the integrated form of the van't Hoff reaction isobar (75), $\Delta H^\circ = \frac{-2.303 R \log \Delta K_p}{\Delta(T^{-1})}$, must be used to calculate

heats of dissociation. The only difference between the two equations is the use of " K_p ", the equilibrium constant expressed in pressures, in the van't Hoff reaction isobar in place of "p" in the Clapeyron equation.

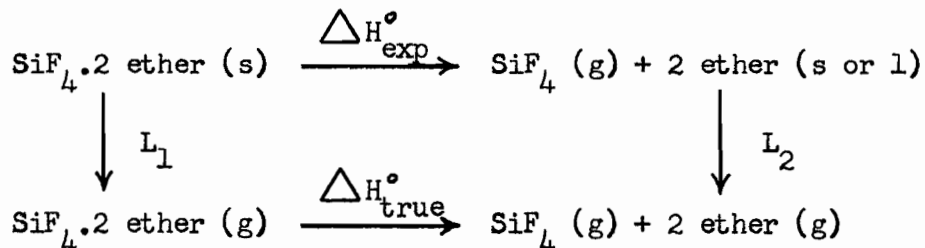
The $\Delta H_{\text{dissc.}}^\circ$ is then calculated from the slope of the linear $\log K_p$ (atm.) vs T^{-1} plot. Values of " K_p " are found from a calculated relationship between " K_p " and "p", i.e., $K_p = \frac{\text{activity of products}}{\text{activity of reactants}}$, where the activities for the assumed ideal gases involved reduces to pressures and the activities of pure solid or liquid are taken as unity.

The equilibrium constant can only be calculated if the dissociation products are in a definite state. Also, if the complexes are not fully dissociated in the gaseous phase the degree of dissociation (α) must be known in order to calculate " K_p ".

In the case of the $\text{SiF}_4 \cdot 2(\text{ether})$ complexes, it was assumed that

the complexes were completely dissociated in the gaseous phase. In the temperature range that dissociation pressures were measured, the dynamic equilibrium present was considered to be $\text{SiF}_4 \cdot 2(\text{ether}) (\text{s}) = 2 \text{ ether} (\text{l}) + \text{SiF}_4 (\text{g})$, except for $\text{SiF}_4 \cdot 2(\text{CH}_2)_5\text{O}$ where the $(\text{CH}_2)_5\text{O}$ would be solid in the temperature range over which pressures were measured. To calculate " K_p " it was necessary to assume that the complex was involatile and that the vapor pressure of the liquid ether was negligible in comparison with the SiF_4 pressure*. Similar assumptions were made for the calculation of thermodynamic data of BF_3 -ether complexes (67). Thus, it is assumed that the dissociation pressure of the complex is due entirely to SiF_4 , which gives simply $K_p = p$ (atm.) and the Clapeyron equation, $\Delta H^\circ = \frac{-2.303 \log \Delta p}{\Delta (T^{-1})}$, can be used to calculate ΔH° , since the plot, $\log K_p$ vs T^{-1} , is equivalent to the plot, $\log p$ vs T^{-1} .

What do the experimental heats of dissociation ($\Delta H^\circ_{\text{exp}}$) mean? The relationship between $\Delta H^\circ_{\text{exp}}$ and $\Delta H^\circ_{\text{true}}$, the actual heat change due to the rupture of both SiF_4 -ether bonds, is shown by the following Hess's law cycle (76), L_1 and L_2 being the latent heats of sublimation of the complex and the ether, respectively.



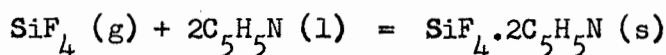
Consequently, $\Delta H^\circ_{\text{exp}} = \Delta H^\circ_{\text{true}} + L_1 - L_2$, or $\Delta H^\circ_{\text{true}} = \Delta H^\circ_{\text{exp}} + L_2 - L_1$.

* This assumption is justified because even $(\text{CH}_3)_2\text{O}$, the most volatile ether used, has a vapor pressure about 100 times less than that of SiF_4 .

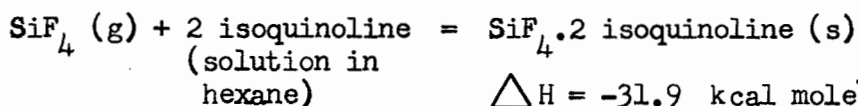
The latent heats of sublimation, L_2 , are only known for $(\text{CH}_2)_2\text{O}$ (7.34 kcal mole⁻¹) and $(\text{CH}_3)_2\text{O}$ (6.32 kcal mole⁻¹) (77). Since L_2 differs by only 1.02 kcal mole⁻¹ for $(\text{CH}_2)_2\text{O}$, a cyclic ether, and $(\text{CH}_3)_2\text{O}$, an acyclic ether, it is not unreasonable to assume that there will be much less difference within the series of aliphatic cyclic ethers. Finally, assuming that L_1 will not vary greatly within a series of similarly coordinated complexes, $\Delta H_{\text{true}}^\circ$ can be related directly to $\Delta H_{\text{exp}}^\circ$.

The actual order found for $\Delta H_{\text{dissc}}^\circ (= \Delta H_{\text{exp}}^\circ)$ for the $\text{SiF}_4 \cdot 2(\text{cyclic ether})$ complexes, shown by Fig. 45, agrees with the order found by other workers (68-71, 73, 78-90) for the basicities of these ethers, thus strengthening the validity of the two previous assumptions. Only Lippert and Prigge (91) disagree with the relative base strength of $(\text{CH}_2)_4\text{O}$ and $(\text{CH}_2)_5\text{O}$, but there appears to be discrepancies in this part of their results as will be shown later.

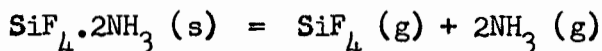
Complexes of SiF_4 with nitrogen electron-pair donor molecules have much higher heats of dissociation than those with oxygen electron-pair donor molecules such as ethers. For example,



$$\Delta H = -33.1 \text{ kcal mole}^{-1} \quad (92)$$



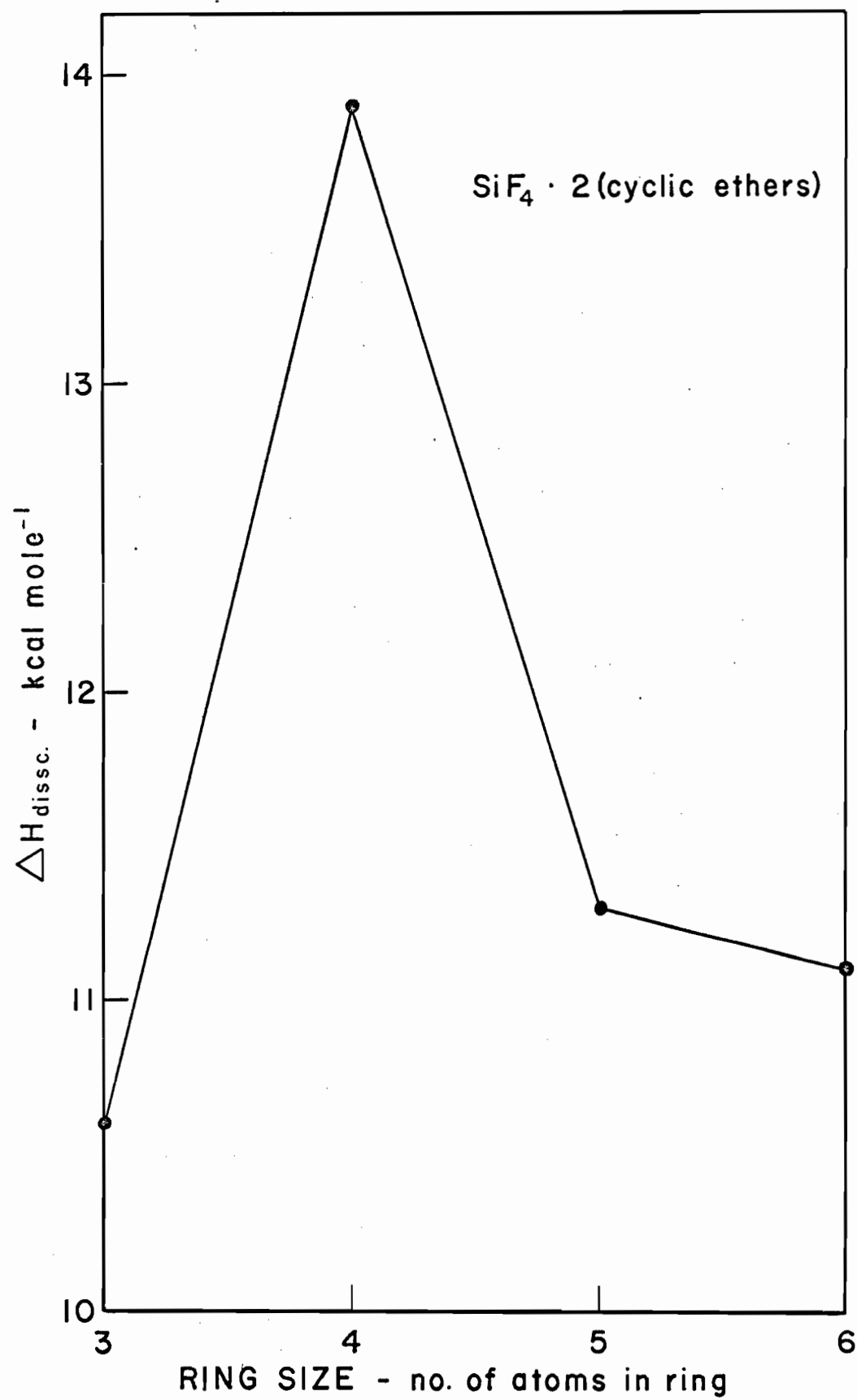
$$\Delta H = -31.9 \text{ kcal mole}^{-1} \quad (92)$$



$$\Delta H = 54.6 \text{ kcal mole}^{-1} \quad (14).$$

FIG. 45

Stability plot of $\text{SiF}_4 \cdot 2(\text{aliphatic cyclic ether})$ complexes,
heats of dissociation against ring size



However, BF_3 .ether complexes appear to have only slightly higher heats of dissociation than those of the $\text{SiF}_4 \cdot 2(\text{ether})$ complexes.

For example, $\text{BF}_3 \cdot (\text{CH}_3)_2\text{O} (\text{s}) = \text{BF}_3 (\text{g}) + (\text{CH}_3)_2\text{O} (\text{g})$

$$\Delta H = 13.3 \text{ kcal mole}^{-1} \quad (69)$$

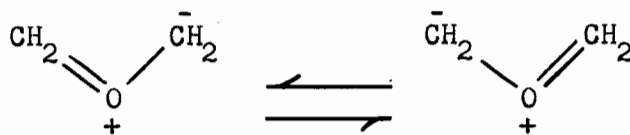
$\text{BF}_3 \cdot (\text{CH}_2)_4\text{O} (\text{s}) = \text{BF}_3 (\text{g}) + (\text{CH}_2)_4\text{O} (\text{g})$

$$\Delta H = 13.4 \text{ kcal mole}^{-1} \quad (69).$$

Nevertheless, $E(\text{Si-O}) < E(\text{B-O})$, where "E" represents the coordinate bond energy, since two Si-O bonds are broken for every molecule of complex that dissociates and therefore, $E(\text{Si-O}) = \Delta H_{\text{dissc.}}^{\circ} / 2$

(b-1) Previous Explanations for the Relative Basicities of Aliphatic Cyclic and Acyclic Ethers

Some attempts have been made to explain the relatively weak base strength of $(\text{CH}_2)_2\text{O}$ (87-89,91). If steric hindrance alone were considered, $(\text{CH}_2)_2\text{O}$ would be the strongest base in the series of ethers investigated, but it is actually the weakest. Searles et al. (87) proposed a delocalization of the nonbonded electrons on the oxygen atom resulting in a small contribution from the following resonance structures,



The idea is supported by the following facts: (i) the dipole moment of $(\text{CH}_2)_2\text{O}$ is less than that of $(\text{CH}_2)_3\text{O}$ (93) and (ii), the C-O bond distance (1.436 Å) in $(\text{CH}_2)_2\text{O}$ is shorter than expected (94). However, the possibility that the nonbonded electrons on the oxygen atom are partly

delocalized into antibonding orbitals of the carbon atoms is not borne out by quantum mechanical analysis (95). It has also been proposed (88,89) that a redistribution of electrons occurs with change in ring size but no further statements were made as to the nature of the distribution.

Lippert and Prigge (91) have offered a more convincing explanation for the relative basicities of the aliphatic cyclic ethers, based on the hybridization of the nonbonded orbitals of the oxygen atom. This depends on the hybridization of the bonded orbitals of the oxygen atom which in turn, is related to the C-O-C bond angle. Table 35 summarizes their proposals. They found that the order of basicities was: $(\text{CH}_2)_3\text{O} > (\text{CH}_2)_5\text{O} > (\text{CH}_2)_4\text{O} > (\text{CH}_2)_2\text{O}$, based on measurements of the hydrogen-bond strengths towards phenol. However their results are contradictory in the case of $(\text{CH}_2)_5\text{O}$, since their values for $\Delta \nu(\text{OH})_{\text{cm}^{-1}}$ and for K_{ass} (the equilibrium constant) indicate that $(\text{CH}_2)_5\text{O}$ is a weaker base than $(\text{CH}_2)_4\text{O}$.

For $(\text{CH}_2)_2\text{O}$, they claim that the nonbonded orbitals on the oxygen atom are not hybridized but remain as pure "s" and pure "p" orbitals. The nonhybridized orbitals would have less overlap potential than that of hybrid orbitals formed by the hybridization of the pure "s" and "p" orbitals (as claimed for the larger ring ethers), thus $(\text{CH}_2)_2\text{O}$ would be the weakest base.

In the case of $(\text{CH}_2)_4\text{O}$, the nonbonded orbitals on the oxygen atom were considered to be essentially sp^3 -hybrid orbitals, each with an s-character of 0.25. This makes $(\text{CH}_2)_4\text{O}$ a stronger donor than $(\text{CH}_2)_2\text{O}$.

TABLE 35

Hybridization of the nonbonded orbitals on the oxygen atom of the
aliphatic cyclic and acyclic ethers (Lippert and Prigge)

	$(\text{CH}_2)_2\text{O}$	$(\text{CH}_2)_3\text{O}$	$(\text{CH}_2)_4\text{O}$	$(\text{CH}_2)_5\text{O}$	R_2O^*
C-O-C, approx. orbital angle ("bent" bond) (95,96)	90°	100°	109.5°	112°	120°
type of bonding orbitals	pure p (no hybrid)	$\text{sp}^{>3}$ hybrid	sp^3 hybrid	$\text{sp}^{<3}$ hybrid	sp^2 hybrid
type of nonbonded orbitals	p, s (no hybrid)	$\text{sp}^{<3}$, $\text{sp}^{<3}$ hybrids	sp^3 , sp^3 hybrids	$\text{sp}^{>3}$, $\text{sp}^{<3}$ hybrids	p, sp^2 hybrid
s-character of nonbonded orbitals	0, 1.0	>0.25, >0.25	0.25, 0.25	<0.25, >0.25	0, 0.33

* R is a bulky group such as t-butyl.

However, $(\text{CH}_2)_3\text{O}$ was considered to have nonbonded orbitals on the oxygen atom each with an s-character greater than 0.25 (and therefore closer to the s-character = 0.5 for maximum overlap) thus resulting in better overlap potential and making this ether the strongest donor.

According to Lippert and Prigge, acyclic ethers theoretically should be stronger bases than $(\text{CH}_2)_4\text{O}$ since their nonbonded orbitals on the oxygen atom are a pure "p" and an sp^2 -hybrid, of which the latter should overlap better than an sp^3 -hybrid orbital. But the steric effect of the "R" groups on the oxygen atom makes the acyclic ethers generally weaker bases than the cyclic ethers.

Finally, they offered the explanation that one of the nonbonded orbitals on the oxygen atom of $(\text{CH}_2)_5\text{O}$ approached those of R_2O , i.e., one orbital is nearly an sp^2 -hybrid and the other nearly a "p". This would support a somewhat stronger basicity for $(\text{CH}_2)_5\text{O}$ than for $(\text{CH}_2)_4\text{O}$.

(b-2) Proposed Explanation

Lippert and Prigge's explanation does not appear to be theoretically plausible for the following reasons. (i) The pure "s" and pure "p" nonbonded orbitals on the oxygen atom of $(\text{CH}_2)_2\text{O}$ would likely hybridize to two equivalent sp -hybrid orbitals perpendicular to the plane of the ring and if their idea of maximum overlap resulting from a hybrid orbital of s-character about 0.5 is correct, then $(\text{CH}_2)_2\text{O}$ would be the strongest base in the series! Also, (ii) there is no reason to suppose that the nonbonded orbitals on the oxygen atom of $(\text{CH}_2)_5\text{O}$ are non-equivalent hybrid orbitals and that a sudden "break" has occurred in going from

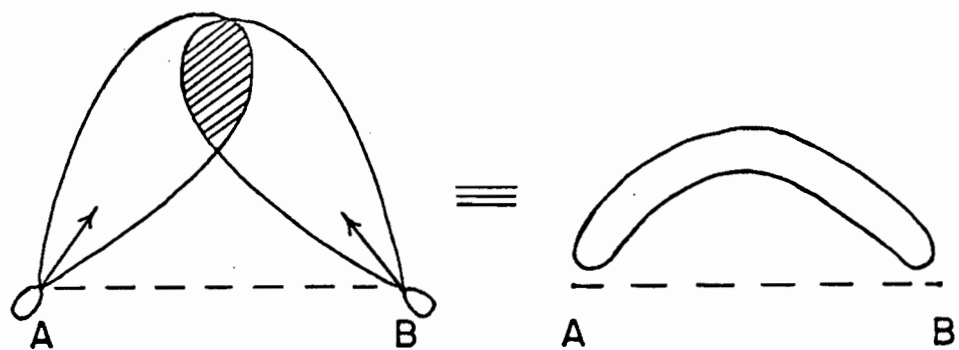
$(\text{CH}_2)_4\text{O}$ to $(\text{CH}_2)_5\text{O}$, i.e., from two nonbonded sp^3 orbitals to a nearly sp^2 and a nearly "p" nonbonded orbital. In fact, the difference in C-O-C bond angle is probably sufficiently small that little change in hybridization would occur on the nonbonded orbitals of the oxygen atom in going from $(\text{CH}_2)_4\text{O}$ to $(\text{CH}_2)_5\text{O}$.

All through their explanation, Lippert and Prigge have assumed that the strongest hydrogen bonds would be formed using sp -hybrid orbitals (s-character = 0.5). But the overlap integral is a maximum only between two similar atomic hybrid orbitals when the effective nuclear charge, Z , is related to the internuclear distance, J , by the condition, $ZJ = 8.0$ (97). Calculations have not yet been made for different overlap conditions and certainly Lippert and Prigge's hydrogen bonds or the Si-O coordinate bond are not formed by the overlap of similar atomic orbitals. It is even possible that as overlap occurs the interatomic bond distance changes in order to strengthen the bond which is being formed.

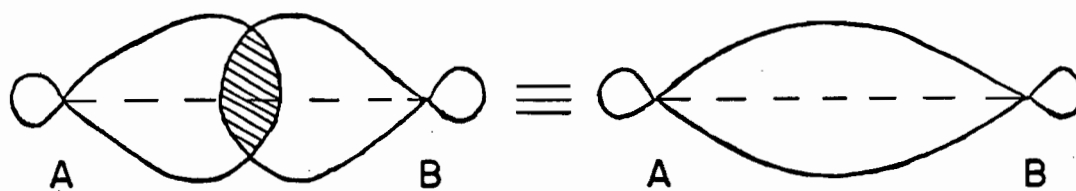
Although the concept of "bent or banana" bonds (Fig. 46) has not yet been applied to the bonding orbitals on the oxygen atom of the aliphatic cyclic ethers, as it has been done for the cycloalkanes (3,4, and 5 membered rings) (98), it seems reasonable to apply the results to these ethers. In the cycloalkanes, the s-character of the $\text{C} \leftarrow \text{C} \rightarrow \text{C}$ bonding orbitals increases as the ring size increases (C-C-C bond angle increasing), thus the s-character of the $\text{H} \leftarrow \text{C} \rightarrow \text{H}$ bonding orbitals decreases as the ring size increases. This is as far as Coulson and Goodwin (98) extended the concept.

FIG. 46

A diagram showing the concept of "bent"
or "banana" bonds



a BENT or BANANA BOND between atoms A and B



a LINEAR BOND between atoms A and B

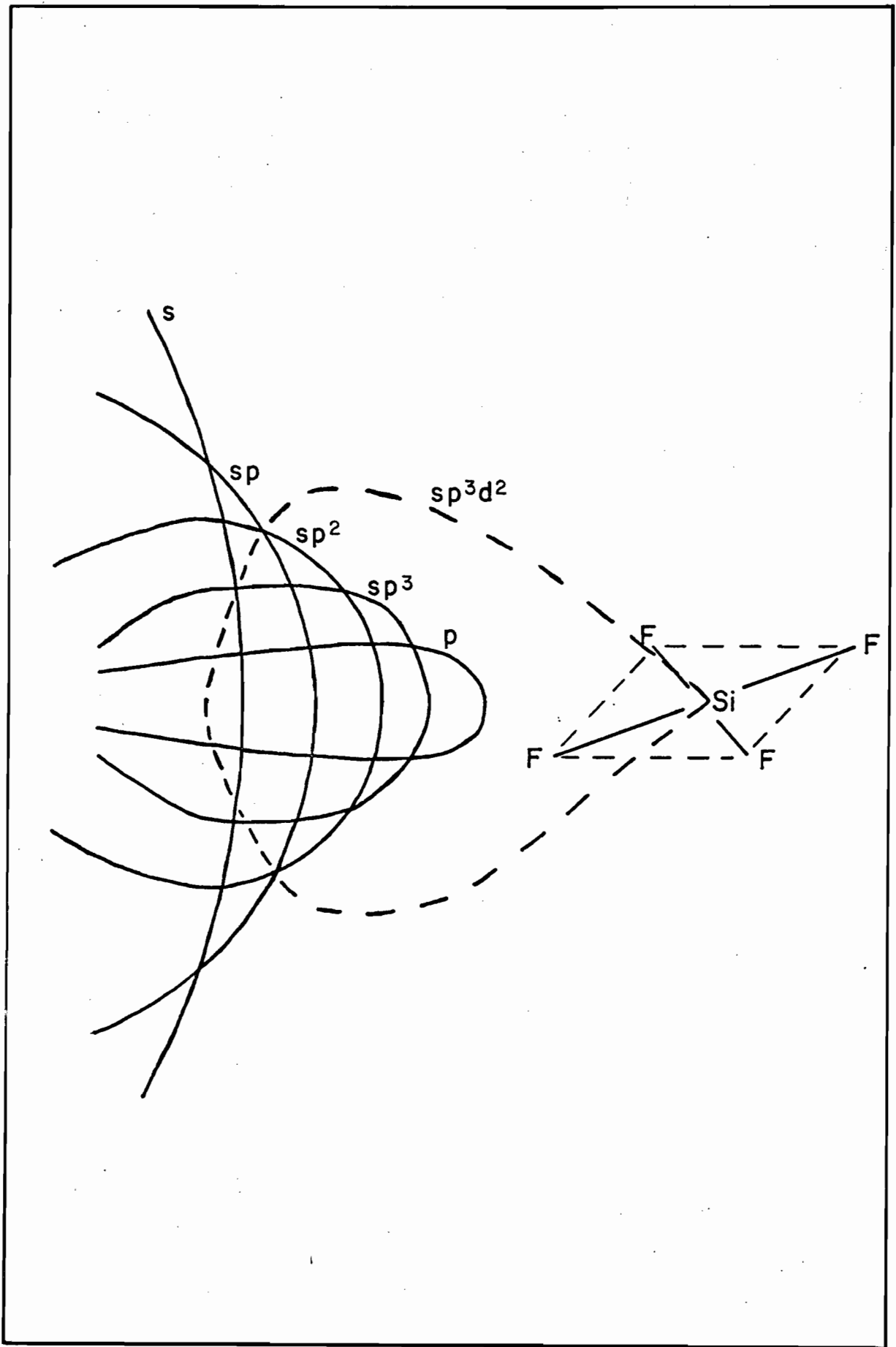
Replacement of a carbon atom by an oxygen atom probably results in slight widening of the original C-C-C bond angle of the cycloalkane, e.g., the C-C-C bond angle in propane increases from 109.5 to 111° in $(\text{CH}_3)_2\text{O}$ (99), but this should not affect the relative magnitudes of the angles and the C-O-C bond angle should also increase with increasing ring size. Applying the Coulson-Goodwin concept, mentioned in the previous paragraph, to the simple aliphatic cyclic ethers, it is reasonable to expect that the s-character of the nonbonded orbital on the oxygen atom would decrease with increasing ring size and therefore, the nonbonded orbitals would become more directional and the angle between them would decrease.

Fig. 47 shows the type of overlap that could occur between a vacant sp^3d^2 -hybrid orbital and hybrid orbitals with varying s-character (from 1.0 to 0). It is clear that pure "s" and pure "p" orbitals overlap the least and that the maximum overlap probably occurs for a hybrid orbital possessing an s-character between 0.5 and 0.25, i.e., between sp and sp^3 -hybrid orbitals, depending on the actual shape of the sp^3d^2 -hybrid orbital. As the s-character of the nonbonded hybrid orbitals on the oxygen atom changes from its value for maximum overlap, the overlap potential must decrease continuously. It is illogical (see Fig. 47) that the overlap potential should suddenly become larger after the maximum has been reached. Yet this is exactly what Lippert and Prigge imply by stating that $(\text{CH}_2)_5\text{O}$ is a stronger base than $(\text{CH}_2)_4\text{O}$.

The observed experimental order of basicity for the aliphatic cyclic ethers towards SiF_4 , plotted for convenience in Fig. 45, can be

FIG. 47

The extent of overlap that may occur between a vacant sp^3d^2 -hybrid orbital and hybrid orbitals of varying s-character

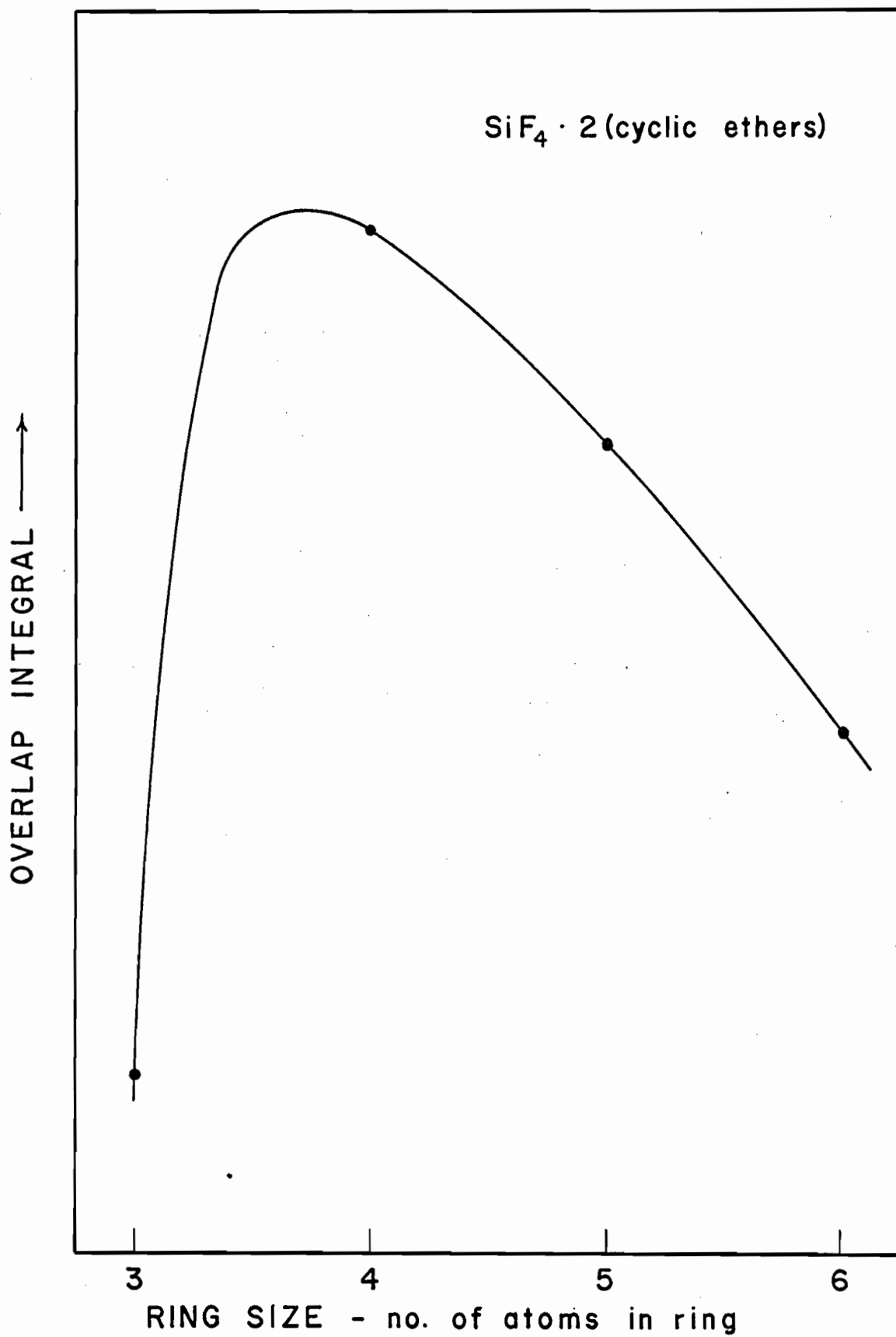


explained as follows. (i) The nonbonding orbitals on the oxygen atom of $(\text{CH}_2)_3\text{O}$ must have the right amount of s and p-character (directional) to make the overlap integral for the coordinate bonds of $\text{SiF}_4 \cdot 2(\text{CH}_2)_3\text{O}$ a maximum. A reasonable guess (assuming a C-O-C true bond angle of about 100°) is that the nonbonded orbitals are equivalent hybrids between sp^2 and sp^3 -hybrid orbitals (probably nearer to sp^2). (ii) For $(\text{CH}_2)_2\text{O}$, the nonbonding orbitals are probably equivalent sp-hybrids (assuming a C-O-C true bond angle of about 90°), 180° to each other and 90° to the plane of the ring, resulting in a smaller overlap integral for the coordinate bonds of $\text{SiF}_4 \cdot 2(\text{CH}_2)_2\text{O}$. (iii) Similarly, the overlap integrals for the coordinate bonds of $\text{SiF}_4 \cdot 2(\text{CH}_2)_4\text{O}$ and $\text{SiF}_4 \cdot 2(\text{CH}_2)_5\text{O}$ must be less than that for the coordinate bonds of $\text{SiF}_4 \cdot 2(\text{CH}_2)_3\text{O}$ but somewhat larger than that for the coordinate bonds of $\text{SiF}_4 \cdot 2(\text{CH}_2)_2\text{O}$. Assuming a C-O-C true bond angle of about 109.5° for $(\text{CH}_2)_4\text{O}$ and one slightly larger for $(\text{CH}_2)_5\text{O}$, the nonbonded orbitals are probably equivalent sp^3 -hybrids for $(\text{CH}_2)_4\text{O}$ and probably equivalent $\text{sp}^{>3}$ -hybrids (but very nearly sp^3) for $(\text{CH}_2)_5\text{O}$.

The overlap integral for the coordinate bonds of the $\text{SiF}_4 \cdot 2(\text{cyclic ether})$ complexes plotted against the ring size of the aliphatic ether might reasonably be expected to result in a plot similar to the one shown in Fig. 48, which would have essentially the same shape as that of Fig. 45, i.e., the overlap integral should be directly proportional to the heat of dissociation.

FIG. 48

The possible form of the plot of the overlap integral for the
coordinate bonds of the $\text{SiF}_4 \cdot 2(\text{aliphatic cyclic ether})$
complexes



III. Coordination of SiF_4 with Pyridine and Other Nitrogen Electron-Pair Donor Molecules

1. Coordination of SiF_4 with Pyridine

(a) Preparation of $\text{SiF}_4 \cdot 2\text{C}_5\text{H}_5\text{N}$

The various methods used for the preparation of $\text{SiF}_4 \cdot 2\text{C}_5\text{H}_5\text{N}$ and the results obtained are summarized in Table 36.

Although the authors' methods were followed carefully, $\text{SiF}_4 \cdot 3/2\text{C}_5\text{H}_5\text{N}$ (12) and $\text{SiF}_4 \cdot \text{C}_5\text{H}_5\text{N}$ (10,11) could not be prepared. Table 36 indicates that various methods of preparation always yielded only the 1:2 complex, $\text{SiF}_4 \cdot 2\text{C}_5\text{H}_5\text{N}$. It is interesting to note that Schnell (8) also obtained only the 1:2 complex.

The reports of combining ratios other than 1:2 are likely incorrect. Hydrolysis of the 1:2 complex releases $\text{C}_5\text{H}_5\text{N}$ while forming $(\text{C}_5\text{H}_5\text{NH})_2\text{SiF}_6$ and SiO_2 , so that as hydrolysis proceeds it would appear that $\text{SiF}_4 \cdot 2\text{C}_5\text{H}_5\text{N}$ is changing into some species with a lower $\text{C}_5\text{H}_5\text{N}$ content. Since $\text{SiF}_4 \cdot 2\text{C}_5\text{H}_5\text{N}$ is easily hydrolyzed, as evidenced by the odor of $\text{C}_5\text{H}_5\text{N}$ on its exposure to moist air, the reports of combining ratios other than 1:2 are probably due to hydrolysis products and loss of $\text{C}_5\text{H}_5\text{N}$.

(b) Properties of $\text{SiF}_4 \cdot 2\text{C}_5\text{H}_5\text{N}$

(i) Stability

The complex, $\text{SiF}_4 \cdot 2\text{C}_5\text{H}_5\text{N}$, was a white stable solid melting at 170-180° with decomposition, had no measurable vapor pressure at 25°, and could be sublimed in a vacuum without decomposition at 60-80°. In an

TABLE 36

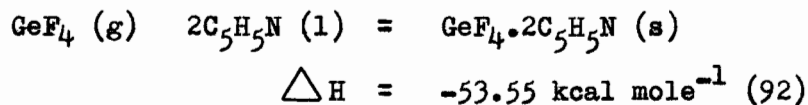
Summary of the analytical data obtained for $\text{SiF}_4 \cdot 2\text{C}_5\text{H}_5\text{N}$
 prepared by various methods

Method of Synthesis	Mole Ratio, $\frac{\text{C}_5\text{H}_5\text{N}}{\text{SiF}_4}$	Fluorine Analysis* (36), %F
direct g-l, vacuum, with excess SiF_4	2.00	28.60
with excess $\text{C}_5\text{H}_5\text{N}$ after sublimation	2.00 -	28.60 29.01
$\text{C}_5\text{H}_5\text{N}$ -diethyl ether solution, stirred in vacuum	-	28.58
bubbling SiF_4 into $\text{C}_5\text{H}_5\text{N}$ -diethyl ether solution	-	29.17
bubbling SiF_4 into $\text{C}_5\text{H}_5\text{N}$ -acetonitrile solution	-	28.64
tensimetric titrations, SiF_4 with $\text{C}_5\text{H}_5\text{N}$	2.01	28.90
$\text{C}_5\text{H}_5\text{N}$ with SiF_4	2.01	28.85

* Calc. for $\text{SiF}_4 \cdot 2\text{C}_5\text{H}_5\text{N}$: %F, 28.95. for $\text{SiF}_4 \cdot \text{C}_5\text{H}_5\text{N}$: %F, 41.50.

atmosphere of dry nitrogen it could be stored indefinitely at 25°, without noticeable change. Recently, the heat of formation of the complex in excess pyridine, -33.1 kcal mole⁻¹, has been measured calorimetrically (92).

The complex, SiF₄·2C₅H₅N, appears to be somewhat less stable than BF₃·C₅H₅N which has a heat of formation in nitrobenzene of -25.0 kcal mole⁻¹ (100). Actually, E(Si-N) = -16.5 kcal mole⁻¹ for SiF₄·2C₅H₅N since two bonds are formed in SiF₄·2C₅H₅N while E(B-N) = -25.0 kcal mole⁻¹ for BF₃·C₅H₅N. Also BF₃·C₅H₅N melts at 48-49° (67) and boils at 300° (101), in each case apparently without decomposition. In contrast, GeF₄·2C₅H₅N is a much more stable white solid with the following heat of formation:



Since NH₂(CH₂)₂NH₂ quantitatively displaced C₅H₅N from SiF₄·2C₅H₅N it is evident that SiF₄·NH₂(CH₂)₂NH₂ is the more stable complex.

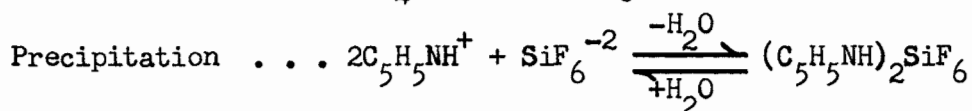
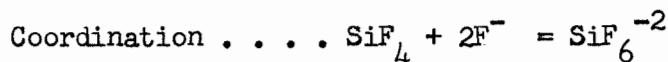
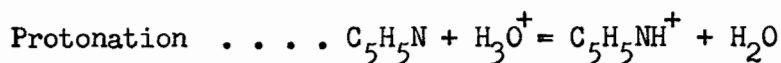
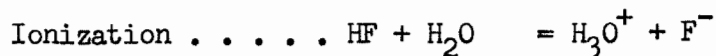
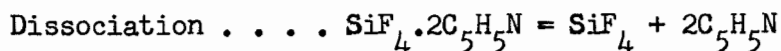
(ii) Displacement Reaction with Ethylenediamine

This experiment was done in order to obtain information about the structure of SiF₄·2C₅H₅N. The idea was, if C₅H₅N ligands were in cis octahedral positions then they could be displaced quantitatively by NH₂(CH₂)₂NH₂, however, if C₅H₅N ligands were in trans octahedral positions then they would not be displaced by NH₂(CH₂)₂NH₂ unless there occurred a change in configuration in going from SiF₄·2C₅H₅N to SiF₄·NH₂(CH₂)₂NH₂. Later it will be shown that the infrared spectrum of SiF₄·2C₅H₅N gives strong evidence indicating that the displacement in fact did occur with a change

in configuration.

(iii) Reaction of $\text{SiF}_4 \cdot 2\text{C}_5\text{H}_5\text{N}$ with aqueous HF

The reaction of $\text{SiF}_4 \cdot 2\text{C}_5\text{H}_5\text{N}$ with aqueous HF is similar to a simple hydrolysis using only H_2O , except that in the latter case SiO_2 is formed as well as the salt, $(\text{C}_5\text{H}_5\text{NH})_2\text{SiF}_6$. The following mechanism is proposed for this reaction.



This latter step is the driving force which shifts the equilibria of the other steps towards the right.

(vi) Infrared Spectrum of $\text{SiF}_4 \cdot 2\text{C}_5\text{H}_5\text{N}$ and Comparison with that of $(\text{C}_5\text{H}_5\text{NH})_2\text{SiF}_6$

Schnell (102) has published the infrared spectra of $\text{SiF}_4 \cdot 2\text{C}_5\text{H}_5\text{N}$ and $(\text{C}_5\text{H}_5\text{NH})_2\text{SiF}_6$ in the range $4000\text{--}650 \text{ cm}^{-1}$, but these spectra were only used to verify a proposed hydrolysis scheme. In this work, the resolution has been improved, the frequency range extended to 265 cm^{-1} , and frequency assignments have been made. Also conclusions are drawn as to the structure of $\text{SiF}_4 \cdot 2\text{C}_5\text{H}_5\text{N}$.

No attempt has been made to correlate the $3220\text{--}3000 \text{ cm}^{-1}$ region

because of the small band separation. The 3400 cm^{-1} band in pure $\text{C}_5\text{H}_5\text{N}$ is not present in either the complex or the salt and the average C-H bond stretching vibration has shifted to slightly higher wave number, from an average 3036 cm^{-1} in $\text{C}_5\text{H}_5\text{N}$ to an average 3090 cm^{-1} in $\text{SiF}_4 \cdot 2\text{C}_5\text{H}_5\text{N}$ and to an average 3103 cm^{-1} in $(\text{C}_5\text{H}_5\text{NH})_2\text{SiF}_6$. The characteristic $(\text{C}_5\text{H}_5\text{NH})_2\text{SiF}_6$ bands not present in the infrared spectrum of $\text{SiF}_4 \cdot 2\text{C}_5\text{H}_5\text{N}$ are 2770 (2720 in KBr), 1630 cm^{-1} , and 1530 cm^{-1} , the first two being due to the formation of an N-H bond. The 1300 - 1000 cm^{-1} region is less resolved in the case of $(\text{C}_5\text{H}_5\text{NH})_2\text{SiF}_6$, perhaps due to a small amount of impurity in the pyridinium salt (such as SiO_2), and shows some shifting of band positions. The Si-F bond stretching vibration has shifted from 798 (792 in KBr) in $\text{SiF}_4 \cdot 2\text{C}_5\text{H}_5\text{N}$ to 720 (740 in KBr) in $(\text{C}_5\text{H}_5\text{NH})_2\text{SiF}_6$. This agrees with the Si-F bond stretching vibration shown to be at higher wave number for most $\text{SiF}_4 \cdot 2(\text{N-donor})$ octahedral complexes ($\sim 740\text{ cm}^{-1}$) (8,19) than for SiF_6^{-2} salts ($\sim 720\text{ cm}^{-1}$) (43,48,103). The 598 cm^{-1} band of $\text{C}_5\text{H}_5\text{N}$ is present in the infrared spectrum of $(\text{C}_5\text{H}_5\text{NH})_2\text{SiF}_6$ but not in the infrared spectrum of $\text{SiF}_4 \cdot 2\text{C}_5\text{H}_5\text{N}$. The coordinate Si-N bond in the complex may make this particular C-H bond deformation vibration inactive.

In the infrared spectrum of $\text{SiF}_4 \cdot 2\text{C}_5\text{H}_5\text{N}$ the Si-F bond stretching vibration near 800 cm^{-1} appears to be perfectly symmetrical and therefore it is unlikely that "splittings" of this band are hidden. Similarly, only one Si-F bond vibration occurs below 650 cm^{-1} near 486 cm^{-1} . Bands in this region are somewhat broader but the scale is considerably expanded allowing more accurate reading of band positions. As predicted by the symmetry considerations of SiF_6^{-2} (46), only two infrared active Si-F

bond fundamental vibrations occur in $(C_5H_5NH)_2SiF_6$, one at 720 cm^{-1} and the other at 485 cm^{-1} .

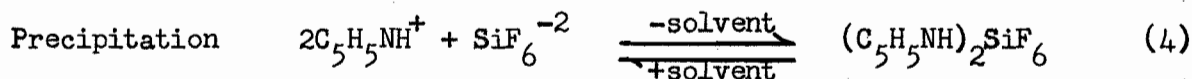
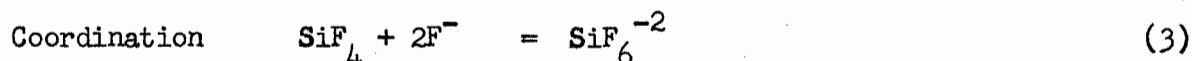
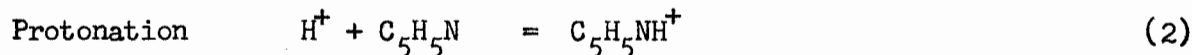
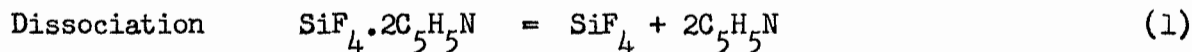
Octahedral complexes with cis configurations should have many more infrared active absorption bands for the Si-F bond. For example, the infrared spectrum (46) of $SiF_4 \cdot \alpha, \alpha'$ -dipyridil (a cis complex because of the steric requirements) has three infrared active octahedral Si-F bond stretching vibrations in the $800-740\text{ cm}^{-1}$ region and six infrared active octahedral Si-F bond "mixed" or "coupled" vibrations in the $460-310\text{ cm}^{-1}$ region. This behavior is also shown qualitatively by the infrared spectrum of $SiF_4 \cdot NH_2(CH_2)_2NH_2$ (also a cis complex by steric requirements) in which at least three octahedral Si-F bond stretching vibrations occur in the region $730-600\text{ cm}^{-1}$ and at least four octahedral Si-F bond "mixed" vibrations in the region $460-325\text{ cm}^{-1}$. Beattie et al. (47) have proposed that $SiCl_4 \cdot 2C_5H_5N$ and $SiBr_4 \cdot 2C_5H_5N$ are cis octahedral complexes because of the similarities in their infrared spectra. However, in the case of $SiF_4 \cdot 2C_5H_5N$, the fact that the Si-F bond stretching and "mixed" octahedral vibrations are not "split" is taken as evidence that the complex has a trans configuration.

(v) "Solubility" of $SiF_4 \cdot 2C_5H_5N$ in Nitromethane

The complex, $SiF_4 \cdot 2C_5H_5N$, was found to be insoluble in a large number of organic solvents but it appeared to be soluble in nitromethane only to the extent of about 5 g.l^{-1} . Analysis of the products remaining after evaporation of the solvent to dryness indicated that $SiF_4 \cdot 2C_5H_5N$ had reacted in nitromethane to yield $(C_5H_5NH)_2SiF_6$, a little SiO_2 , and a

little unreacted complex.

Four mechanisms are proposed for the reaction of $\text{SiF}_4 \cdot 2\text{C}_5\text{H}_5\text{N}$ in nitromethane. The following are common to all four mechanisms.

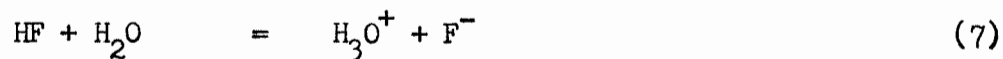


(This step is the driving force)

The four mechanisms differ in the reaction used to produce a H^+ (which must originate in CH_3NO_2 or in its H_2O content) and a F^- (which must result from the cleavage of an Si-F bond). In the two non-aqueous mechanism, the H^+ is produced by the ionization of CH_3NO_2 , a weak acid ($K_a = 6.3 \times 10^{-11}$) (104).



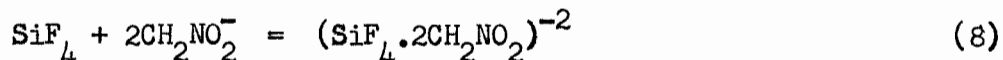
In the two aqueous mechanisms, the H^+ is produced by the ionization of HF (produced by the irreversible action of H_2O on SiF_4) in H_2O .



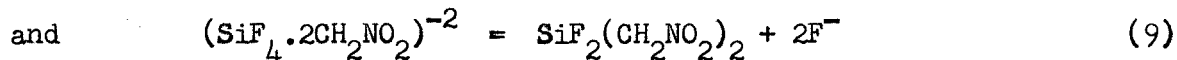
But each mechanism differs in its production of F^- .

Mechanism A (non-aqueous)

Reactions (1), (5), (2), followed by

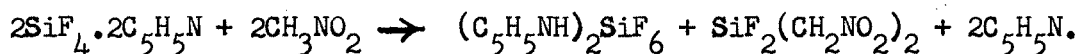


the formation of a charged octahedral complex,



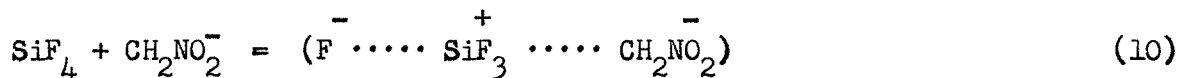
the cleavage of two Si-F bonds; formation of an uncharged octahedral complex, in addition to (3) and (4).

The overall reaction then becomes,

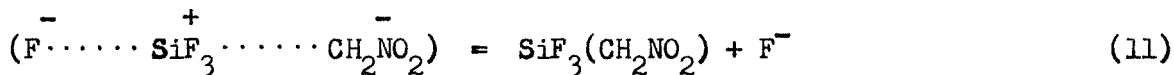


Mechanism B (non-aqueous)

Reactions (1), (5), (2), followed by

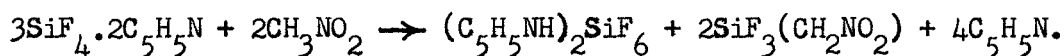


cleavage of an Si-F bond,



formation of an ion-pair, in addition to (3) and (4).

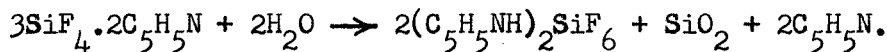
The overall reaction may then be written as,



Mechanism C (aqueous)

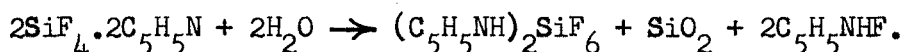
Reactions (1), (6), (7), (2), followed by (3) and (4).

The overall reaction becomes,

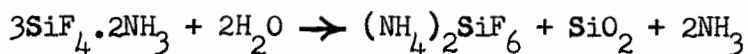


Mechanism D (aqueous)

This mechanism is similar to "mechanism C" but differs in the overall reaction, the $\text{C}_5\text{H}_5\text{N}$ not being liberated.



This latter mechanism can immediately be rejected since free C_5H_5N is produced experimentally. In fact, comparison of the mechanisms with the overall reaction in the hydrolysis of $SiF_4 \cdot 2NH_3$ (14),



indicates that "mechanism C" is probably correct.

All the mechanisms proposed (except "mechanism D") indicate the liberation of free C_5H_5N in the same way. But all of them differ in the ratio of $SiF_4 \cdot 2C_5H_5N$ consumed to $(C_5H_5NH)_2SiF_6$ produced. "Mechanisms A, B, C, and D" have ratios, $SiF_4 \cdot 2C_5H_5N$ consumed / $(C_5H_5NH)_2SiF_6$ produced, equal to 2, 3, 1.5, and 2. Comparison with the actual experimental ratio, 1.6, confirms that "mechanism C" is probably correct. Schnell (102) also proposes the same overall reaction for the hydrolysis of $SiF_4 \cdot 2C_5H_5N$.

Assuming "mechanism C" to be valid, the amount of water in the nitromethane can be calculated from the amount of SiO_2 produced experimentally. This turns out to be 0.01%, a not unreasonable value.

Summarizing, it is probably the small water content (perhaps 0.01%) in nitromethane that is responsible for the solubility of $SiF_4 \cdot 2C_5H_5N$ with the reservation that the nitromethane may participate in the reaction with the complex. This is stated because the other solvents tried did not dissolve or "dissolve with reaction" $SiF_4 \cdot 2C_5H_5N$ to any appreciable extent, even though they very likely were not much drier than the nitromethane used.

(vi) Cryoscopic Molecular Weight Determination of $\text{SiF}_4 \cdot 2\text{C}_5\text{H}_5\text{N}$ in Nitromethane

The observed molecular weight ($M = 130$), indicates that $\text{SiF}_4 \cdot 2\text{C}_5\text{H}_5\text{N}$ ($M = 262.3$) is not the species in solution. In fact, the value found supports the solubility data that $\text{SiF}_4 \cdot 2\text{C}_5\text{H}_5\text{N}$ reacts with nitromethane to form mainly $(\text{C}_5\text{H}_5\text{NH})_2\text{SiF}_6$ ($M = 100.8$). The somewhat larger than expected value found, i.e., expected for $(\text{C}_5\text{H}_5\text{NH})_2\text{SiF}_6$ in solution, is probably due to some association of the ionic species or perhaps some undissociated $\text{SiF}_4 \cdot 2\text{C}_5\text{H}_5\text{N}$ molecular species. This is likely at the freezing point of nitromethane, -29° .

(vii) Conductivity of $\text{SiF}_4 \cdot 2\text{C}_5\text{H}_5\text{N}$ in Nitromethane

The measurements confirm the conclusion from the previous solubility and cryoscopic data. The linear plot of the molar conductance against the square root of the concentration indicated that the conductivity was due to an ionic species (p. 141 of the discussion), i.e., a strong electrolyte, as would be the case for the ionic salt, $(\text{C}_5\text{H}_5\text{NH})_2\text{SiF}_6$, in nitromethane. The abnormally large decrease in molar conductance (a deviation from linearity) at concentrations higher than about $0.003 \text{ mole l}^{-1}$ was probably due to excessive ion-pair formation (as the cryoscopic data had indicated) and a decrease in ionic mobilities (due to solvent interaction) in accord with the Debye-Hückel theory (105).

The conductivity data show again that the species in nitromethane is the ionic salt, $(\text{C}_5\text{H}_5\text{NH})_2\text{SiF}_6$, and therefore, nitromethane is not a solvent for $\text{SiF}_4 \cdot 2\text{C}_5\text{H}_5\text{N}$.

(c) Structure of $\text{SiF}_4 \cdot 2\text{C}_5\text{H}_5\text{N}$

In summary, the experimental data reveal that the complex in the solid state (i) has the composition represented by $\text{SiF}_4 \cdot 2\text{C}_5\text{H}_5\text{N}$, (ii) is negligibly dissociated at 25° , (iii) contains octahedral Si-F bonds, and (iv) can readily be hydrolyzed to the ionic salt, $(\text{C}_5\text{H}_5\text{NH})_2\text{SiF}_6$. The infrared data strongly favor a trans arrangement of $\text{C}_5\text{H}_5\text{N}$ ligands rather than a cis arrangement (structures I and II, respectively of Fig. 49).

The displacement reaction with $\text{NH}_2(\text{CH}_2)_2\text{NH}_2$ then must involve a change in spatial configuration (trans \rightarrow cis) through a relatively low energy barrier. Since a complex stepwise mechanism is improbable, the best reaction path is probably the initial trace dissociation of $\text{SiF}_4 \cdot 2\text{C}_5\text{H}_5\text{N}$ yielding SiF_4 which easily reacts with $\text{NH}_2(\text{CH}_2)_2\text{NH}_2$ forming the cis octahedral complex, $\text{SiF}_4 \cdot \text{NH}_2(\text{CH}_2)_2\text{NH}_2$. The removal of SiF_4 would result in further dissociation of $\text{SiF}_4 \cdot 2\text{C}_5\text{H}_5\text{N}$ until it had all been converted to the cis complex.

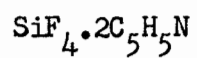
2. Coordination of SiF_4 with Ethylenediamine, Pyrrolidine, and Piperidine (N-donors)

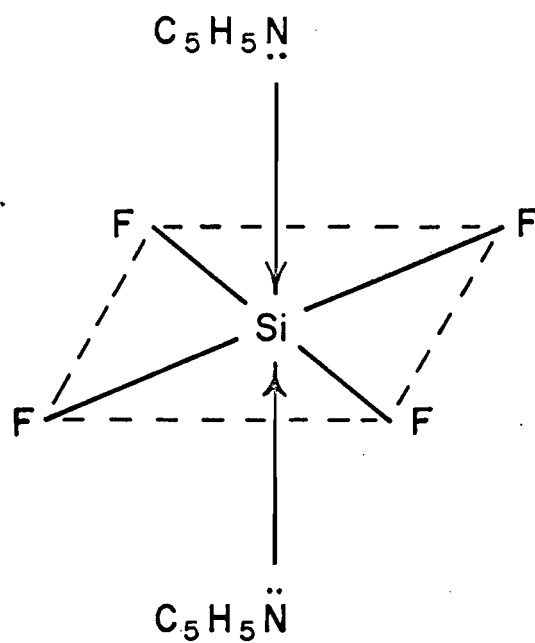
(a) Preparation of the Complexes

Direct vacuum synthesis of the complexes invariably yielded slightly impure pale yellow solids although combining ratios were good. With $(\text{CH}_2)_4\text{NH}$ and $(\text{CH}_2)_5\text{NH}$ the 1:2 complexes, $\text{SiF}_4 \cdot 2(\text{CH}_2)_4\text{NH}$ and $\text{SiF}_4 \cdot 2(\text{CH}_2)_5\text{NH}$, were obtained; with $\text{NH}_2(\text{CH}_2)_2\text{NH}_2$, a bidentate ligand, the 1:1

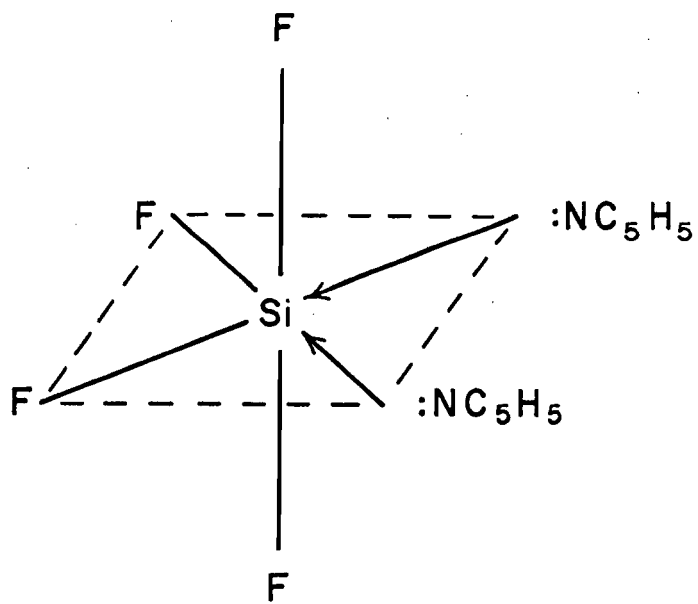
FIG. 49

The two possible spatial arrangements of C_5H_5N
ligands coordinated to SiF_4 in the complex,





TRANS



CIS

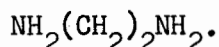
complex, $\text{SiF}_4 \cdot \text{NH}_2(\text{CH}_2)_2\text{NH}_2$, resulted. Vacuum sublimation gave analytically pure white solids.

The purest complexes were obtained by bubbling SiF_4 through precooled solutions of the base in acetonitrile. The precipitated solids were always white, although the solvent had a tinge of yellow, and they analyzed to the pure complexes without further purification. The slight yellow coloring of the solvent is probably due to the corrosive nature and slight instability of the bases as well as to the high heat of formation of the complexes. All react with stopcock grease. By using the bubbling technique most of these difficulties encountered in the direct vacuum synthesis were eliminated.

(b) Properties of the Complexes

All the complexes were involatile, white, hygroscopic solids at 25°. The complex, $\text{SiF}_4 \cdot \text{NH}_2(\text{CH}_2)_2\text{NH}_2$, could be sublimed in a vacuum at 120° and melts with decomposition near 300°. Both $\text{SiF}_4 \cdot 2(\text{CH}_2)_4\text{NH}$ and $\text{SiF}_4 \cdot 2(\text{CH}_2)_5\text{NH}$ sublime in a vacuum at 80° but the former melts with decomposition at 205-210° and the latter with decomposition at 185-190°. They appear to have about the same stability as $\text{SiF}_4 \cdot 2\text{C}_5\text{H}_5\text{N}$.

The infrared spectrum of $\text{SiF}_4 \cdot \text{NH}_2(\text{CH}_2)_2\text{NH}_2$ has previously been used to show qualitatively that $\text{SiF}_4 \cdot 2\text{C}_5\text{H}_5\text{N}$ is probably a trans complex (p. 173). Its noteworthy features were the multiple infrared active Si-F bond absorption bands in the regions 730-600 cm^{-1} and 460-325 cm^{-1} . Such "splittings" of infrared absorption bands are characteristic of an asymmetric structure as would be the case for the cis complex, $\text{SiF}_4 \cdot$



The infrared spectrum of $\text{SiF}_4 \cdot 2(\text{CH}_2)_5\text{NH}$ is marked by many more absorption bands than occur in the infrared spectrum of $\text{SiF}_4 \cdot 2(\text{CH}_2)_4\text{NH}$. But this is not too surprising since liquid $(\text{CH}_2)_5\text{NH}$ has many more absorption bands than liquid $(\text{CH}_2)_4\text{NH}$. Table 31 shows that the band near 750 cm^{-1} has been assigned to the octahedral Si-F bond stretching vibration. This has been done mainly on the basis that it is a strong, slightly broad band and that the other bands near this region can be assigned to ligand vibrations. Also in most $\text{SiF}_4 \cdot 2(\text{N-donor})$ complexes the octahedral Si-F bond stretching vibration is usually strong and somewhat broad occurring near 740 cm^{-1} (8,19). Multiple bands occur in the region $695-275 \text{ cm}^{-1}$ some of which can be assigned to $(\text{CH}_2)_5\text{NH}$ vibrations but most of which are probably due to octahedral Si-F bond "mixed" vibrations (46). The infrared evidence therefore favors a cis octahedral arrangement of $(\text{CH}_2)_5\text{NH}$ ligands in $\text{SiF}_4 \cdot 2(\text{CH}_2)_5\text{NH}$ with the reservation that the observed "splittings" assigned to Si-F bond vibrations may actually be $(\text{CH}_2)_5\text{NH}$ vibrations which are infrared active only in the complex. A cis configuration for $\text{SiF}_4 \cdot 2(\text{CH}_2)_5\text{NH}$ would mean that the band near 750 cm^{-1} is not a true singlet but must contain one or more unresolved infrared active bands.

It is difficult to assign unambiguously the octahedral Si-F bond stretching vibration (or vibrations) in the infrared spectrum of $\text{SiF}_4 \cdot 2(\text{CH}_2)_4\text{NH}$ (Table 30) since the resolution is poor in the $800-700 \text{ cm}^{-1}$ region but the three strong bands in this region have thus been tentatively assigned. In this case it is possible that the three strong broad bands in the infrared spectrum of liquid $(\text{CH}_2)_4\text{NH}$ in the region $900-800 \text{ cm}^{-1}$

could be shifted to lower wave number in the complex, i.e., to the 800-740 cm^{-1} region, with the result that the octahedral Si-F bond stretching vibration would be "masked". This seems unlikely since it would result in bands in the region 945-820 cm^{-1} for $\text{SiF}_4 \cdot 2(\text{CH}_2)_4\text{NH}$ to have no correspondence with those of liquid $(\text{CH}_2)_4\text{NH}$ and it is unlikely that the octahedral Si-F bond stretching vibration occurs at wave numbers much higher than 800 cm^{-1} . But assuming that the three bands in the 800-740 cm^{-1} region are Si-F bond vibrations, then $\text{SiF}_4 \cdot 2(\text{CH}_2)_4\text{NH}$ is probably a cis complex as has been proposed for $\text{SiF}_4 \cdot 2(\text{CH}_2)_5\text{NH}$. The two octahedral Si-F bond mixed vibrations (46) in the 490-400 cm^{-1} region are further evidence for this.

Summarizing, the infrared data (i) confirm the cis configuration of $\text{SiF}_4 \cdot \text{NH}_2(\text{CH}_2)_2\text{NH}_2$, (ii) give strong evidence that $\text{SiF}_4 \cdot 2(\text{CH}_2)_5\text{NH}$ is also a cis complex, and (iii) indicate that $\text{SiF}_4 \cdot 2(\text{CH}_2)_4\text{NH}$ probably has a cis configuration.

IV. Attempted Preparation of SiF_4 Complexes with Hydrogen Sulfide, Dimethyl Sulfide, Phosphine, and Nitromethane

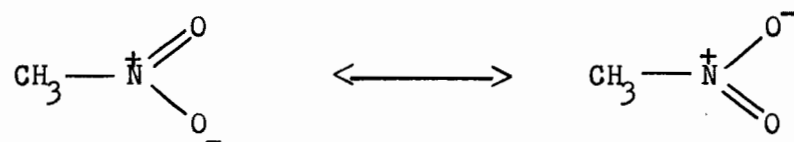
There is no observable interaction between SiF_4 and H_2S , $(\text{CH}_3)_2\text{S}$, PH_3 , and CH_3NO_2 in the temperature range -95 to 25° at pressures less than one atmosphere. Weak complexes might have been formed at lower temperatures but it was not possible to detect their presence with the available apparatus. Recently, a low temperature infrared cell, which may be used to detect complex formation at temperatures in the extended range -195 to 25° , has been acquired in this laboratory. Low-temperature vacuum distillation of the volatile components at -129° indicated that no stable involatile complex was formed at that temperature. This did not, however, exclude the possibility of the formation of a volatile complex at this temperature.

The results show that sulfur and phosphorus electron-pair donor molecules such as H_2S , $(\text{CH}_3)_2\text{S}$, and PH_3 seem to be much less basic than the corresponding oxygen electron-pair donor molecules (NH_3 corresponds to PH_3). This is expected on the basis of electronegativities since sulfur and phosphorus have considerably smaller values than oxygen or nitrogen. A more meaningful explanation should include a description of the electronic distribution around the sulfur and phosphorus atoms of the above compounds and compare this with that around the oxygen and nitrogen atoms of the corresponding compounds.

The valence-bond method is probably the most useful approach and was previously used to explain the behavior of the aliphatic cyclic ethers towards SiF_4 (p. 163). If one examines the nonbonded orbitals on

the sulfur or phosphorus atoms of H_2S , $(\text{CH}_3)_2\text{S}$, and PH_3 , it is found that these possess much greater s-character (and therefore less directional properties) than those of H_2O , $(\text{CH}_3)_2\text{O}$, and NH_3 . Also, the nonbonded orbitals of H_2S , $(\text{CH}_3)_2\text{S}$, and PH_3 are hybrids which use s and p orbitals with principle quantum number three thus resulting in even more diffuse hybrid orbitals than those of H_2O , $(\text{CH}_3)_2\text{O}$, and NH_3 which use principle quantum number two. This large decrease in directional property probably results in less overlap potential towards an sp^3d^2 -hybrid orbital of SiF_4 ; therefore, H_2S , $(\text{CH}_3)_2\text{S}$, and PH_3 are poor electron-pair donor molecules towards SiF_4 . Table 37 shows the ideas involved in the proposed explanation.

Nitromethane also had no observable basic properties towards SiF_4 . This may be due to resonance resulting in a delocalization of the slight negative charge on the oxygen atoms of CH_3NO_2 .



Steric requirements make it improbable that both oxygen atoms would behave as electron donors simultaneously. And more simply, it may be that steric hindrance due to the presence of two oxygen atoms on the same nitrogen atom prevents the near approach of CH_3NO_2 to SiF_4 .

TABLE 37

The type of hybridization of the nonbonded orbitals on the S, P, and N atoms of some acyclic compounds used in this investigation, with comparisons

Compound	NH_3	PH_3	H_2O	H_2S	$(\text{CH}_3)_2\text{O}$	$(\text{CH}_3)_2\text{S}$
Angle between bonding orbitals	107.3°	93.3°	104.5°	92.1°	111°	105°
Reference	106	107	108	109	99	110
type of bonding orbitals	sp^3	p	$\text{sp}^{>3}$, $\text{sp}^{>3}$	p, p	sp^3 , sp^3	$\text{sp}^{>3}$, $\text{sp}^{>3}$
type of nonbonded orbitals	sp^3	s	$\text{sp}^{<3}$, $\text{sp}^{<3}$	sp, sp	sp^3 , sp^3	$\text{sp}^{<3}$, $\text{sp}^{<3}$
s-character of nonbonded orbitals	0.25	1.0	>0.25 , >0.25 $<<0.5$, $<<0.5$	0.5, 0.5	0.25, 0.25	>0.25 , >0.25
directional characteristic	more	less	more	less	more	less

SUMMARY AND CONTRIBUTIONS TO KNOWLEDGE

1. Silicon tetrafluoride reacts with CH_3OH in a 1:4 mole ratio, forming the complex, $\text{SiF}_4 \cdot 4\text{CH}_3\text{OH}$, which freezes to a glass at -20° and is completely dissociated in the gas phase at 25° .
2. Conductivity measurements show clearly that $\text{SiF}_4 \cdot 4\text{CH}_3\text{OH}$ is a very weak electrolyte in methanol solution. Its infrared spectrum does not contain an Si-O bond stretching absorption band. Proton magnetic resonance measurements provide strong evidence of hydrogen bonding between SiF_4 and CH_3OH .
3. The experimental data indicate that the complex in the liquid state is tetrahedral with strong hydrogen bonds between CH_3OH and each of the four fluorine atoms.
4. At low temperature, SiF_4 forms stable solid 1:2 complexes, $\text{SiF}_4 \cdot 2(\text{ether})$, with $(\text{CH}_2)_n\text{O}$ (where $n = 2, 3, 4,$ and 5) and $(\text{CH}_3)_2\text{O}$. At 25° , all are unstable and either dissociate completely, as do $\text{SiF}_4 \cdot 2(\text{CH}_2)_4\text{O}$, $\text{SiF}_4 \cdot 2(\text{CH}_2)_5\text{O}$, and $\text{SiF}_4 \cdot 2(\text{CH}_3)_2\text{O}$, or decompose into SiF_4 and a polymer, as do $\text{SiF}_4 \cdot 2(\text{CH}_2)_2\text{O}$ and $\text{SiF}_4 \cdot 2(\text{CH}_2)_3\text{O}$. In the range -94 to 25° and at pressures less than one atmosphere, 1,4-dioxane and SiF_4 do not coordinate.
5. Heats of dissociation follow the order:
 $\text{SiF}_4 \cdot 2(\text{CH}_2)_3\text{O} > \text{SiF}_4 \cdot 2(\text{CH}_2)_4\text{O} \geq \text{SiF}_4 \cdot 2(\text{CH}_2)_5\text{O} > \text{SiF}_4 \cdot 2(\text{CH}_2)_2\text{O} > \text{SiF}_4 \cdot 2(\text{CH}_3)_2\text{O}$,
indicating that this is the relative order of basicities of the ethers towards SiF_4 .

6. A theoretical explanation based on the hybridization of the nonbonded orbitals on the oxygen atom of the ethers was proposed to explain the experimental trend found for the heats of dissociation of $\text{SiF}_4 \cdot 2(\text{aliphatic cyclic ether})$ complexes. A previous explanation for the basicity trend of the aliphatic cyclic ethers was shown to be less satisfactory.

7. The $\text{SiF}_4 \cdot 2(\text{ether})$ complexes probably have octahedral structures with either cis or trans arrangement of ether ligands, but it was only possible to obtain direct evidence for this in the case of $\text{SiF}_4 \cdot 2(\text{CH}_2)_3\text{O}$; the other complexes were too unstable.

8. Silicon tetrafluoride forms much stronger adducts with nitrogen electron-pair donor molecules than with oxygen electron-pair donor molecules. With $\text{C}_5\text{H}_5\text{N}$, $(\text{CH}_2)_4\text{NH}$, and $(\text{CH}_2)_5\text{NH}$, stable solid 1:2 complexes are formed. The 1:1 complex, $\text{SiF}_4 \cdot \text{NH}_2(\text{CH}_2)_2\text{NH}_2$, results from the interaction of SiF_4 with $\text{NH}_2(\text{CH}_2)_2\text{NH}_2$. These complexes are easily hydrolyzed and have no measurable vapor pressures at 25°.

9. The interaction of $\text{SiF}_4 \cdot 2\text{C}_5\text{H}_5\text{N}$ with either aqueous HF or nitromethane yields the ionic salt, $(\text{C}_5\text{H}_5\text{NH})_2\text{SiF}_6$. Conductivity and cryoscopic measurements on $\text{SiF}_4 \cdot 2\text{C}_5\text{H}_5\text{N}$ in nitromethane further indicate the presence of such an ionic species.

10. Infrared measurements indicate that (i) $\text{SiF}_4 \cdot 2\text{C}_5\text{H}_5\text{N}$ has a trans octahedral structure and that (ii) $\text{SiF}_4 \cdot 2(\text{CH}_2)_4\text{NH}$, $\text{SiF}_4 \cdot 2(\text{CH}_2)_5\text{NH}$, and $\text{SiF}_4 \cdot \text{NH}_2(\text{CH}_2)_2\text{NH}_2$ have cis octahedral structures.

11. Temperature-pressure measurements showed that no observable interaction occurs between SiF_4 and H_2S , $(\text{CH}_3)_2\text{S}$, PH_3 , and CH_3NO_2 in the temperature range -95 to 25° and at pressures below one atmosphere. Possible theoretical explanations for the poor electron donor capacity of these compounds towards SiF_4 are discussed.

REFERENCES

1. J.L. Gay-Lussac and J.L. Thenard. Mem. Soc. D'Arcueil. 2, 210 (1809).
2. J. Davy. Phil. Trans. 102, 353 (1812).
3. M. Besson. Compt. Rend. 110, 80 (1890).
4. G.N. Lewis. J. Franklin Inst. 226, 293 (1938).
5. Nomenclature of Inorganic Chemistry. Int. Union Pure Appl. Chem. Butterworths Scientific Publication. London. 1959.
6. J.E. Fergusson, D.K. Grant, R.H. Hickford, and C.J. Wilkins. J. Chem. Soc. 99 (1959).
7. C.J. Wilkins and D.K. Grant. J. Chem. Soc. 927 (1953).
8. E. Schnell. Monatsh. Chem. 93, 1136 (1962).
9. N. Miller. Nature (London). 158, 950 (1946).
10. E.L. Muetterties. J. Am. Chem. Soc. 82, 1082 (1960).
11. J. Goubeau and H. Grosse-Ruyken. Z. anorg. Chem. 264, 230 (1951).
12. U. Wannagat and R. Schwarz. Z. anorg. Chem. 277, 73 (1954).
13. J.A. Gierut, F.J. Sowa, and J.A. Niewland. J. Am. Chem. Soc. 58, 786 (1936).
14. D.B. Miller and H.H. Sisler. J. Am. Chem. Soc. 77, 4998 (1955).
corr. 78, 6421 (1956).
15. W.G. Mixter. J. Am. Chem. Soc. 2, 153 (1881).
16. W.C. Schumb and P.S. Cook. J. Am. Chem. Soc. 75, 5133 (1953).
17. T.S. Piper and E.G. Rochow. J. Am. Chem. Soc. 76, 4318 (1954).
18. R.C. Aggarwal and M. Onyszchuk. Can. J. Chem. 41, 876 (1963).
19. V. Gutmann, P. Heilmayer, and K. Utvary. Monatsh. Chem. 92, 322 (1961).
20. K. Issleib and H. Reinhold. Z. anorg. Chem. 314, 113 (1962).
21. A.V. Topchiev and N.F. Bogomolova. Dokl. Akad. Nauk S.S.S.R. 88, 487 (1953).

22. L. Holzapfel, E. Borchers, and H. Kettner. In *Silicium, Schwefel, Phosphate, Colloq. Sek. Anorg. Chem. Intern. Union Reine u. Angew. Chem. Munster. 1954.* p. 63.
23. M. Schmeisser and S. Elischer. *Z. Naturforsch.* 7b, 583 (1952).
24. R.C. Aggarwal and M. Onyszchuk. *Proc. Chem. Soc.* 20 (1962).
25. J.E. Griffiths. "Some Derivatives of Germane". Ph.D. Thesis. McGill University, Montreal. 1958.
26. R.T. Sanderson. "Vacuum Manipulation of Volatile Compounds". John Wiley and Sons, Inc. New York. 1948.
27. W.G. Paterson. "The Reaction of Some Lewis Acids with Hydrazine". Ph.D. Thesis. McGill University, Montreal. 1959.
28. D.J. LeRoy. *Can. J. Research.* 288, 492 (1950).
29. F. Feher, G. Kuhlborsh, and H. Luhlreich. *Z. anorg. allgem. Chem.* 303, 294 (1960).
30. D.R. Stull. *Ind. and Eng. Chem.* 39, 517 (1947).
31. *Handbook of Physics and Chemistry.* 41st ed. Chemical Rubber Publishing Co., Cleveland, Ohio. 1959.
32. J.P. Guertin and M. Onyszchuk. *Can. J. Chem.* 41, 1477 (1963).
33. C.R. Noller and R. Adams. *J. Am. Chem. Soc.* 48, 1080 (1926).
34. L.S. Levitt. *Chem. Ind. (London).* 1621 (1961).
35. F. Daniels, J.H. Mathews, J.W. Williams, P. Bender, and R.A. Alberty. "Experimental Physical Chemistry". McGraw-Hill, New York, Toronto, London. 1956.
36. R. Belcher and J.C. Tatlow. *Analyst.* 76, 593 (1951).
37. P.G. Stecher, M.J. Finkel, O.H. Siegmund, and B.M. Szafranski. "The Merck Index". 7th ed. 1960. Merck and Co., Inc. Rahway, N.J., U.S.A.
38. T. Shedlovsky and R.L. Kay. *J. Phys. Chem.* 60, 151 (1956).
39. J.P. Butler, H.I. Schiff, and A.R. Gordon. *J. Chem. Phys.* 19, 752 (1951).
40. F.E. Malherbe and H.J. Bernstein. *J. Am. Chem. Soc.* 74, 4408 (1952).
41. E.D. Bergmann and S. Pinchos. *Rec. trav. chim.* 71, 161 (1952).

42. S.C. Burket and R.M. Badger. *J. Am. Chem. Soc.* 72, 4397 (1950).
43. W.R. Heslop, J.A.A. Ketelaar, and A. Buchler. *Spectrochim. Acta.* 16, 513 (1960).
44. E.A. Coulson, J.L. Hales, and E.F.G. Herington. *J. Chem. Soc.* 2125 (1951).
45. R.H. Nuttall, D.W. Sharp, and T.C. Waddington. *J. Chem. Soc.* 4965 (1960).
46. H. Hickie. Private Communication. McGill University, Montreal. 1964.
47. I.R. Beattie, T. Gilson, M. Webster, and (in part) G.P. McQuillan. *J. Chem. Soc.* 238 (1964).
48. I.R. Beattie, G.P. McQuillan, L. Rule, and M. Webster. *J. Chem. Soc.* 1514 (1963).
49. D.A. Long, F.S. Murfin, J.L. Hales, and W. Kynaston. *Trans. Faraday Soc.* 53, 1171 (1957).
50. C.H. Kline, Jr., and J. Turkevich. *J. Chem. Phys.* 12, 300 (1944).
51. L. Corrsin, B.J. Fax, and R.C. Lord. *J. Chem. Phys.* 21, 1170 (1953).
52. J.K. Willmshurst and H.J. Bernstein. *Can. J. Chem.* 35, 1183 (1957).
53. L.J. Bellamy. "Infrared Spectra of Complex Molecules". N.Y.: John Wiley and Sons, Inc. London: Methuen and Co. Ltd. 1959. p. 277.
54. L. Elias. Ph.D. Chemistry Thesis. McGill University, Montreal. 1956. p. 8.
55. A. Sabatini and S. Califano. *Spectrochim. Acta.* 16, 677 (1960).
56. M. Freymann. *Compt. Rend.* 205, 852 (1937).
57. R.A. Heacock and L. Marion. *Can. J. Chem.* 34, 1783 (1956).
58. H.M. Randall, N. Fuson, R.G. Fowler, and J.R. Dangle. "Infrared Determination of Organic Structure". D. Van Nostrand Company, Inc. New York. 1949.
59. M. Freymann, *Ann. chim. (Paris)*. 11, 11 (1939).
60. N.N. Greenwood and R.L. Martin. *J. Chem. Soc.* 757 (1953).
61. H. Meerwein and W. Panwitz. *J. prak. Chem.* 141, 123 (1934).
62. B. Sternback and A.G. MacDiarmid. *J. Am. Chem. Soc.* 81, 5109 (1959).

63. E.A.V. Ebsworth, M. Onyszchuk, and N. Sheppard. *J. Chem. Soc.* 1453 (1958).
64. R.H. Pierson, A.N. Fletcher, and E. St. Clair Gantz. *Anal. Chem.* 28, 1218 (1956).
65. C. Reid and T.M. Conner. *Nature (London)*. 180, 1192 (1957).
66. W.G. Schneider. In "Hydrogen Bonding". Edited by D. Hadzi. Pergamon Press, London. 1959.
67. N.N. Greenwood and R.L. Martin. *Quart. Revs. (London)*. 8, No. 1, 1 (1954).
68. D.E. McLaughlin, M. Tamres, and S. Searles, Jr. *J. Am. Chem. Soc.* 82, 5621 (1960).
69. H.C. Brown and R.M. Adams. *J. Am. Chem. Soc.* 64, 2557 (1942).
70. J. Grimley and A.K. Holliday. *J. Chem. Soc.* 1215 (1954).
71. H.E. Wirth, M.J. Jackson, and H.W. Griffiths. *J. Phys. Chem.* 62, 871 (1958).
72. R.C. Aggarwal. Private Communication. McGill University, Montreal. 1962.
73. J.D. Edwards, W. Gerrard, and M.F. Lappert. *J. Chem. Soc.* 348 (1957).
74. J. Furukawa, T. Saigusa, and N. Mise. *Makromol. Chem.* 38, 244 (1960).
75. S.H. Maron and C.F. Prutton. "Principles of Physical Chemistry". Macmillan Company. 1959. p. 352.
76. H.J. Emeleus and G.S. Rao. *J. Chem. Soc.* 4245 (1958).
77. "Selected Values of Chemical Thermodynamic Properties". Circular 500. National Bureau of Standards. U.S. Government Printing Office, Washington, D.C. 599 (1952).
78. B. Rubin, H.H. Sisler, and H. Schecter. *J. Am. Chem. Soc.* 74, 877 (1952).
79. J.G. Whanger and H.H. Sisler. *J. Am. Chem. Soc.* 75, 5188 (1953).
80. J. Grimley and A.K. Holliday. *J. Chem. Soc.* 1212 (1954).
81. J.D. Edwards, W. Gerrard, and M.F. Lappert. *J. Chem. Soc.* 1470 (1955).
82. H.H. Sisler and P.E. Perkins. *J. Am. Chem. Soc.* 78, 1135 (1956).

83. A.G. Massey and A.K. Holliday. *J. Chem. Soc.* 1893 (1961).
84. H.E. Wirth and P.I. Slick. *J. Phys. Chem.* 66, 2277 (1962).
85. F.J. Cioffi and S.T. Zenchelsky. *J. Phys. Chem.* 67, 357 (1963).
86. S. Searles and M. Tamres. *J. Am. Chem. Soc.* 73, 3704 (1951).
87. S. Searles, M. Tamres, and E.R. Lippincott. *J. Am. Chem. Soc.* 75, 2775 (1953).
88. H.S. Gutowsky, R.L. Rutledge, M. Tamres, and S. Searles. *J. Am. Chem. Soc.* 76, 4242 (1954).
89. Sister M. Brandon, O.P., M. Tamres, S. Searles, Jr. *J. Am. Chem. Soc.* 82, 2129 (1960).
90. Sister M. Brandon, O.P., M. Tamres, S. Searles, Jr. *J. Am. Chem. Soc.* 82, 2134 (1960).
91. E. Lippert and H. Prigge. *Ann. Chem.* 659, 81 (1962).
92. J.M. Miller. Private Communication. McGill University, Montreal. 1964.
93. H.D. Robles. *Rec. trav. chim.* 58, 111 (1939).
94. G.L. Cunningham, A.W. Boyd, R.J. Myers, W.D. Gwin, and W.I. LeVan. *J. Chem. Phys.* 19, 676 (1951).
95. C.A. Coulson and W.E. Moffit. *Phil. Mag.* (7) 40, 1 (1949)
96. C.A. Coulson and W.E. Moffit. *J. Chem. Phys.* 15, 151 (1947).
97. A. Maccoll. *Trans. Faraday Soc.* 46, 369 (1950).
98. C.A. Coulson and T.H. Goodwin. *J. Chem. Soc.* 2851 (1962). corr. *J. Chem. Soc.* 3161 (1963).
99. L.E. Sutton and L.O. Brockway. *J. Am. Chem. Soc.* 57, 473 (1935).
corr. L. Pauling and L.O. Brockway. *J. Am. Chem. Soc.* 57, 2684 (1935).
100. H.C. Brown and R.H. Horowitz. *J. Am. Chem. Soc.* 77, 1730 (1955).
101. P.A. van der Meulen and H.A. Heller. *J. Am. Chem. Soc.* 54, 4404 (1932).
102. E. Schnell. *Monatsh. Chem.* 93, 65 (1962).
103. F.A. Miller and C.H. Wilkins. *Anal. Chem.* 24, 1253 (1952).
104. F.G. Bordwell. "Organic Chemistry". Macmillan Company. New York. Collier-Macmillan Ltd., London. 1963. p. 138.

105. P. Debye and E. Huckel. Physik. Z. 24, 185 (1923).
106. M.T. Weiss and W.P. Strandberg. Phys. Rev. 83, 567 (1951).
107. M.H. Sirvetz and R.E. Weston. J. Chem. Phys. 21, 898 (1953).
108. D.W. Posener and M.W.P. Strandberg. Phys. Rev. 95, 374 (1954).
109. C.A. Burrus and W. Gordy. Phys. Rev. 92, 274 (1953).
110. L.O. Brockway and H.O. Jenkins. J. Am. Chem. Soc. 58, 2036 (1936).

